GEOLOGY OF THE RAMONA PEGMATITES, SAN DIEGO COUNTY, CALIFORNIA

Thesis by

Dale Rodekohr Simpson

In Partial Fulfillment of the Requirements

For the Degree of

Doctor of Philosophy

California Institute of Technology

Pasadena, California

1960

ACKNOWLEDGMENTS

The investigations upon which this report is based were started at the suggestion of Dr. R. H. Jahns of the California Institute of Technology. His continued interest, suggestions, and detailed comments during the course of the work and the preparation of this summary are greatly appreciated.

Laboratory facilities for the project were generously provided by the California Institute of Technology and the Pennsylvania State University. Permission to use the thin section and photographic laboratories and the advice from Mr. R. von Huene is greatly appreciated. The hydrothermal investigations, conducted at the latter institution, could not have been completed without the wholehearted support and counsel of Dr. C. W. Burnham. Determinations of the quantity of water soluble in a magma that the writer was unable to complete before his departure from Penn State have been generously provided by Dr. C. W. Burnham. The water solubility determinations not completed by the writer include all determinations at pressures greater than 3 kilobars. These determinations are marked with an asterisk in the section on hydrothermal investigations.

Financial support for the hydrothermal investigations and analytical determinations was provided by the National Science Foundation through a research grant to Dr. R. H. Jahns. A research assistantship and the Harvey Mudd Summer Fellowship, both under the aegis of the California Institute of Technology helped make this study possible.

The property owners within the Ramona district have been actively cooperative in many ways. In this connection, particular thanks for many personal kindnesses are due Mr. and Mrs. L. B. Spaulding of Ramona. Mr. Hal Weber, of the California Division of Mines, generously provided a historical summary of the ownership of the several deposits in the district.

Abstract

The Ramona pegmatite district of central San Diego County, California, has been known as a source of gem garnet, tourmaline, and topaz since the early 1900's. All the occurrences of known commercial importance lie within an area of about 1.5 square miles.

The dominant rocks of the district are tonalites and granodiorites of the Cretaceous southern California batholith. The nearest outcrop of older rocks, the Triassic Julian schist, is about one mile from the main group of pegmatites. Eocene Poway conglomerate caps hills and ridges in a west-trending belt that lies south of the district.

The pegmatite bodies, ranging from small stringers to large dikes about 8 feet thick, are remarkably persistent along their strike. They form a pattern of subparallel anastomosing units with a general northwest strike and a westward dip of 35 to 45 degrees. The dikes occur mainly in the tonalites, and appear to have been emplaced along a well-developed set of fractures. These fractures are not systematically related to other structural features of the area, and they transect a major contact between plutons of different composition.

Most of the pegmatite dikes are asymmetrically zoned, each with a footwall unit of layered aplite and a hanging-wall unit rich in graphic granite. Typical inner zones of the dikes consist of quartz-perthite pegmatite, pocket-bearing pegmatite, and albite-quartz rock.

Aplite generally constitutes about one-third of the containing pegmatite body. It is a soda-rich rock, with about 40 percent of modal albite. Garnet-tourmaline layers in the aplite are roughly parallel to the footwall of the pegmatite body.

Typical graphic granite, which also forms about one-third of the containing pegmatite body, has a quartz-perthite ratio of 1:3. The microcline-albite ratio within the perthite is about 2:1. Studies of mineral orientation show that the quartz rods in a single specimen of graphic granite have a common crystallographic orientation, but that this orientation is different for different specimens and is not consonant with any crystallographic law. Moreover, the c axis of quartz is generally not the axis of elongation of the rod, nor does the c axis have a systematic angular relation to the walls of the pegmatite dike. Successive surfaces cut in a block of graphic granite show many interconnections of the quartz rods.

The quartz-perthite pegmatite commonly contains large euhedral crystals of perthite and ragged-edged blocks of graphic

granite in an allotriomorphic groundmass consisting mainly of quartz, perthite, and albite.

Albite-quartz rocks occur as fracture fillings and irregular masses within the pegmatite dikes. The albite commonly has a curved cleavelandite form. Modally these rocks have an albite-quartz ratio of 2:1.

The pocket pegmatite, which ordinarily occurs in the quartz-perthite rock, consists mainly of smoky quartz with some cleavelandite and topaz. The pockets themselves form spherical voids to thin openings with irregular outlines.

A period of corrosion and secondary mineralization followed crystallization of the pegmatites. The sequence of removal of minerals was quartz→microcline→albite, and the sequence of secondary mineralization was albite→orthoclase (with an adularia habit)→quartz with a typical low-temperature crystal form. Spessartite and secondary tourmaline most likely crystallized during the end stages of the corrosion or the beginning of the albite mineralization.

Pseudomorphs of manganese oxide after garnet (?), as well as pseudomorphs of muscovite after tourmaline, are present in otherwise unaltered quartz-feldspar rocks.

The bulk mineralogical composition of the pegmatite bodies is 30 to 35 percent for each of the minerals quartz, microcline, and albite. Muscovite, garnet, and tourmaline form about 5 percent of the total rock.

The experimentally determined liquidus for a composite sample of the pegmatite under various water-vapor pressures is about 50°C. higher than the corresponding liquidus for the ternary minimum of the system $KAlSi_3O_8$-$NaAlSi_3O_8$-SiO_2-H_2O. Similarly, the pegmatite solidus is about 50 degrees lower than that for the ternary minimum, and it can be further lowered by the addition of fluorine-bearing minerals to the rock melt. Water is soluble in a melt of the composite sample of pegmatite to the extent of about 3.5 and 5.0 weight percent at 1 and 2 kilobars, respectively, of water-vapor pressure.

Laboratory crystallization of the pegmatite melts was found to be a fairly slow process, requiring several weeks to form 1 or 2 percent of crystals. The crystals are larger and form more rapidly in melts under high water-vapor pressure and with little undercooling. Spherulitic crystal aggregates form with undercooling of 75 degrees or more.

The natural pegmatites probably crystallized from a magma and a coexisting vapor that were residual from the magma forming

the large composite southern California batholith. An hypothesis of crystallization in a restricted system best explains the features of the pegmatite bodies. Spatial relationships indicate that the dikes crystallized from the walls inward.

Hypotheses are presented to explain the layered aplites either as products of rhythmic crystallization and crystal settling or as products of in-situ rhythmic crystallization progressing upward from the footwalls of the dikes. The rhythmic crystallization could have been a result of pressure fluctuations.

Graphic granite cocrystallized with the layered aplite. All available evidence indicates simultaneous crystallization of quartz and feldspar, with the graphic texture a result of accelerated growth of one mineral alternating with accelerated growth of the other mineral. Temperature and water vapor-pressure during crystallization of the graphic granite and layered aplite were most likely about 690° to 715°C. and 3000 to 4500 bars, respectively.

The graphic granite and the quartz-perthite pegmatite probably crystallized from a melt and a coexisting vapor, and the layered aplite from the melt. The other pegmatite units are thought to be products of crystallization from a hydrothermal fluid that was mainly in the form of a vapor.

TABLE OF CONTENTS

FIGURES

FIGURES (continued)

FIGURES (continued)

TABLES

TABLES (continued)

I. INTRODUCTION

Nature of Investigation

The Ramona pegmatites in eastern San Diego County, California, have been known since 1903 for their yield of gem-quality tourmaline, topaz, garnet, and quartz, and hence have received considerable attention from students of mineralogy. In contrast, the present investigation of these interesting dikes has been petrologic, and has been aimed primarily at problems of their genesis. To this end, detailed field studies were supplemented with both petrographic and experimental work in the laboratory.

The first objective of the study was to establish the field relationships of the pegmatite dikes and their various rock types, as well as the paragenesis of their contained minerals. Field mapping was begun in March 1957 and was carried on intermittently to February 1960. A total of about 25 days was devoted to this work. The pegmatite district, about half a square mile in area, was mapped on a scale of 400 feet to one inch. Enlargement of an air photograph furnished by the Agricultural Adjustment Administration was used as the base for the original plotting of geologic data, which subsequently were transferred to an enlargement of part of the 7.5 minute Ramona Quadrangle published by the United States Geological Survey in 1955. The final map appears in this report as plate 1.

Two mines were mapped in much greater detail, one at a scale of 5 feet to the inch and the other at a scale of 10 feet to the inch. In addition, 10 cross sections of well exposed

dikes were prepared in the field at a scale of 2 feet to the inch. Maps of the mines and the cross sections appear in this report as plates 2, 3, and 4.

The second part of the study was concerned with the petrography and mineralogy of specimens obtained from the pegmatite dikes. It involved the microscopic examination of 186 thin-sections and 85 samples of crushed minerals. The thin-sections were studied primarily to determine the mineralogical composition and the paragenetic relations of the rock. The crushed samples were examined in index oils to determine the optical properties and the indicated chemical composition of the minerals. Also included in this part of the study is mineral orientation work on 30 thin-sections and the determination of the crystal forms in two rocks.

The third part of the work, also done in the laboratory, consisted of hydrothermal investigations of silicate melts. Some of these represented the bulk composition of the pegmatite dikes, and others the composition of individual pegmatite zones. Of a total of 30 months of laboratory work, begun in May 1957 and ending November 1959, about 6 months was devoted to the hydrothermal investigation.

The results of the entire investigation are presented in five sections of this report. The first deals with the general geological setting of the pegmatites. The second comprises detailed descriptions of the pegmatite zones. The third section deals with the mineralogy and the bulk mineralogical composition of the pegmatites, and the fourth is a description and discussion

of data from the hydrothermal studies. In the final section the mode of origin of each pegmatite is discussed, and a coordinated hypothesis for the genesis of the pegmatite dikes and their constituent rock types is presented and evaluated.

Previous Investigations

In an early report of the State Mineralogist, Fairbanks (1893) described the principal rock of the Ramona area as a light granite becoming a dark diorite east of the town. Also mentioned in this report are pegmatite dikes containing tourmaline, garnet, and muscovite. However, no note is made of mining in the area at that time. Gem-quality minerals evidently were first recognized in the Ramona pegmatites in 1903, and the first report on the deposit was published two years later (Kunz, 1905). This report was concerned principally with the general nature of the pegmatites and descriptions of the gem minerals. Merrill (1914) subsequently listed the names and owners of the mining claims in the district, but he did not describe the pegmatites.

During the period of 1904 to 1924, Schaller studied the mineralogy and geological relationships of asymmetrically zoned pegmatites in southern California. In the report of this study (unpublished manuscript) Schaller describes briefly the geologic relationships of the Ramona pegmatite zones and dikes. An analysis of a black tourmaline crystal from the Ramona pegmatites is also listed in the report by Schaller.

Mining activities essentially ceased in 1913, but were revived on a small scale in 1950. Sinkankas (1957) described

the geologic setting of the pegmatites and the mineral discoveries recently made in several of them.

Several published papers of a more general nature, but which are pertinent to the geology of the Ramona area, include a discussion by Miller (1935) of the geomorphology of the Southern Peninsular Range and a comprehensive treatment by Larsen (1948) of the rocks in the Corona, Elsinore, and San Luis Rey quadrangles. Several of the rock units in the Ramona quadrangle are briefly described and one rock analysis is listed in Larsen's report.

Merriam (1941) stated that a large ring-dike of a light colored tonalite was recognized during the course of general geological mapping in the southwestern part of the Ramona quadrangle. This is of particular interest, as the pegmatite dikes of the Ramona district lie on or very near the contact between the ring and a central boss of a dark colored tonalite. Later Merrian (1946) published a geologic map of the southern half of the Ramona quadrangle and described the major rock units therein. Still later, in 1954, Merriam presented a geologic map of the area between Ramona and Julian in Geologic Guide Number 5 of the bulletin on the Geology of Southern California (1954). Unfortunately there is not good agreement in names of rock units and positions of contacts among Merriam's three published maps; in particular, several of the rock units have been renamed and one rock name is introduced that is not described in the literature.

Physical Features

The Ramona pegmatites are about four miles east of the

town of Ramona in San Diego County, California. The Pacific Ocean lies 27 miles to the west and the Mexican border 34 miles to the south. The remains of the Hatfield Stage Station are about 1000 feet south of the main group of dikes (fig. 1).

The pegmatites crop out in a hilly region about 2000 feet above sea level, and in general they are about 500 feet higher than the adjacent Santa Maria Valley and the town of Ramona further west. Drainage of the area is to the west via Hatfield Creek and the San Dieguito River to the Pacific Ocean.

Climatically the area can be considered as warm semi-arid. Most of the precipitation falls during the winter months. Larsen (1948) reports the extreme temperatures at Escondido, 15 miles west of Ramona, to be 13° and 106°F. The difference between the average temperature of the warmest month and of the coldest month is about 30°F.

Vegetation is predominately sage with some manzanita in the hilly areas and abundant grass cover in the valleys. Oak trees are present in some areas adjacent to stream courses, all of which are dry during most of the year. Parts of the valley land are cultivated, with grain and alfalfa as the main crops. Turkey farming and small scale cattle grazing operations are carried on in the hilly region east of Ramona.

The paved Old Julian Road, connecting the town of Ramona and Ballena Valley, is about one half mile south of the pegmatites. A dirt road that extends through the Bernhardt turkey ranch connects the mine area with the paved road.

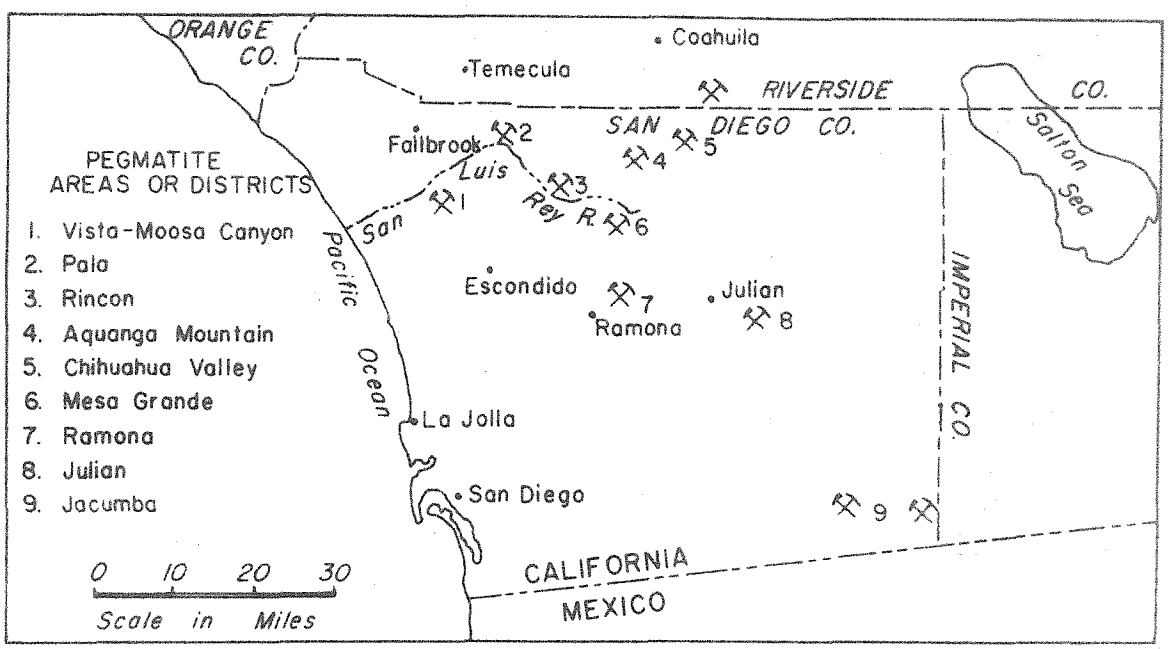

Figure 1. Index map showing locations of principal pegmatite areas and districts in San Diego County, California

Location and Ownership of Mines and Claims

Since the first discoveries of gem minerals in the Ramona pegmatites in 1903, many of the original claims have been relocated and later patented. Table 1, compiled from unpublished information generously supplied by Hal Weber of the California Division of Mines, summarizes the present ownership of the deposits. Table 2, also based upon information supplied by Mr. Weber, provides comments on the abandoned claims and claims of unknown ownership. A claim location map is shown in figure 2.

TABLE 1

LIST OF CLAIMS, LOCATIONS, OWNERSHIP, AND REMARKS

Name of Claim, Mine, or Group	Location	Owner	Remarks
A. B. C.	NW 1/4 NW 1/4 Sec. 8, T13S, R2E, SBM, Ramona district, about 2-2/3 miles east-northeast of Ramona.	Victor L. Baldwin, 3624 Wilcox, San Diego 6, and A. L. Baldwin, 2045 Pacific Highway, San Diego 1, hold 3 unpatented claims which cover about 40 acres (1957).	First discovered in November 1903 and developed by Henry Daggett, San Diego, and Alexander McIntosh, Ramona. The property was worked until the early 1910's and was then idle until 1922, when it was relocated by L. B. Spaulding, Ramona. Mr. Baldwin purchased the property from Mr. Spaulding in 1937. There has been little activity in recent years.
Daggett group	Ramona district		The original name given to the A. B. C. group by one of its discovers, Henry Daggett. See A. B. C.
Black Panther	NW 1/4 SE 1/4 Sec. 8, T13S, R2E, SBM, Ramona district, about 4 miles east-northeast of Ramona in Hatfield Creek Valley	L. B. Spaulding, P. O. Box 15, Ramona (1957).	A northwest-trending claim located in 1947 by Mr. Spaulding partly on the site of the old Sunrise cabin. Developed by a shallow northwest-trending trench. Adjoins the Fraction claim which lies to the east. Idle.
Fraction	E 1/2 NW 1/4 SE 1/4 2nd S 1/2 SE 1/4 SW 1/4 NE 1/4 Sec. 8 T13S, R2E, SBM, Ramona district about 4 miles east-northeast of Ramona in Hatfield Creek Valley	Charles H. Davis, 213 Via Cordova, Lido Isle, Newport Beach (1957).	A north-trending claim located in the late 1930's and patented in 1948. Adjoins the Little Three property which lies to the east, the Little Three Extension and Black Panther claims which lie to the west and patented ranch land to the south. Shallow workings only. No record of Production. Small house on property.
Hercules	Mainly in the SE 1/4 NE 1/4 Sec 8 small part in S 1/2 NE 1/4 NE 1/4 Sec. 8. T13S, R2E, SMB, Ramona district about 4-1/2 miles east-northeast of Ramona.	Robert B. Winstead, 225 3rd Street, Ramona and George Converse (1957).	Borders the Little Three property on the north. Originally located in August 1903 by A. V. Pray, S. G. Ingle, and Harry Titus as 2, end to end, north-northwest-trending claims. Most of the development work was done by Pray. In 1954 the present owners relocated a single north-trending claim. Developed by shallow open cuts and a 50 ft. adit driven northwestward from the south border of the claim.
Little Three	NE 1/4 SE 1/4 Sec. 8, T13S, R2E, SBM, Ramona district	Louis B. Spaulding, P. O. Box 15, Ramona (1957).	Discovered by H. W. Robb in 1903 and later purchased by Robb, McIntosh, and Schnack from John Ferguson. The property was mined until 1910 and then lay idle until 1950 and 1951 when Mr. Spaulding leased and then purchased the property. The deposit was worked continuously from 1955 to 1959.
Little Three Extension	E 1/2 SE 1/4 NW 1/4, W 1/2 NE 1/4, and N 1/2 NW 1/4 SE 1/4, Sec. 8, T13S, R2E, SBM, Ramona district about 4 miles east-northeast of Ramona in Hatfield Creek Valley	L. B. Spaulding, P. O. Box 15, Ramona (1957).	A northwest-trending claim located by owner in 1947. Adjacent to the Black Panther claim to the south and the Fraction claim to the east. Idle.
New A. B. C.	SE 1/4 NW 1/4 2nd N 1/2 NE 1/4 SW 1/4 Sec. 8, T13S, R2E, SBM; Ramona district about 4 miles east-northeast of Ramona in Hatfield Creek Valley	L. B. Spaulding, P. O. Box 15, Ramona (1957).	A northwest-trending claim that was located in 1947 by the present owner on land partly covered in the early 1900's by the Cable and Sunrise claims. Principal workings are on the site of the extreme northwest part of the Sunrise claim. Developed by a northwest-trending trench 35 ft. long, 10 to 25 ft. wide and about 10 ft. deep. Idle.
Prospect	W 1/2 NW 1/4 SW 1/4 Sec. 5, T13S, R2E, SBM, Ramona district, about 4 miles east-northeast of Ramona and 200 ft. east of Highway 78	Henry Taylor, Julian Road, Ramona (1957).	On patented ranch land. Located by H. A. Warnock and J. P. Sutherland of Ramona in September 1904 on property owned by Warnock. Abandoned within several years thereafter. Developed by 25 ft. cut. No production.
Surprise	W 1/2 SW 1/4 SW 1/4 Sec. 9, T13S, R2E, SBM, Ramona district, about 4-1/2 miles east-northeast of Ramona in Hatfield Creek Valley	J. J. Bernhardt Bernhardt Ranch Ramona, Calif. (1957)	Discovered in 1903 by Mrs. J. W. Booth just north of her residence, which was a station on the Forster-Julian stage route. Mrs. G. M. Stone, owner of the land, Mr. Booth, and A. J. Farley worked the deposit for a short time. The deposit, now located in the Bernhardt turkey pen, has been abandoned since the early 1900's.

TABLE 2

ABANDONED CLAIMS AND CLAIMS OF UNKNOWN OWNERSHIP

Name of Claim Mine, or Group	Location	Remarks
Cable	Mainly in SE 1/4 NW 1/4 Sec. 8 and partly in NW 1/4 NE 1/4 SW 1/4 Sec. 8, T13S, R2E, SBM, Ramona district	A northwest-trending claim located in 1903 by a Dr. Cable, Los Angeles. It adjoined the Sunrise claim on the northwest. No recorded gem discoveries. Long idle. Parts of this property relocated more recently as the New A. B. C. and Little Three Extension claims.
Beryl	Part of Old Hercules Group, Ramona district	Reported by Tucker and Reed (1939) as one of two claims that comprised the Hercules mine. No longer valid.
Lookout	Center NE 1/4, Sec. 8, T13S, R2E, SBM, Ramona district	A northwest-trending claim located by S. G. Ingle, H. Titus and A. W. Pray in July 1903. It adjoined the original Hercules claims on the northeast. Developed by shallow open cuts long idle. Now partly covered by the new Hercules claim.
Sonny Boy	Reported as center of E 1/2 E 1/2, Sec. 8, probably more nearly SE 1/4 SE 1/4 NE 1/4, Sec. 8, T13S, R2E, SBM, Ramona district	A 600 ft. square claim that was located in the early 1900's east of the Hercules claim. No longer valid. Tucker and Reed (1939) reported that Edward Richmond, San Diego, owned the Sonny Boy mine which was developed by a 50 ft. adit. No evidence for this. However, the Hercules claim is developed by a 50 ft. adit.
Sunrise	Ramona district. NW 1/4 SE 1/4 Sec. 8, and the E 1/2 NE 1/4 SW 1/4 Sec. 8, T13S, R2E, SBM, Ramona district	A northwest-trending claim that was located in 1903 by a Mr. Batcheller, Ramona. It adjoined the Cable claim on the southeast. Long idle until 1947 when most of the property was relocated as the Black Panther claim.

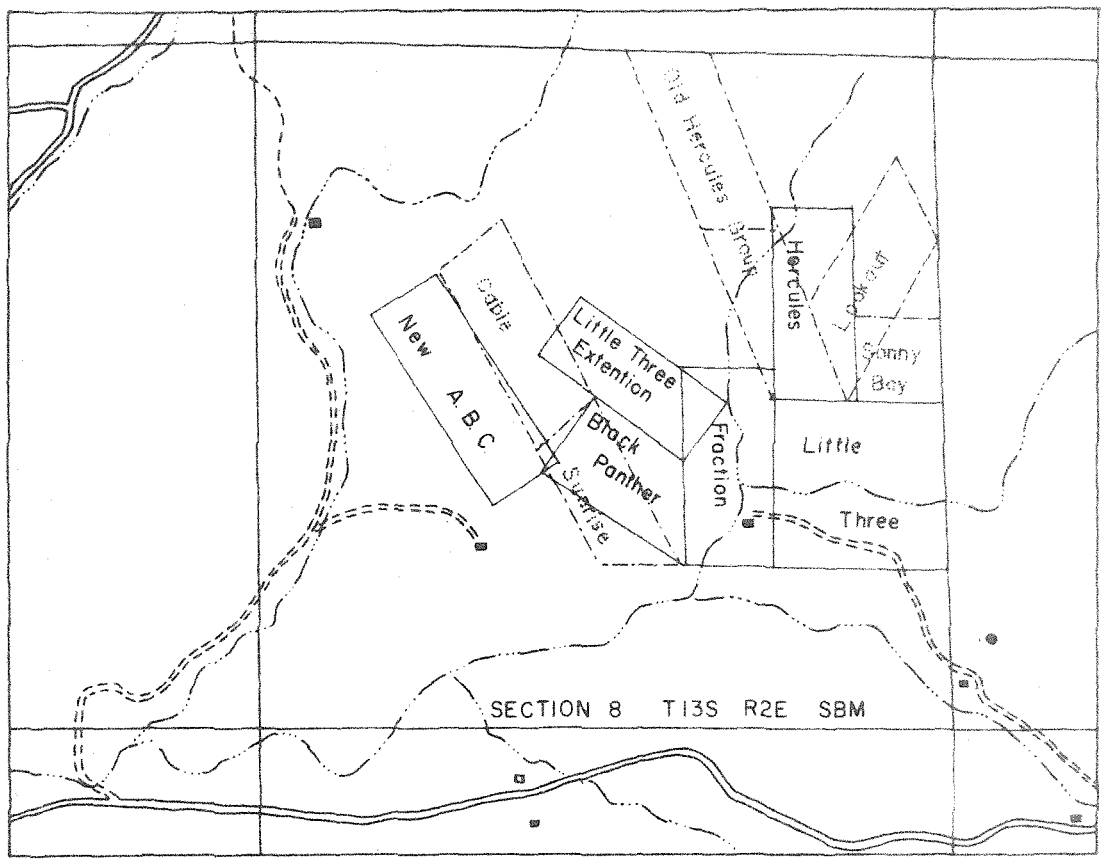

Figure 2. Index map of the Ramona district showing the location of claims

II. GEOLOGIC SETTING

General Features

The Ramona district is underlain by intrusive rocks that are part of the large and complex southern California batholith of the Peninsular Range province. This batholith, of late Mesozoic age, comprises many separate intrusive units, or plutons, that generally are in the granodiorite to gabbro range of composition. Three of these plutons form the country rock of the Ramona district. Metamorphic rocks of pre-batholith age are found as septa, screens, or inclusions in areas within several miles of the main group of pegmatites. Sedimentary rocks of Eocene age cap some of the high ridges and hills in the Ramona area.

Metamorphic Rocks

The metamorphic rocks of the Ramona region, chiefly quartz-mica schist, occur as isolated masses among large bodies of younger plutonic rocks. They have been termed the Julian schist by Merriam (1946). The outcrop of schist nearest to the pegmatites is about one mile east of the main group of dikes on the contact between the central boss of dark colored tonalite and the ring dike of light colored tonalite described by Merriam (1941). Within a three-mile radius of the main group of pegmatites, the metamorphic rocks constitute about one percent of the exposed bedrock terrane.

Igneous Rocks

Green Valley Tonalite

The Green Valley tonalite, a rather uniform medium- to

coarse-grained rock, is exposed mainly north of the pegmatite area. The major minerals in this rock are plagioclase, quartz, and biotite. The biotite and the gray color of the quartz and feldspar give the rock an overall bluish-gray color. Large poikilitic biotite crystals are readily visible on a fractured surface.

Microscopically the rock is seriate textured with grains ranging in size from 1/2 to 4 mm. The largest crystals are anhedral to subhedral plagioclase. Inclusions of ferromagnesian minerals give the plagioclase a poikilitic texture. Small euhedral crystals of plagioclase are present in lath-like forms. Much of the plagioclase has normal zoning that ranges in composition from $An_{(43)}$ to $An_{(53)}$. The ferromagnesian minerals, listed in order of decreasing abundance, are brown and green-brown biotite, hypersthene, and green hornblende. Quartz is present mostly as anhedral crystals interstitial to the plagioclase and ferromagnesian minerals.

A mafic facies of the Green Valley tonalite overlies the pegmatite at the Little Three mine. A typical surface of this rock has a salt-and-pepper texture caused by the abundant crystals of black hornblende and brown-stained plagioclase.

Two modes of representative specimens of Green Valley tonalite and one mode of a specimen from the mafic facies are listed in table 3.

Lakeview Mountain Tonalite

The Lakeview Mountain tonalite, one of the major rock types in the district, crops out in the area south of the Little

Three mine. This rock is medium- to coarse-grained, nearly white in color, and rather uniform in character. Biotite is widely distributed in the rock, and locally inclusions of biotite and other mafic minerals are present. Microscopically the rock is mainly plagioclase (An_{37-40}), quartz, and biotite with an allotriomorphic texture. Microcline is represented in some specimens to a maximum of about 14 percent; where present, it is generally interstitial and sporadically veins the other minerals. It appears to be a late constituent, like the accompanying interstitial quartz. Megascopically, specimens containing microcline cannot be distinguished from specimens with little or no microcline. The Lakeview Mountain tonalite weathers to a nearly white rock with scattered black plates of biotite.

Petrographic study of the Lakeview Mountain tonalite (for distribution of specimens examined, see the generalized geologic map, figure 3) reveals no systematic relationship between microcline content and distance of the rock from exposed pegmatites. This is well shown by specimen 59-R-1, in which tonalite that is in contact with pegmatite contains no potash feldspar. It seems unlikely that the variation of potash feldspar in the Lakeview Mountain tonalite can be ascribed to metasomatic action related to the pegmatites; instead, this variation must reflect original inhomogeneities in the tonalite.

The Lakeview Mountain tonalite is characterized by an increasing abundance of oriented inclusions as the contact with the Green Valley tonalite is approached. These oriented inclusions impart a definite streaking to the tonalite. Near the contact

the inclusions appear to be typical Green Valley tonalite, and dark streaks can be traced into bodies of Green Valley tonalite. The presence of inclusions and streaks of Green Valley lithology within the Lakeview Mountain tonalite indicates that the Lakeview Mountain is the younger of the two rock units.

Woodson Mountain Granodiorite

The Woodson Mountain granodiorite is of particular interest because a boss about 300 feet in longest dimension lies on or very near the contact of the tonalites. The contacts of the granodiorite and the tonalites are not visible although they can be located within about 10 feet. In general there is an absence of features as banding, gneissic structures, and inclusions that would indicate the relative age relations of the tonalite and the granodiorite. In other regions, for example the area studied by Larsen (1948), the Woodson Mountain granodiorite is younger than the Green Valley tonalite and other tonalites. Based primarily on the age relations established in other regions, the Woodson Mountain granodiorite in the pegmatite district is probably a small pluton that has been intruded along the contact of the Lakeview Mountain tonalite and the Green Valley tonalite.

The granodiorite is light- to medium-gray, commonly stained yellow-brown to red-brown. It is uniformly coarse grained, and contains scattered flakes of biotite. Outcrops of the granodiorite are jointed and deeply weathered, and the rock is veined with quartz in the area of the pegmatites. Quartz veins were not observed in the Woodson Mountain granodiorite of other areas near the Ramona district, and their occurrence hence may be

related to the pegmatites.

Microscopically the Woodson Mountain granodiorite shows a variation from medium to coarse in grain size of the major minerals, quartz, microcline, and plagioclase. The plagioclase is zoned, ranging in composition from about An_{15} to An_{30} with average ones of about An_{27}. The microcline and quartz appear to have formed later than the plagioclase and ferromagnesian minerals because they occur interstitial to and rarely veining these minerals. The modes of six specimens from the boss near the Little Three mine are listed in table 3.

Three specimens were collected near the town of Ramona. Two of these specimens, 59-R-16 and 59-R-17, are from outcrops about 1.7 miles south of the town. The location of the third specimen, 59-R-18, is shown on the map of the Ramona area, figure 3. The modes of the rocks are listed in table 3. The rock of the area from which these specimens were collected has been classified by Merriam (1946) as Bonsall tonalite, and later (Merriam, 1954) as Ramona tonalite, although no petrographic description has been published for the latter rock name. Because the mineral composition, texture, and megascopic appearance of the rock are very similar to corresponding features of the Woodson Mountain granodiorite, including that of the type locality about 6 miles southwest of Ramona, there is little basis for introducing a new rock name or even for identifying the rock as tonalite. The present writer therefore has modified the geologic map of Merriam (1954) by referring the Ramona tonalite to the Woodson Mountain granodiorite.

TABLE 3

MODAL ANALYSES OF COUNTRY ROCK SPECIMENS

GREEN VALLEY TONALITE

Specimen Number	Quartz	Plagioclase	Biotite	Hypersthene	Hornblende	Magnetite	Apatite	Total	Points Counted	Area in cm^2
59-R-12	14.2	58.0	11.9	11.9	3.6	0.5	0.0	100.0	1431	8.0
59-R-14	22.3	55.3	14.9	1.1	6.1	0.3	0.0	100.0	1190	7.5
57-R-39	1.4	51.2	3.1	7.8	34.4	1.7	0.3	99.9	1567	7.0

LAKEVIEW MOUNTAIN TONALITE

	Quartz	Microcline	Plagioclase	Biotite	Hornblende	Magnetite	Others	Total	Points Counted	Area in cm^2
57-R-12a	34.1	0.7	49.3	15.9	0.0	0.0	0.1	100.1	1464	5.0
59-R-1	22.4	0.0	56.7	16.5	3.9	0.3	0.2	100.0	1751	9.5
59-R-2	24.2	0.0	56.7	11.4	7.2	0.3	0.5	100.0	2004	11.0
59-R-10	31.6	9.1	44.8	10.7	3.8	0.1	0.1	100.2	1168	7.5
59-R-20	19.0	0.0	52.6	12.7	13.0	0.5	2.3	100.1	1040	7.5
59-R-22	28.6	11.6	45.7	8.8	5.0	0.0	0.2	99.9	1178	7.5
59-R-23	21.9	8.3	56.7	7.2	5.9	0.0	0.0	100.0	1117	7.5
59-R-24	26.7	14.2	47.6	6.8	0.0	0.6	4.3	100.2	1065	7.5

WOODSON MOUNTAIN GRANODIORITE

	Quartz	Microcline	Plagioclase	Biotite	Magnetite	Muscovite	Others	Total	Points Counted	Area in cm^2
59-R-3	38.2	24.3	32.9	3.8	tr	0.6	tr	99.8	2000	7.5
59-R-9a	32.4	20.6	40.2	6.1	0.5	0.2	0.0	100.0	1000	7.5
59-R-9b	29.2	24.6	41.2	4.6	0.2	0.0	0.0	99.8	1000	7.5
59-R-9c	36.2	22.7	38.4	2.6	0.0	0.2	0.0	100.1	1000	6.5
59-R-13	29.8	23.5	41.6	4.9	0.1	0.0	0.1	100.0	1420	7.5
59-R-15	35.9	21.9	37.3	4.1	0.5	0.1	0.0	99.8	1295	7.5
59-R-16	39.0	28.3	31.9	0.8	0.0	0.0	0.0	100.0	1000	7.5
59-R-17	40.7	16.2	38.9	2.9	0.0	0.0	1.3	100.0	1000	4.5
59-R-18	33.9	22.2	39.5	2.5	0.0	0.0	1.9	100.0	1000	6.0

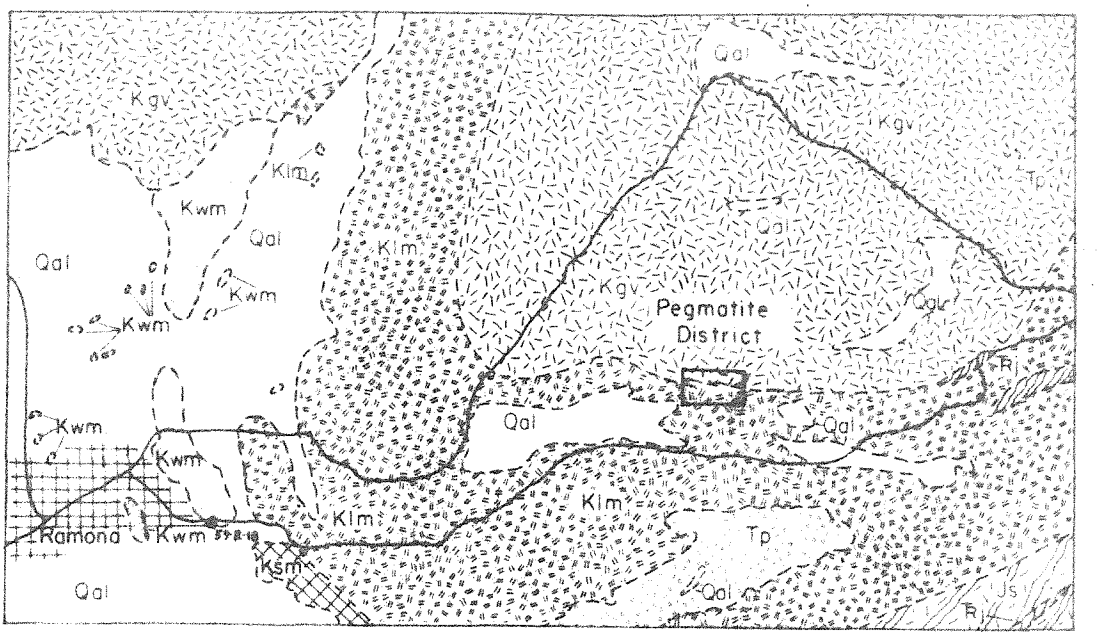

Geology after Richard Merriam (1954) modified by D. R. Simpson

EXPLANATION

Qal — Alluvium (Recent)

Tp — Poway conglomerate (Eocene)

Kwm — Woodson Mountain granodiorite (Cretaceous)

Klm — Lakeview Mountain tonalite (Cretaceous)

Kgv — Green Valley tonalite (Cretaceous)

Ksm — San Marcos gabbro (Cretaceous)

Js — Stonewall granodiorite (Jurassic)

Rj — Julian schist (Triassic)

ONE MILE

Figure 3. Generalized geologic map of the Ramona area

Pegmatite

Dikes of granitic pegmatite ranging in thickness from several inches to about 10 feet occur as a series of long anastomosing dikes that trend northwest and dip shallowly toward the west. These dikes cut the Green Valley tonalite and the Lakeview Mountain tonalite but are not in contact with the Woodson Mountain granodiorite. They probably are younger than the granodiorite, as suggested by the occurrence of possibly related quartz veins only in nearby parts of the granodiorite. Further, dikes of similar pegmatites transect Woodson Mountain granodiorite in the Pala district (Jahns and Wright, 1951) and the Rincon district (Hanley, 1951) in more northerly parts of San Diego County. It seems likely that the pegmatites represent the end of known igneous activity in the Ramona district.

Sedimentary Rocks

Poway Conglomerate

The Poway conglomerate caps the high hills and ridges in a discontinuous belt extending from Whale Mountain, east of Ramona, to the Pacific Ocean. This formation, of Eocene age, is a pebble to cobble conglomerate with abundant well rounded clasts of rhyolitic rocks. At Whale Mountain the conglomerate crops out at an altitude of about 3000 feet; about 3 miles southwest of the pegmatite area the outcrop altitude is about 2100 feet.

Quaternary Sediments

Quaternary alluvium, chiefly sand to pebble size, is present as valley fill and for the most part forms the floor of

the Hatfield Creek. Slope debris is present on most of the hills. This debris ranges in size from small grus fragments to boulders 10 to 15 feet in diameter.

Structure

Regional Structure

The Ramona area is in a major structural block about 40 miles wide and probably several hundred miles long. The Elsinore fault, trending about north 45° west, bounds this block on the east. The west margin of the block is not known, but it cannot be far west of the present coastline because the fault-bounded San Diego trough, as shown by Emery (1954), is only about 15 miles offshore.

Cretaceous sedimentary rocks are exposed in an area about 5 miles southeast of Carlsbad, in the core of an anticline near Soledad Mountain about 2 miles east of the town of La Jolla, and in a narrow zone along the coast between La Jolla and San Diego. In the Carlsbad area these rocks lie unconformable upon crystalline rocks of the southern California batholith and have a dip of about 3° northwest (Hertlein and Grant, 1954). In the narrow zone between La Jolla and San Diego they are nearly horizontal. Northeast of the summit of Soledad Mountain the sedimentary rocks have been folded, and the north limb of the main anticline dips steeply (Hertlein and Grant, 1954).

Eocene sedimentary rocks crop out in a discontinuous belt roughly parallel with the coast line. The Eocene Poway conglomerate covers a large area east of La Jolla and extends as a

discontinuous tongue in a northeasterly direction to Whale mountain east of Ramona.

Structural Features in the Ramona Area

The general trend of the prominent structural features in the area of the pegmatites is northwest. The features include the pegmatite dikes, a major set of joints, a small fault exposed west of the main group of pegmatites, and the contact between the two tonalites. Additional structural features are the gneissic layering in the tonalites trending in a northwest direction, and joint sets that do not trend in the same direction as the pegmatites.

Despite the anastomosing nature of the pegmatite dikes, their trend is generally about north 60° west. Their dip is extremely variable, but on the average is about 45° southwest.

The attitudes of joint planes in the country rock of the district were measured, and no obvious relation was found between the attitude of the joints and the size and shape of the plutons. Although there are many exceptions, most of the joints are concordant with the pegmatite dikes. Good examples of this joint set are visible on the west bank of Hatfield Creek near Spaulding Ledge. It is thought that the pegmatites were emplaced along joints of this set. The origin of these joints is problematic as they cannot be related to large scale structural features as the Elsinore fault. It may be that these joints are caused by contraction during the cooling of the batholith.

The trend of the one mappable fault in the area is about north 70° west, and its dip is southwesterly at an angle of about

60°. Poorly preserved slickensides indicate some left lateral movement on this fault.

The contact between the two tonalites is very irregular with a general intertonguing of the tonalites. The trend of the contact and the axis of the tongues is about north 70° west. Gneissoid segregations result from the increased number of inclusions of Green Valley tonalite arranged in a streaked fashion in the Lakeview Mountain tonalite near the contact of the two plutons. The attitude of these gneissic structures is nearly vertical, and the contact between the tonalites also may be essentially vertical.

Structural History of the Ramona Area

The Ramona pegmatites lie nearly in the center of a fault block more than 40 miles wide and several hundred miles long. By comparison, the mountains of the basin and range province and the Sierra Nevada Mountains are tilted horsts, but the tilting is rarely more than about 5 degrees.

Upper Cretaceous sedimentary rocks crop out along the coast about 30 miles from the Ramona pegmatite district. They overlie the batholithic rocks with profound unconformity, and their attitude indicates that there has been no major folding or tilting of the structural block in post-Cretaceous time. Near Soledad Mountain a small anticline, which appears to grade into a fault (Hertlein and Grant, 1954), furnishes the only known evidence of deformation since the Cretaceous period.

A tongue-like remnant of the Eocene Poway conglomerate

extends from the La Jolla area eastward to Whale Mountain. Bellemin and Merriam (1958) consider the thickness of this formation to be 1000 feet or less. Had there been tilting of the structural block or much uplift since Eocene time, the Poway conglomerate would have been eroded from the high areas where it is now preserved.

To summarize, all available evidence indicates that there was no substantial tilting of the structural block after emplacement of the pegmatites, and hence that the present attitude of the dikes approximates their initial attitude.

General Features of the Pegmatites

Distribution and Occurrence

The main pegmatite dikes of the Ramona district occur in an area about one half mile wide and one mile long. Within this area are exposed three major groups of anastomosing dikes that range from a single outcrop several feet long to one half mile in length. These include all pegmatites of known commercial interest.

The pegmatite bodies vary greatly in size and surface expression, although all tend to be generally tabular. In thickness the pegmatite dikes range from a few inches to about six feet. Most are two to four feet thick, and those of commercial interest are slightly thicker than the average.

The pegmatite dikes are more resistant to erosion than the country rock, and they typically form low ridges on the hillsides. They generally weather to angular fragments, whereas

the country rock weathers to grus and spheroidal boulders. Commonly the dikes are continuously exposed along their strike, although their border portions generally are covered with rock debris.

The dip of the pegmatite contacts with the country rock ranges from 30 to about 60 degrees southwest. The average angle of dip is about 45 degrees. The strike of the pegmatite dikes is also variable in direction but averages about north 45 degrees west. The strike of the pegmatite dikes does not change where the dikes transect the contact between the two tonalites.

The outcrop pattern of the pegmatite dikes is largely a function of their branching nature and tendency to form dip-slope exposures.

General Structural Features

The contacts between pegmatite and country rock are sharp. Many are irregular in detail, some are nearly planar, and others are broadly and irregularly curved. A particularly well exposed undulation in the Hercules ledge is downslope from the Hercules adit, where it plunges west with a dip of 19 degrees. It is discordant with other structural features such as joints, contact between the two tonalites, and gneissic segregations.

In general the pegmatite dikes are parallel in strike but not in dip to other planar features such as the gneissic segregations, the contact between the two tonalites, and the local fault. However, the dikes are concordant with a well-defined

joint set, which suggests that they were emplaced along fractures of this set. These breaks are not related systematically to other structural features such as the contact of the plutons or known local or major faults.

III. PEGMATITE ZONES

General Features of the Dikes

Many of the Ramona pegmatites are essentially homogeneous fine- to medium-grained aggregates of microcline-perthite[1] and quartz with scattered tourmaline, garnet, and muscovite. Distinct larger irregular blocks or euhedral crystals of perthite with some graphically intergrown quartz are scattered irregularly throughout these pegmatites.

Other pegmatite dikes in the district have well developed internal zoning, in that they consist of several lithologically distinct rock units that are arranged asymmetrically. The basal zone is an albite-rich aplite with thin layers of tourmaline and garnet, whereas the uppermost zone is dominated by coarse grained perthite graphic granite. The central zones are: a granitoid textured unit that consists predominantly of perthite and anhedral quartz with abundant tourmaline and garnet and some muscovite, a quartz core of large anhedral quartz crystals, and pockets containing euhedral cleavelandite and quartz with some topaz, tourmaline, and other rare minerals. Zones not concordant within the host pegmatite dike are cleavelandite-quartz fracture fillings and corroded rocks containing spessartite garnet. An idealized cross

1. In subsequent pages, perthitic intergrowth of microcline and albite will be called perthite in order to prevent misunderstanding concerning the use of the mineral species names microcline or albite and a perthite name such as microcline-perthite. On plates and figures accompanying this report, where misunderstanding concerning the use of the name is unlikely, the more complete name microcline-perthite is used.

section of an asymmetrically zoned pegmatite dike is shown in figure 4, and a detailed description of the individual zones is given in the following pages.

Footwall Aplite

Occurrence

The layered aplite, locally called "line rock" by the miners, occurs in sharp contact with the tonalites on the footwall side of the pegmatite dikes. The layered aplite ranges from several inches to about 3 feet in thickness and on an average forms about one third to one half of the zoned pegmatite dikes. Overlying this aplite, commonly with a sharp contact, is either granitoid or graphic-textured pegmatite. In those places where the upper contact is gradational, the change is one of texture rather than composition.

Megascopic Features

The aplites are light gray in general appearance, although individual layers commonly range in color from brown through dark gray to white. The layers range in thickness from 0.5 cm. to 3 cm. with an average of about 1 cm. The thick bands commonly are coarser grained than the narrow ones. All are parallel to subparallel, and are essentially planar to broadly undulatory.

These rocks are distinguished by the typical sugary granular texture of aplites. The crystals of plagioclase, microcline, quartz, and garnet are equant, and for the most part are in the size range of 0.1 to 1 mm. in diameter. Tourmaline present in the coarser bands is as much as 1 cm. in length.

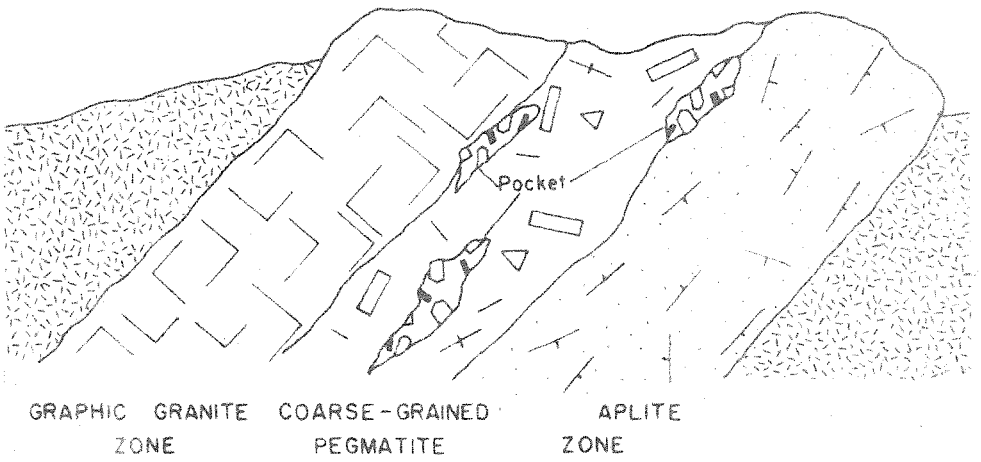

Figure 4. Idealized section of an asymmetrical zoned pegmatite in the Ramona district

Microscopic Features

Mineralogy and Texture

The aplite consists mostly of albite, quartz, and microcline. The quartz occurs in two forms. One is characterized by equant crystals, hexagonal to rounded in outline, that are about 0.5 mm. in average diameter. Crystals of the other form also are equant, but are large and anhedral, and commonly enclose smaller equant crystals of quartz and feldspar. Most of the large crystals are about 2 mm. in diameter, and they generally show a marked undulatory extinction.

Albite is the predominant feldspar. It also occurs in two forms: small, commonly prismatic crystals about 0.5 mm. in length, and large anhedral crystals, 1 to 4 mm. in diameter, that commonly enclose smaller crystals of quartz and albite. The plagioclase shows typical albite twinning.

Large anhedral crystals of microcline, about 1 to 4 mm. in diameter, enclose the small albite and quartz crystals. Rarely the microcline is perthitic.

Tourmaline, pleochroic from a pinkish purple to dark blue, is present as euhedral crystals with the characteristic rounded triangular cross section. A basal section of these crystals commonly show an internal zone that is darker blue in color than the outer zone. A core of feldspar, either microcline or albite, and quartz is present in a few of the tourmaline prisms.

Garnet occurs as euhedral crystals 0.5 mm. or less in diameter. Muscovite, in books about 1 mm. in diameter, is

rarely present in the layered aplites.

Mineral Paragenesis

Interpretation of the mineral paragenesis is complicated by the rhythmic layering of the rock and by the occurrence of the major constituents in two generations. In these rocks, the most useful criteria for determining the age relation of minerals are: (a) the enclosure of one mineral by another mineral, (b) the embayment of a mineral suggesting corrosion of the mineral, (c) the occurrence of a given mineral along contacts of other minerals, and (d) interlocking of the minerals suggesting that the minerals co-crystallized. Caution must be exercised in applying these criteria because they are not wholly diagnostic; however when used in combination they have proved useful in determining the mineral sequence.

It appears likely that the large anhedral crystals of quartz, microcline, and albite are later in the crystallization sequence than the small euhedral crystals of quartz, albite, tourmaline, and garnet because they enclose the small crystals (see figure 5). Muscovite and needle-like crystals of tourmaline occur along contacts of the large anhedral quartz, albite, and microcline thus suggesting that this muscovite and tourmaline post-date the large anhedral crystals.

The allotriomorphic texture or mutually interfering crystal boundaries of the large anhedral crystals suggests that these minerals co-crystallized.

A generalized mineral sequence is shown in figure 6.

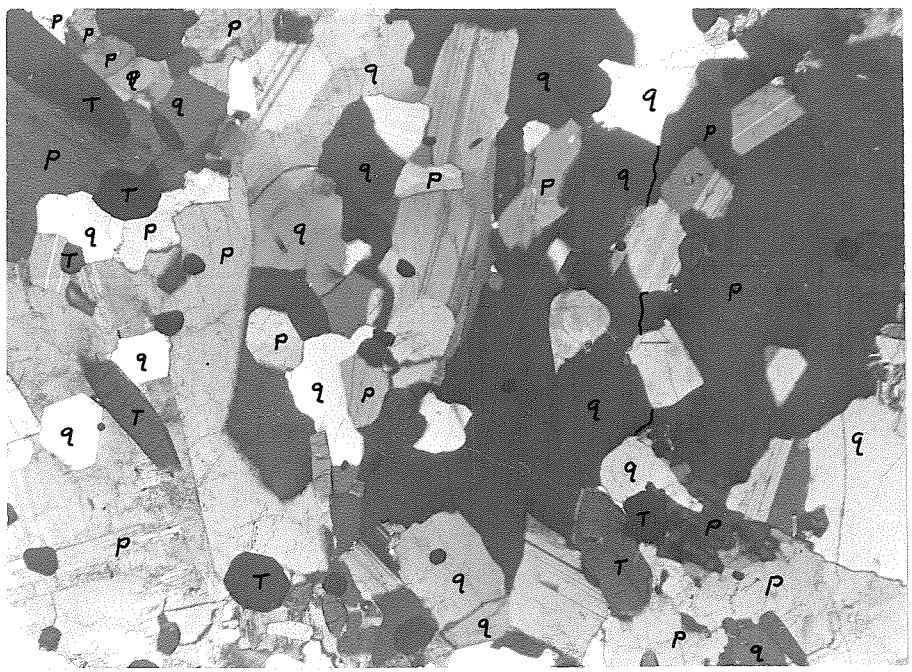

Figure 5. Layered aplite 57-R-14-4 showing bimodal size distribution of minerals (X 40)

Garnet

Tourmaline (continuity not established)

Quartz
(small euhedral crystals)

Albite
(small euhedral crystals)

Muscovite

Quartz
(large anhedral crystals)

Albite
(large anhedral crystals)

Microcline
(large anhedral crystals

Figure 6. Generalized mineral sequence for the layered aplites.

Bulk Composition

Total Rock

Because of the large variations in mineralogical composition of the layered aplite over small distances, it is meaningless to discuss the composition of a single specimen. For this reason modes were completed on what appears megascopically to be representative specimens.

Thirty modal analyses were made by the Chayes point-count method using between 1000 and 1500 points per slide. The traverses were on an area of about 7.5 cm^2. All slides were stained to facilitate the identification of quartz, potash feldspar, and albite. The linear-traverse or point count method of microscopic analysis and the limits of the method have been thoroughly discussed in the literature (Chayes, 1956) so that it needs no explanation here. For example, Chayes shows that the observed or expected error is about 1 percent of the whole for minerals constituting about 30 percent of the total rock. Campbell (1959) considered the problem of reproducibility of thin-section analysis from a more practical point of view. On the basis of these variation tests with standard size thin sections of medium-grained rocks and modes of about 1400 points, he concluded that one can expect to be able to reproduce the results of point count modal analysis within 1 percent of the whole for each major mineral.

Variations within a single hand specimen of layered aplite were studied by cutting 4 to 10 thin sections from each of three

specimens. The sampling of these specimens is shown in figure 7. The mineralogical composition obtained from the modes of the three specimens and from other layered aplites are listed in table 4. The major mineral composition of the layered aplite is quartz 35.8 percent, potash feldspar 17.5 percent, and plagioclase 41.2 percent with standard deviations of 5.4, 7.5, and 5.8 respectively.

Variation between Layers

The variation within and between layers in a thin section was studied by separately point counting the garnet and tourmaline bearing layers and the layers barren of these minerals. To accomplish this the individual layers were outlined with ink on the cover glass of the thin section, and the minerals in the areas between the inked lines were then counted. The results of these analyses along with the size of the area sampled and the number of points for each mode are listed in table 5. In order to plot these results, the quartz and feldspar percentages were recalculated to yield a sum of 100 percent. These adjusted values were then used to establish the position of the rock analysis on a triangular quartz-albite-microcline plot (figure 8). Results of the 30 model analyses of entire thin sections, as listed in table 4, are also plotted on figure 8.

Considering only the modal quartz, albite, and microcline, as shown in figure 8, it can be readily observed that the variation when layers are compared is not much greater than the

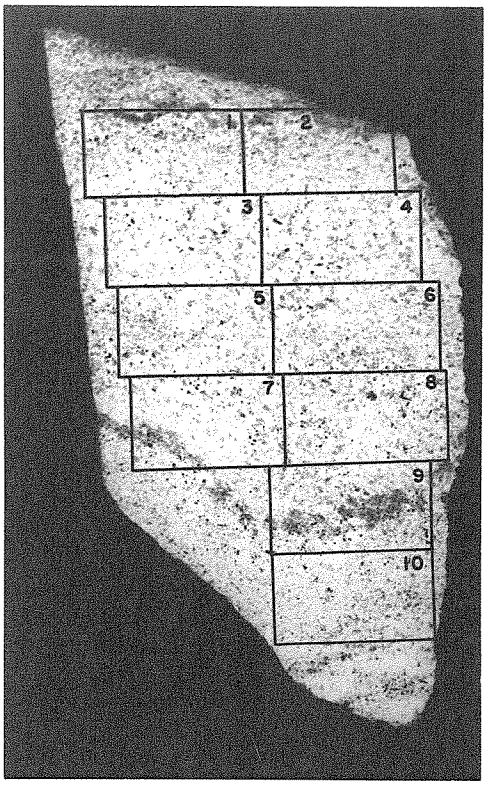

57-R-14

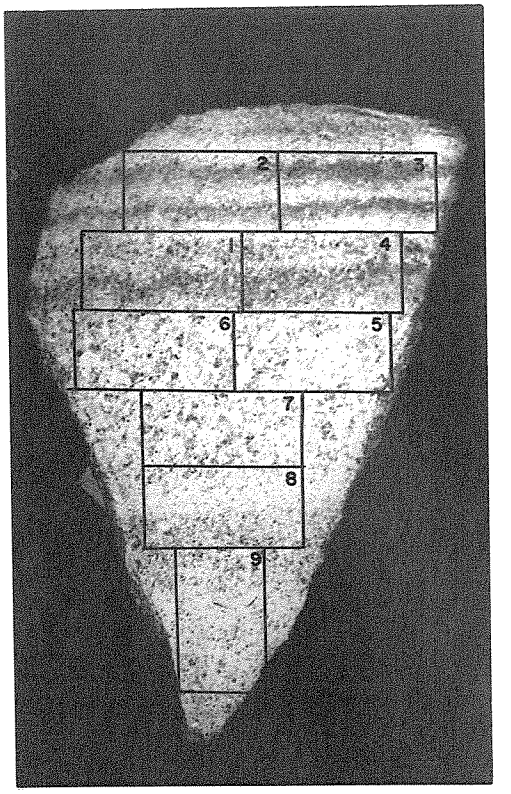

57-R-28

57-R-31

0 1 2
Inches

Figure 7. Specimens of layered aplite with outlines of areas represented by thin sections

TABLE 4

MODAL ANALYSES OF LAYERED APLITE FROM THE RAMONA DISTRICT

(area of about 7 cm^2 sampled with 1000 or more points)

Specimen Number	Quartz	Potassium Feldspar	Plagioclase	Tourmaline	Muscovite	Garnet	Total
57-R-14-1	41.8	9.6	43.8	4.6	0.0	0.1	99.9
57-R-14-2	44.5	12.7	38.1	4.7	0.0	0.0	100.0
57-R-14-3	40.4	11.9	40.6	6.5	0.1	0.4	99.9
57-R-14-4	40.8	12.1	41.5	4.6	0.1	0.8	99.9
57-R-14-5	38.4	9.7	46.0	5.3	0.4	0.0	99.8
57-R-14-6	36.1	17.0	41.7	4.9	0.2	0.0	99.9
57-R-14-7	37.7	18.6	39.7	4.0	0.0	0.0	100.0
57-R-14-8	35.8	13.1	45.6	5.2	0.3	0.0	100.0
57-R-14-9	34.6	15.5	43.8	5.7	0.2	0.0	99.8
57-R-14-10	35.5	16.9	42.9	4.6	0.0	0.0	99.9
57-R-28-1	35.1	13.4	42.0	4.9	1.3	3.3	100.0
57-R-28-2	41.3	7.0	41.7	3.7	1.8	4.5	100.0
57-R-28-3	24.5	10.1	58.7	3.6	1.0	2.1	100.0
57-R-28-4	35.3	9.5	46.7	5.3	1.3	1.8	99.9
57-R-28-5	29.6	25.6	36.5	7.3	0.7	0.1	99.8
57-R-28-6	32.6	29.3	32.2	5.3	0.3	0.5	100.2
57-R-28-7	29.8	22.8	43.0	3.9	0.6	0.0	100.1
57-R-28-8	34.9	20.3	36.5	8.1	0.3	0.1	100.2
57-R-28-9	27.7	29.6	40.4	2.0	0.1	0.2	100.0
57-R-31-1	39.7	29.6	26.7	3.8	0.2	0.0	100.0
57-R-31-3	46.9	14.3	38.6	0.0	0.0	0.0	99.8
57-R-31-5	44.1	14.6	40.5	0.3	0.3	0.0	99.8
57-R-31-6	32.8	18.0	47.2	1.6	0.5	0.0	100.1
58-R-1	32.7	23.9	40.1	3.2	0.1	0.0	100.0
58-R-5	33.3	31.8	31.5	3.1	0.3	0.0	100.0
58-R-9	34.6	20.1	37.3	1.8	6.1	0.1	100.0
58-R-12	33.8	14.7	45.1	5.3	0.1	1.0	100.0
58-R-14	30.2	29.9	35.0	4.9	0.0	0.0	100.0
58-R-15	36.0	4.7	47.3	6.3	0.9	4.8	100.0
58-R-17	32.1	20.2	43.5	4.1	0.0	0.0	99.9
Avg.	35.8	17.5	41.2	4.3	0.6	0.7	100.1
S	5.4	7.5	5.8				

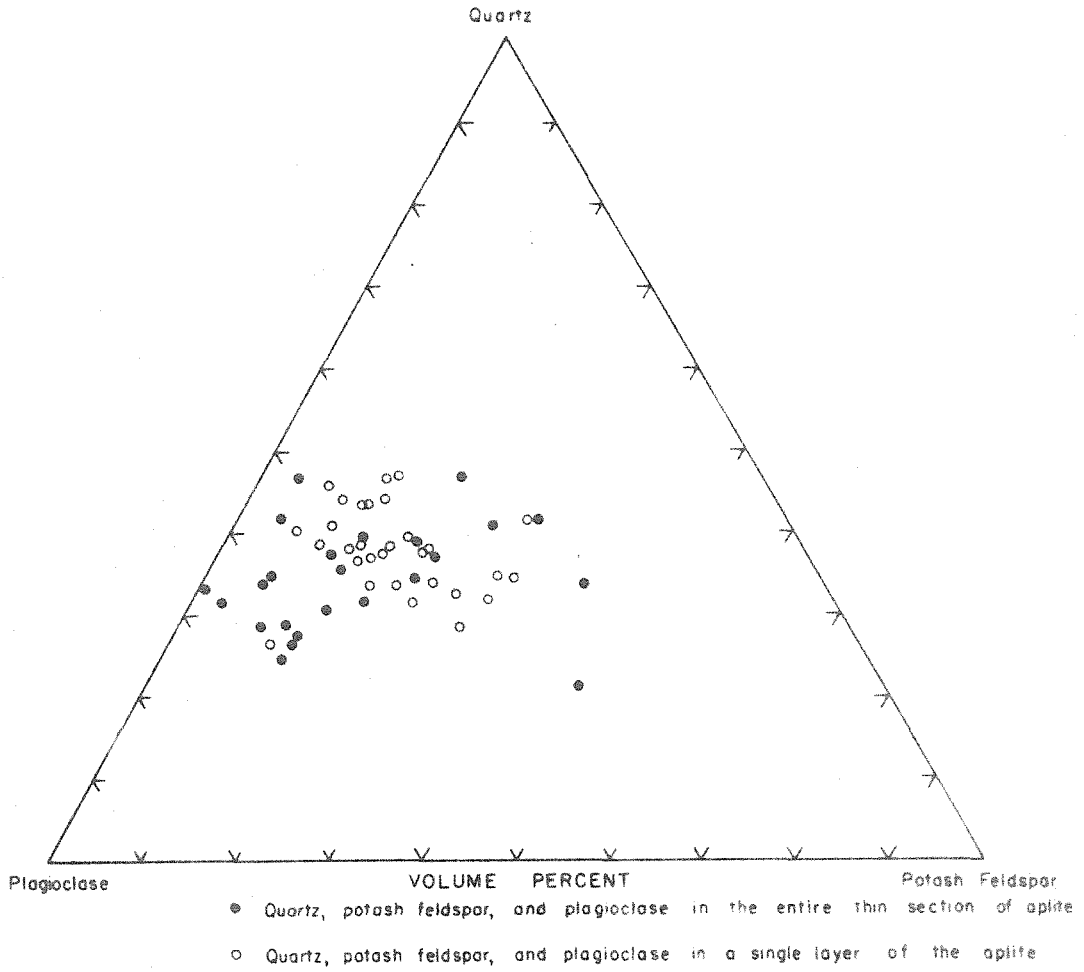

Figure 8. Volume percent relationship of quartz, potash feldspar, and plagioclase in the layered aplite from the Ramona district

TABLE 5

MODAL ANALYSES OF INDIVIDUAL LAYERS IN THE LAYERED APLITE FROM THE RAMONA PEGMATITES

Specimen Number	Layer Notation	Quartz	Potassium Feldspar	Plagioclase	Tourmaline	Muscovite	Garnet	Total	Points Counted	Approx. Area in cm^2
57-R-28-2	a	26.9	13.1	58.3	0.9	0.7	0.1	100.0	667	1.2
	b	27.2	5.4	48.5	9.3	1.7	8.0	100.1	485	1.3
	c	27.1	10.2	56.8	1.4	2.2	2.1	99.8	722	1.8
	d	26.7	13.2	47.7	5.6	0.7	6.1	100.0	460	1.4
	e	23.8	12.6	60.4	1.1	0.2	2.0	100.1	454	1.2
57-R-28-3	a	29.8	6.3	50.7	7.3	1.2	4.8	100.1	777	1.1
	b	27.1	9.0	59.7	2.2	1.2	1.0	100.2	819	1.6
	c	26.1	3.0	54.3	9.3	0.6	6.6	99.9	632	1.2
	d	25.9	13.7	59.8	0.7	1.0	0.3	100.4	724	1.6
	e	30.8	10.8	52.2	3.8	1.1	1.4	100.1	714	1.5
57-R-31-3	a	37.2	22.0	40.6	0.2	0.0	0.0	100.0	540	1.4
	b	35.5	27.2	22.3	11.3	0.2	2.9	99.4	485	1.4
	c	36.9	19.3	38.7	5.2	0.2	0.0	100.1	955	4.2
57-R-31-4	a	37.8	25.6	29.2	7.4	0.0	0.0	100.0	352	0.9
	b	39.4	14.3	46.0	0.2	0.2	0.0	100.1	645	1.0
	c	29.9	36.3	22.3	10.9	0.4	0.3	100.0	777	2.4
57-R-31-6	a	36.8	23.4	39.3	0.6	0.0	0.0	100.1	788	3.0
	b	43.0	19.5	29.2	8.3	0.0	0.0	100.0	544	1.5
	c	34.0	13.4	48.3	3.7	0.6	0.2	100.2	630	2.0
58-R-15	a	31.4	0.4	62.3	5.1	0.0	0.8	100.0	509	1.5
	b	32.6	3.4	42.0	4.5	1.5	16.0	100.0	464	1.0
	c	43.9	4.1	46.4	4.3	0.5	0.9	100.1	565	2.0
	d	33.1	10.9	44.9	6.4	1.5	3.3	100.1	814	2.5
58-R-1	a	18.5	40.8	28.2	12.5	0.0	0.2	100.2	578	2.2
	b	32.6	21.9	41.3	4.0	0.2	0.0	100.0	543	2.0
	c	31.6	18.3	50.0	0.0	0.0	0.0	99.9	436	1.8

variation when entire thin sections of the layered aplite are compared. Some of the greater variation may be due to sampling error from counting the minerals of the rock in small areas between layers. From this variation study it is concluded that, with the exception of tourmaline and garnet, no significant mineralogical variation was found among individual layers of the aplite.

As compared with rocks from other concordant zones of the pegmatite dikes, the layered aplite contains more soda feldspar and less potash feldspar than the other rocks.

Graphic Granite

Occurrence

Graphic granite generally occurs as the uppermost unit within the zoned pegmatite dikes. This hanging-wall zone, best developed in the dikes exposed at the Little Three mine, reaches a maximum thickness of about two feet. At the Little Three mine and the dike shown in cross section J-J', plate 1 and 2, a thin selvage is found between the graphic granite and the country rock. This selvage is similar to the graphic granite except that it contains a minor amount of biotite. The contact between the graphic granite or selvage and the country rock is sharp. The lower contact of the graphic granite is commonly gradational in that the texture of the rocks changes over a distance that may be as much as several feet from a typical graphic granite texture to an extremely coarse grained allotriomorphic texture.

The graphic granite has two general modes of occurrence.

One involves euhedral crystals of perthite with enclosed graphic or runic shaped rods of quartz scattered through a granitoid or aplitic textured rock. In the other, the entire rock unit consists of graphic granite.

Megascopic Features

The graphic granite is a perthite-quartz rock that is light tan to gray on a fresh surface and tan to brown on a weathered surface. This rock is primarily perthite crystals, anhedral to euhedral, ranging in size from about 2 inches to several feet. The typical perthite is subhedral and about 4 to 8 inches in its longest dimension. On fractured surfaces of the rock, the crystallographic continuity of the perthite is well shown by reflection from the cleavage surfaces. The second most abundant mineral in the graphic granite is quartz. This mineral is generally in the form of rods or plates in nearly parallel orientation. The rods range in diameter from microscopic sizes to about 2 cm. with an average diameter of about 0.5 cm. The plates are rarely greater than 2 cm. in width and 0.5 cm. in thickness with an average width and thickness of about 0.8 and 0.2 cm. respectively. The rods and plates may reach a length greater than 30 cm., but the average length is about 6 to 12 cm. Other minerals in the graphic granite in minor amounts are tourmaline and garnet. The tourmaline generally is about 1 cm. in diameter and 4 to 6 cm. in length, but it may reach a maximum size greater than 2 cm. in diameter and 15 cm. in length. The garnet rarely is more than 1 cm. in diameter.

Fractured surfaces of the graphic granite parallel to the length of the quartz rods show that these rods are spindle shaped with irregular boundaries with some rods splitting or branching into two rods. In cross section the rods commonly have an angular form as a triangle, parallelogram, square, I-shape, L-shape, or V-shape, or these rods may have an irregular rounded form. On a fractured surface of the rock roughly perpendicular to the long axis of the rods, the angular forms of the quartz rods appear similar to Runic or Hebraic writing. Because of this similarity between the outline of the quartz rods on the surface of the rock and writing or script, the rock appears graphic textured and is called graphic granite.

Commonly the rock does not show a graphic texture because the quartz rods do not have an angular habit. These rocks are referred to in the following pages as graphic granite with "poorly developed graphic characters" in contrast to graphic granite with "well developed graphic characters" or graphic granite in which the quartz has angular forms.

Microscopic Features

Microscopically the feldspar host is perthite being comprised of the minerals microcline and albite. In these rocks the albite occurs as irregular platy masses about 2 to 3 mm. in diameter and 0.2 mm. thick in a microcline host. This albite does not rim, nor is it concentrated, around the quartz rods.

The quartz rods are generally a single crystal; although rods have been found with several quartz crystals in different

orientations. In the few observed multicrystalline quartz rods, the habit of the rod was not noticeably different from unicrystalline quartz rods. The quartz generally has numerous bubble trains and included minerals. Because of the prismatic outline, the minute included minerals have been tentatively identified as tourmaline.

Rarely crystals of tourmaline ranging in size from about 0.1 mm. to several centimeters and small crystals of garnet are present in the graphic granite. The tourmaline is dark blue in color and has indices close to that of schorlite. Commonly the tourmaline crystals are zoned or have quartz-microcline cores that extend parallel to the c axis of the tourmaline. The quartz and microcline in the core of the tourmaline are anhedral, and in cross section the crystals do not reflect the spherical triangular habit of the tourmaline.

Composition

In 1881, it was pointed out by Brögger that the texture in graphic granite is due to simultaneous crystallization. In subsequent years, some investigators considered graphic granite to have a quartz-feldspar ratio of about 1:3, and the relative constancy of this ratio was cited in support of a theory of eutectic crystallization for the formation of graphic granite. During the same period other investigators questioned whether the quartz-feldspar ratio is constant in graphic granites, and they cite analyses with large variation in the quartz content as evidence

that graphic granites did not crystallize in eutectic proportions. Still other investigators considered most graphic granites to form by replacement processes and thus there is no requirement for a constant quartz content of the rocks.

In order to determine the mineralogical composition of graphic granite from the Ramona pegmatites, modal analyses of 1000 or more points were made on each of 19 of these rocks. The results of these modes and a triangular diagram of the three major minerals recalculated to yield a sum of 100 percent are shown in table 6 and figure 9. The average of the modes is 22.9, 55.7, and 20.6 percent with values ranging from 14.4 to 30.6, 43.5 to 63.5, and 11.9 to 23.3 percent for quartz, microcline, and albite respectively.

One specimen of graphic granite (57-R-23), about 14 inches long with a 4 by 6 inch cross section, was investigated in detail. This sample, a single perthite crystal with quartz rods averaging at least 6 cm. in length, was cut into three blocks and thin sections were obtained from each block as shown in figure 10. In this manner, four thin sections were made from each of the three blocks. On the surface of each block of the graphic perthite there are areas with different textures arranged in a manner suggesting that they might represent a relic texture inherited from a pre-existing rock. The composition of the rock of the different textural areas was investigated by outlining the unlike areas and point counting the minerals present in each textural area. The areas outlined with their corresponding thin sections are shown in

TABLE 6

MODAL ANALYSES OF GRAPHIC GRANITE FROM THE RAMONA PEGMATITES

(area of about 7 cm^2 sampled with 1000 or more points)

Number	Quartz	Microcline Albite		Tourmaline	Muscovite	Garnet	Total
57-R-6	21.5	55.3	23.1	0.1	0.0	0.0	100.0
57-R-9	17.9	54.6	27.3	0.2	0.0	0.0	100.0
57-R-10	14.4	60.9	24.3	0.2	0.0	0.0	99.8
57-R-19	18.9	61.0	20.0	0.1	0.0	0.0	100.0
57-R-20	24.8	53.8	21.2	0.1	0.0	0.0	99.9
57-R-22[1]	22.4	51.8	25.5	0.3	0.1	0.0	100.1
57-R-22[2]	18.1	54.3	26.5	0.9	0.0	0.1	99.9
57-R-25	20.6	62.9	16.1	0.2	0.2	0.0	100.0
58-R-11	25.2	57.2	17.0	0.2	0.4	0.0	100.0
58-R-13	20.7	60.8	16.0	2.3	0.2	0.0	100.0
58-R-16	30.6	49.1	19.9	0.1	0.1	0.1	99.9
58-R-20	29.6	53.2	11.6	5.5	0.0	0.1	100.0
58-R-27	20.3	54.2	25.0	0.3	0.3	0.0	100.1
58-R-30	29.3	43.5	23.1	4.7	0.0	0.3	99.9
59-R-25	27.1	54.6	17.6	0.6	tr	0.0	99.9
59-R-26	24.6	57.6	17.5	0.2	0.0	0.0	99.9
59-R-27	19.7	63.5	15.8	0.9	0.0	0.0	99.9
59-R-28	26.4	59.1	14.3	0.2	0.0	0.0	100.0
Avg.	22.9	55.7	20.6	0.9	0.1	tr.	100.2

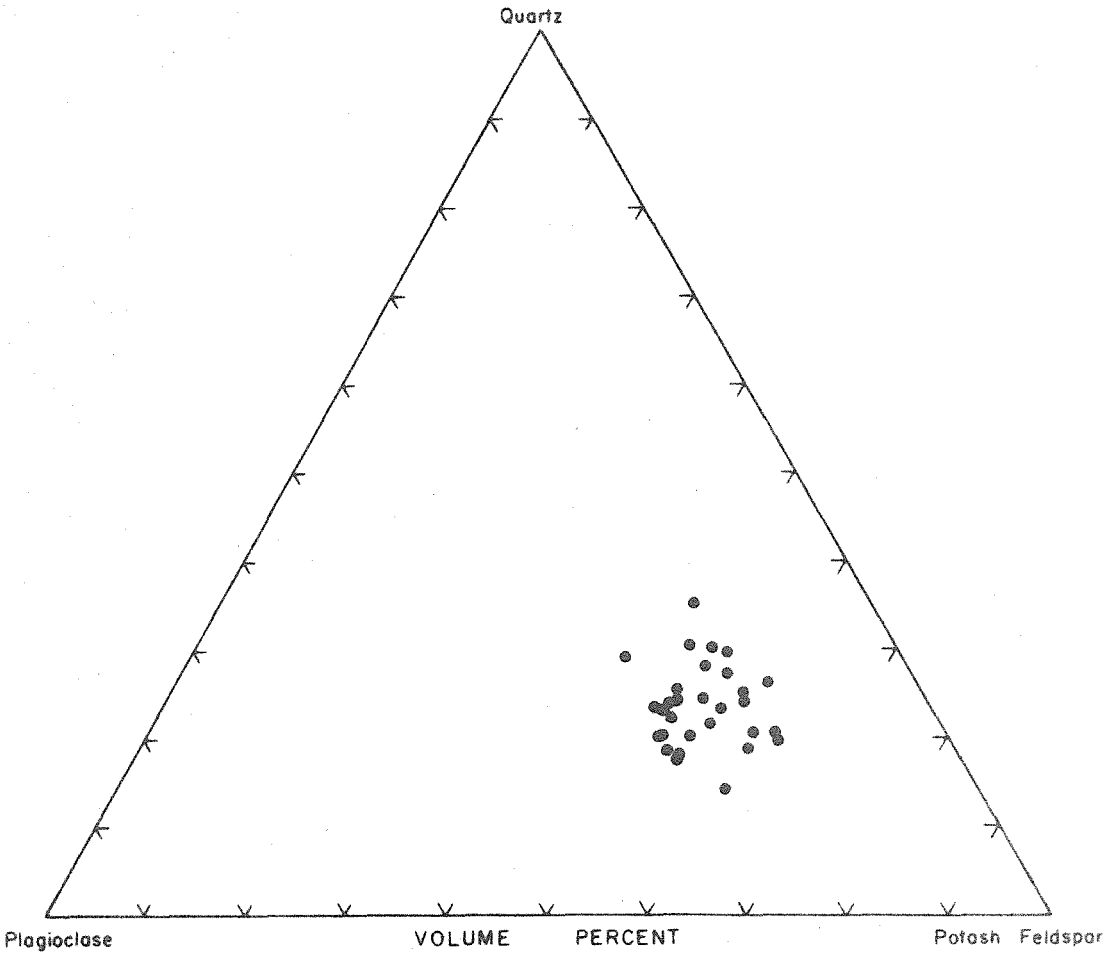

Figure 9. Volume percent relationship of quartz, potash feldspar, and plagioclase in graphic granite from the Ramona district. The feldspar is a perthite.

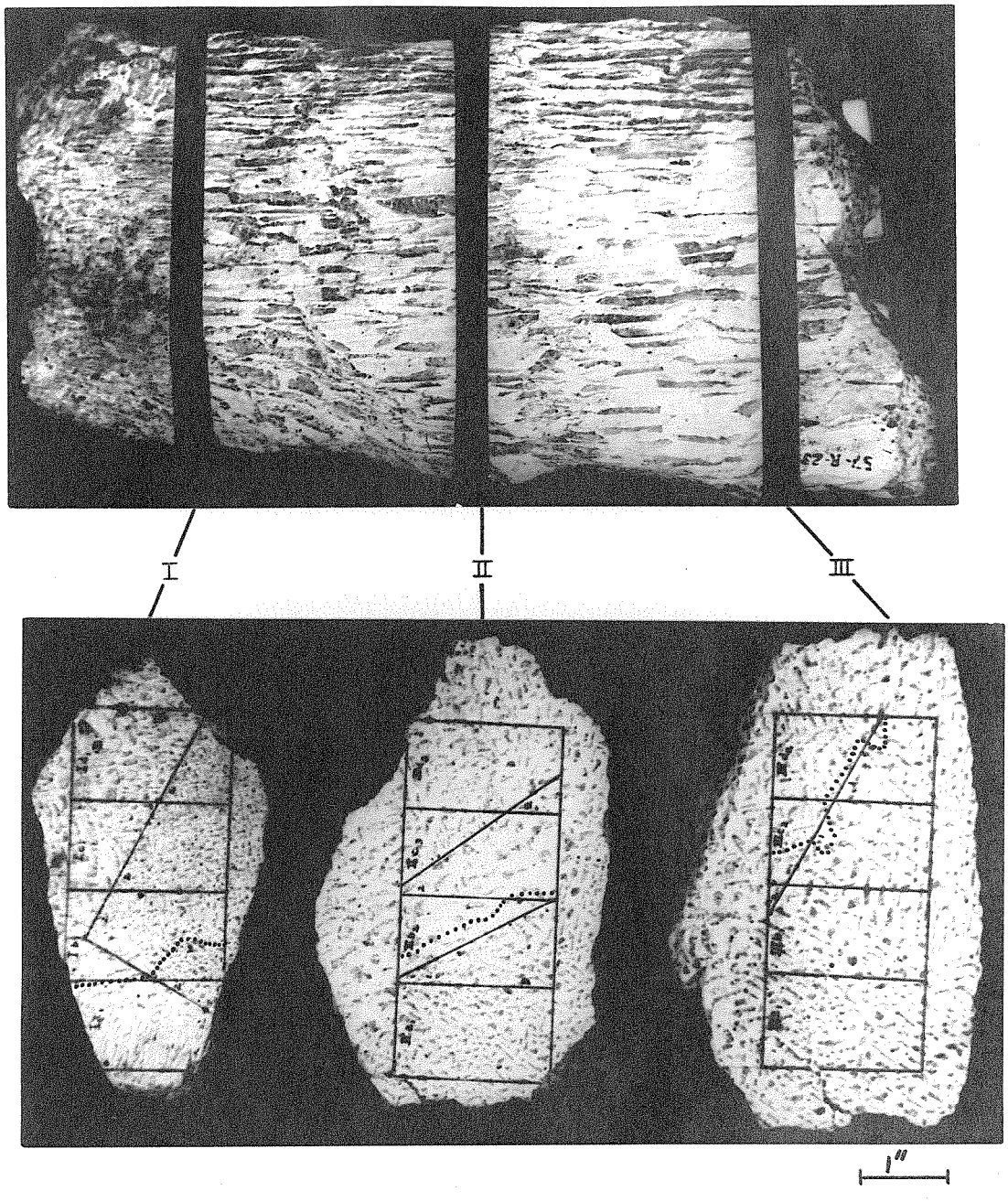

Figure 10. Specimen 57-R-23. Graphic granite showing, on the slab faces, outlines of areas represented by thin sections. Areas of different textures are also outlined and designed 1 or 2. The dotted line separates quartz rods of different orientation.

figure 10. Table 7 shows the modal composition within a textural area of the rock and the average for each block of graphic granite. These modal analyses indicate that there is little difference between the texturally dissimilar areas of rock within a single block of the graphic granite, and that greater compositional differences exist among the averages for each of the three blocks.

Graphic granite from Ramona was further studied by comparing it compositionally with 21 analyzed graphic granites as listed by Fersman (1931 pp. 77-78), Washington (1917), and Staatz and Trites (1955, p. 32). The analysis listed by Staatz and Trites is a split from a 1 ton sample of graphic granite. The chemical compositions, norms, and the localities of the samples are listed in tables 8a and 8b. A plot of the norms, with the quartz-feldspar content adjusted to 100 percent, is shown in figure 11. It is clear that the position of the main cluster of points in figure 11 is very similar to the position of the cluster of points in figure 9. In view of the data from the Ramona district and other districts, it is concluded that rocks which different investigators consider to be graphic granite, probably on the basis of the texture, have a quartz-feldspar ratio of about 1:3. No doubt these rocks should be considered the most typical graphic granite and therefore do not represent the limits of compositional variations for the rock type. Nevertheless the similarity in composition of these "most typical graphic granites" is a feature, not unique to the Ramona pegmatite district, that must be accounted for in considering various modes of origin for the rocks.

TABLE 7

MODAL ANALYSES OF AREAS OF DIFFERENT TEXTURES IN GRAPHIC GRANITE

SPECIMEN 57-R-23

(see figure 10)

Rock Slab	Textural Area	Quartz	Microcline	Albite	Tourmaline	Muscovite	Total	Points Counted	Area$_2$ in cm^2
I	1	28.8	53.0	18.1	tr	tr	99.9	3261	22
I	2	29.9	51.2	18.8	tr	tr	99.9	3071	16
II	1	27.5	48.9	23.2	0.5	0.0	100.1	2197	15
II	2	17.6	55.8	26.3	0.3	0.0	100.0	1944	14
II	3	24.1	49.3	26.4	0.2	tr	100.1	1637	14
III	1	22.2	51.0	26.4	0.3	tr	99.9	4712	38
III	2	20.4	49.8	29.5	0.3	tr	100.0	1115	9

TABLE 8a

NORMS OF GRAPHIC GRANITE FROM OTHER PEGMATITE DISTRICTS

[from analyses as listed by Fernman, A. (1931, pp. 77-78), Washington, H. S. (1917, pp. 73, 95, 109 and 113), and Staatz, M. H. and Trites, A. F. (1955, p. 32)]

Number	Quartz	Orthoclase	Albite	Anorthite	Corundum	Wollastonite	Others	Sum
1	26.0	55.6	16.8	1.4	0.4	--	--	100.2
2	24.5	53.4	20.4	1.7	--	0.1	--	100.1
3	34.0	42.3	16.8	3.6	2.7	--	--	99.4
4	22.8	51.7	25.2	--	--	0.8	--	100.5
5	21.5	59.5	18.3	--	--	0.2	0.3	99.8
6	29.6	57.8	10.0	1.4	0.3	--	--	100.1
7	31.2	8.9	51.4	8.3	0.2	--	--	100.0
8	38.4	2.8	44.5	13.3	0.1	--	0.1	99.2
9	39.8	6.1	49.3	11.1	--	0.8	4.4	101.6
10	33.0	37.3	26.7	0.6	0.1	--	1.8	99.5
11	30.6	58.4	7.9	0.6	0.3	--	1.4	99.2
12	34.0	49.5	5.8	7.2	--	1.5	1.0	99.0
13	18.5	3.9	54.0	23.1	--	0.1	--	99.6
14	27.1	53.4	17.8	--	0.5	--	0.3	99.1
15	27.1	53.4	17.8	--	1.0	--	0.3	99.6
16	22.9	55.0	19.9	1.1	1.1	--	--	100.0
17	26.0	54.5	16.8	1.4	--	--	0.4	99.1
18	22.6	46.7	28.3		1.0	--	0.5	100.2
19	25.4	56.2	16.8	0.6	0.4	--	0.9	101.3
20	29.4	50.6	17.8	1.1	--	0.1	0.5	99.5
21	31.8	45.6	21.0	0.8	0.1	--	--	99.3
22	38.5	2.8	44.1	13.3	1.1	--	--	99.8
23	35.2	3.9	47.7	11.1	0.4	--	0.6	98.9
24	18.0	59.5	19.4	1.7	--	--	0.6	99.2
25	17.6	51.2	28.8	1.1	--	--	0.9	99.6
26	48.5	13.9	22.5	5.6	4.2	--	4.3	99.0
27	36.9	20.6	32.5	--	--	--	10.2	100.2
28	20.0	64.5	14.1	0.4	--	--	--	99.0

TABLE 8b

SPECIMEN LOCALITIES FOR GRAPHIC GRANITE FROM OTHER PEGMATITE DISTRICTS

[after A. Fersman (1931), H. Washington (1917), and M. Staatz and A. Trites (1955)]

1. Östre Road, Mölard, Arendal, Norway
2. Hitterö, Norway (Vogt, 1904)
3. Raade, Smaalenene, Norway (Vogt, 1904)
4. Arendal, Norway (Vogt, 1904)
5. Elfkarleö (detached block) Norway (Bygden, 1906)
6. Skarpö, Stockholm, Sweden (Bygden, 1906)
7. Evje, Saetersdalen, Norway (Oligoclase graphic granite)
8. Ytterby, Sweden (oligoclase graphic granite)
9. Gubbe, Rodö, Sweden (albite micropegmatite)
10. Selgapajalax, Gohland Island, Finland
11. Idem
12. Stauner Rock, Kington, England
13. Beef Island, West India (oligoclase graphic granite)
14. Maine (Bastin, 1911)
15. Idem
16. Idem
17. California (Schraeder)
18. Idem
19. Evje (Klüver-Vogt, 1930) (Traces of S; CO_2-0.06%)
20. Svinö, Aland, Sweden Sundius (1926)
21. Moursinka (Sundius, 1926)
22. Oligoclase graphic granite of Hitterö (Vogt, 1927)
23. Idem
24. Wilsons Creek, Omeo, Victoria
25. Portland, Connecticut
26. Schneeqrube, Riesengebirge
27. East Greenwich, Rhode Island
28. Bucky mine, Quartz Creek District, Colorado (Split from 1 ton sample)

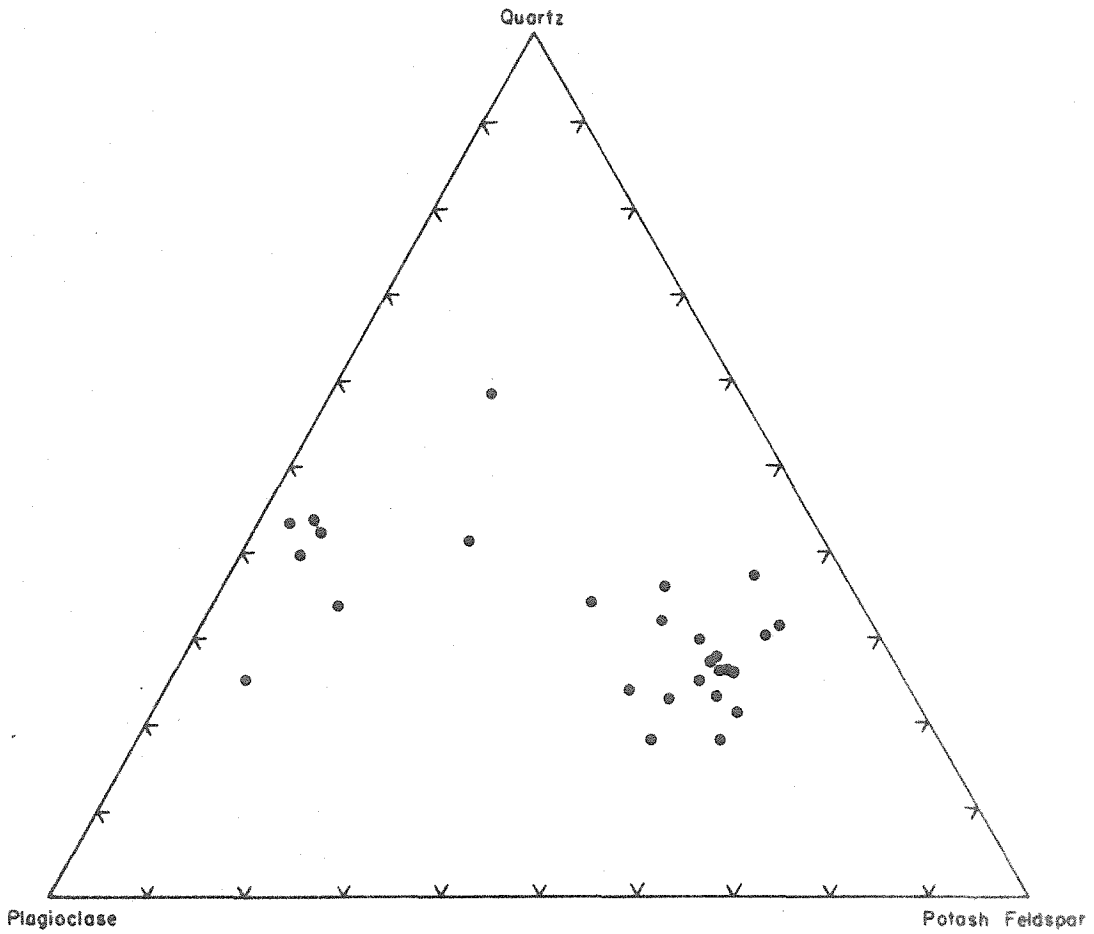

Figure 11. Normative quartz, potash feldspar, and plagioclase in graphic granites from other pegmatite districts as listed by Washington (1917) and Fersman (1931).

Orientation of Quartz

The orientation of quartz in graphic granite has been a subject of much interest and investigation. An excellent summary of work by Fersman (1928), Schiebold (1927), and Spangenberg and Neuhaus (1930) is presented by Wahlstrom (1939), along with new orientation data on about thirty specimens of graphic granite.

The so-called "trapezohedral law" was advocated by Fersman because in the specimens he examined, 88 percent were characterized by the growth of quartz in such a manner that one of its trapezohedron zones coincides with the prism zone of the feldspar. In such occurrences there is a parallelism between the prism edge of the feldspar and an edge between two adjacent rhombohedral faces of the quartz. Modifications have been proposed for the trapezohedral law (also known as "Fersman's Law"), but a characteristic feature of both the law and its modifications is that the c axis of the feldspar should make an angle of 42° 16' with the c axis of the quartz.

Wahlstrom (1939) did not find any consistent orientation of the quartz in the feldspar, and his view is therefore in direct contradiction to those expressed by Fersman and others. Minor concentrations of the positions of the quartz c axis found by Wahlstrom are not near the 42° 16' difference in the position of the axis orientation of the quartz and feldspar as is demanded by the trapezohedral law. Wahlstrom (1939, p. 690) states. "The present investigation is not comprehensive enough

to determine whether or not quartz statistically favors any particular direction or directions in the feldspar, but it does indicate that the relation probably does not conform to the requirements of a definite set of crystallographic laws."

In order further to study the orientation relationships in graphic granites, thirty thin sections from the Ramona pegmatites were examined on a universal stage. Of these thin sections, 12 were from specimen 57-R-23 as shown in figure 10. The orientation of the quartz was determined by the extinction method and the orientation of the perthite was determined by attitudes of cleavage and twin planes. The determination of cleavage directions (001) and (010) and the pericline and albite twin direction is sufficient to orient correctly the perthite crystal. Supplementary information concerning the orientation of the perthite can be obtained from interference figures of the mineral.

An area of the thin section about 4.8 cm^2, including from 9 to 164 quartz grains, was sampled. The size of the area sampled was limited by universal stage. The measured orientation was plotted on an equal area projection. These plots were then rotated so that 100 and 010 of the perthite lie on the periphery of the projection and 001 lies 26^o from the pole of the projection. With the perthite crystals sharing a common orientation with each other, the results were transferable to a composite plot. Table 9 summarizes the data obtained from this study. Commonly the orientation of the c axis of the quartz rods in a graphic granite specimen is unidirectional; although in some specimens

TABLE 9

ROCK DESCRIPTION AND DISTRIBUTION OF c AXIS POSITIONS OF QUARTZ IN GRAPHIC GRANITE

Specimen Number	Distribution of c Axis Positions of Quartz in an Equal Area Projection	Number of Quartz Rods Measured	Rock Description
57-R-6	Unidirectional	35	Perthite host crystal with quartz rods about 6 mm. by 40 mm. The rock has a well developed graphic texture.
57-R-9	Unidirectional	9	Quartz rods about 3 mm. by 15 mm. in a perthite host crystal. The rock has a poorly developed graphic character.
57-R-10	Unidirectional	18	Perthite host crystal with quartz rods about 3 mm. by 15 mm. The rock has a well developed graphic character.
57-R-19	Bidirectional	24	Perthite host crystal with quartz rods about 4 mm. by 30 mm. The rock has well developed graphic character. One group of the bidirectional distribution is from one quartz rod being composed of several crystals with slightly different orientations.
57-R-20	Unidirectional	48	The rock has a well developed graphic character. The quartz rods are about 2 mm. by 20 mm. in a perthite host crystal.
57-R-22	Unidirectional	15	Perthite host crystal with quartz rods about 5 mm. by 25 mm. The rock has a poorly developed graphic character.
57-R-22a	Bidirectional	18	Quartz rods about 3 mm. by 15 mm. in a perthite host crystal. The rock has a poorly to average developed graphic character.
57-R-25	Unidirectional	57	The rock has a poorly developed graphic character. Perthite host crystal with quartz rods about 5 mm. by 30 mm.
58-R-13	Bidirectional	57	The rock has a very poorly developed graphic character. The quartz rods are about 2 mm. by 10 mm. in a perthite host crystal.
58-R-16	Bidirectional	86	Perthite host crystal with quartz rods about 1 mm. by 10 mm. The rock has a well developed graphic character.
58-R-27	Bidirectional	17	Perthite host crystal with quartz rods about 2 mm. by 20 mm. and minor concentrations of tourmaline. The rock has a very poorly developed graphic character.
58-R-30a	Quatre directional	37	Quartz rods about 5 mm. by 8 mm. in a perthite host crystal. The rock has a very poorly developed graphic character.
59-R-27	Bidirectional	35	Perthite host crystal with quartz rods about 4 mm. by 40 mm. The rock has a well developed graphic character.
59-R-28	Quatre directional	54	Quartz rods about 2 mm. by 30 mm. in a perthite host crystal. The rock has a very poorly developed graphic character.
57-R-23	Bidirectional -- Summary of data from 12 thin sections		Perthite host crystal with quartz rods about 4 mm. by 80 mm. The rock has a well developed graphic character in most parts; however the edge of the specimen has a poorly developed graphic character.

the orientation of the c axis is bi-, tri-, or quatre-directional. The composite plot of all the results, except measurements from thin section 59-R-25, are shown in figure 12. Specimen 59-R-25 was excluded because in the plot of orientation data from this rock, there is no suggestion of a pattern. The plot of each of the other graphic granite specimens shows a well defined pattern, but the composite plot of all of these specimens does not show a pattern.

Most investigators have concluded that graphic granite may form either by a replacement of solid potassium feldspar by quartz, by simultaneous crystallization of quartz and feldspar, or by a combination of the two processes. If the Ramona graphic granite were formed by more than one process, it would be possible that a fabric on the composite plot, figure 12, of graphic granite formed by simultaneous crystallization would be obscured by a fabric, on the same plot, produced by graphic granite formed by replacement. In order to investigate this possibility, only those specimens with well formed graphic characters were plotted as shown in figure 13. There does not appear to be a definite fabric in this plot. To further investigate this problem, the data from specimens with anhedral, or poorly developed graphic characters, were plotted as shown in figure 14. In this case also, no fabric was found in the plot.

For each specimen of graphic granite the relationship between the optic axis and the axis of elongation of the quartz rods was investigated by comparing megascopic measurements

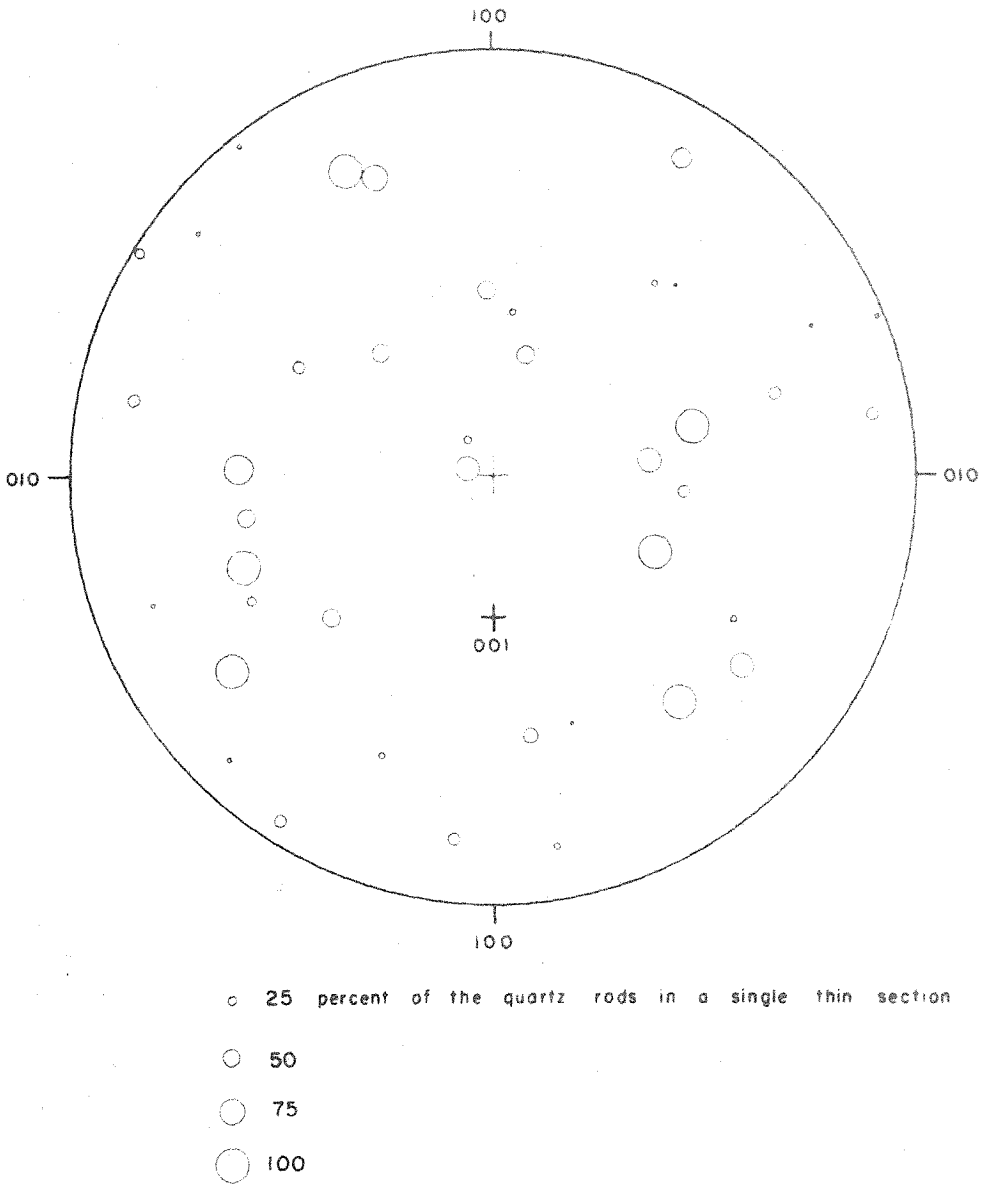

Figure 12. Composite plot of orientation data from thirty thin sections of graphic granite from the Ramona district showing the points of emergence of the c axis of quartz on an equal area projection of a monoclinic potash feldspar. The diameter of the circles indicates the percent of the quartz in a single thin section having that plotted orientation.

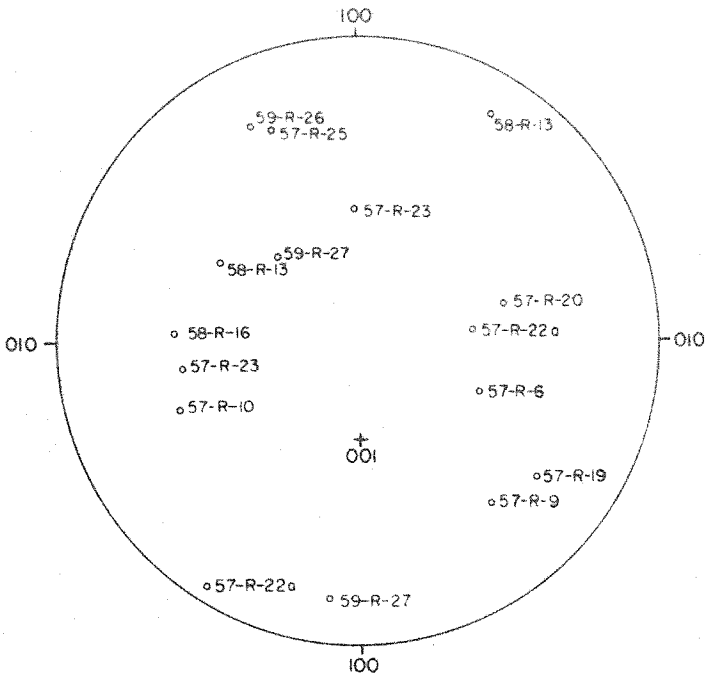

Figure 13. Plot of orientation data from thin sections of graphic granite with well developed graphic characters showing the points of emergence of the c axis of quartz on an equal area projection of a monoclinic potash feldspar.

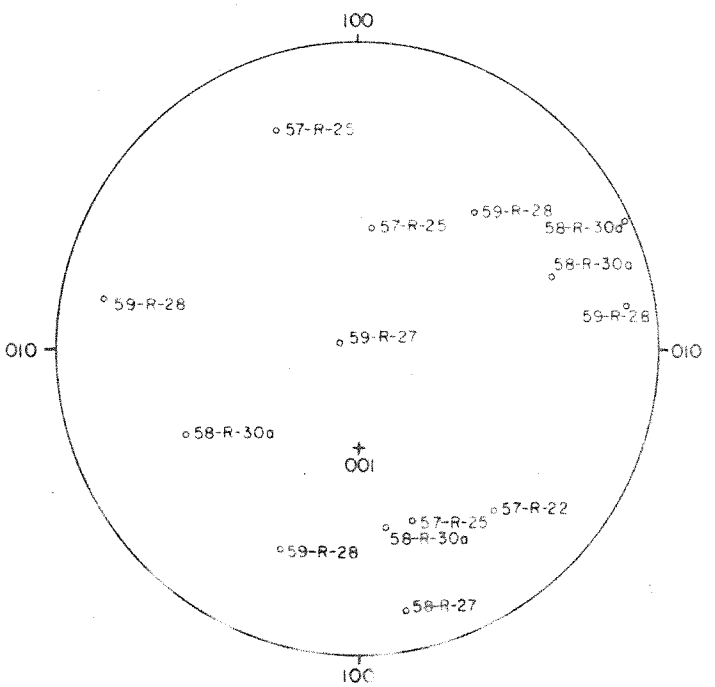

Figure 14. Plot of orientation data from thin sections of graphic granite with poorly developed graphic characters showing the points of emergence of the c axis of quartz on an equal area projection of a monoclinic potash feldspar.

of the direction of the axis of elongation with microscopic measurements of the direction of the c axis. The results of this work are shown in figure 15. There is considerable possibility for error in measurements, and for compounding errors when megascopically and microscopically oriented specimens are compared. Nevertheless, it is evident that the c axis is generally not the axis of elongation of the quartz rods.

Two of the thin sections of graphic granite each contained two differently oriented perthite crystals. From these specimens it is possible to determine whether the quartz in one feldspar is in the same optical orientation as the quartz in the adjacent feldspar. There is no shift in the orientation of the axis of elongation of the quartz rods in the two adjacent feldspars; but as pointed out in a prior paragraph, the axis of elongation is generally not the c axis of the quartz rods. The data from the orientation study of these specimens is listed in table 10. In both specimens it was found that the c axis orientation of quartz in one of the perthite crystals is unidirectional; whereas in the adjacent perthite crystal, the c axis of quartz is oriented in several directions of which one is the same as the unidirectional orientation in the adjacent perthite.

Because only the optic axis of quartz was determined, the crystals could not be uniquely oriented. However, some information on the orientation of quartz could be obtained by measuring the planes of contact between the quartz rods and the perthite host. This problem is complicated because the planes of contact may be any one of the possible crystal faces of quartz

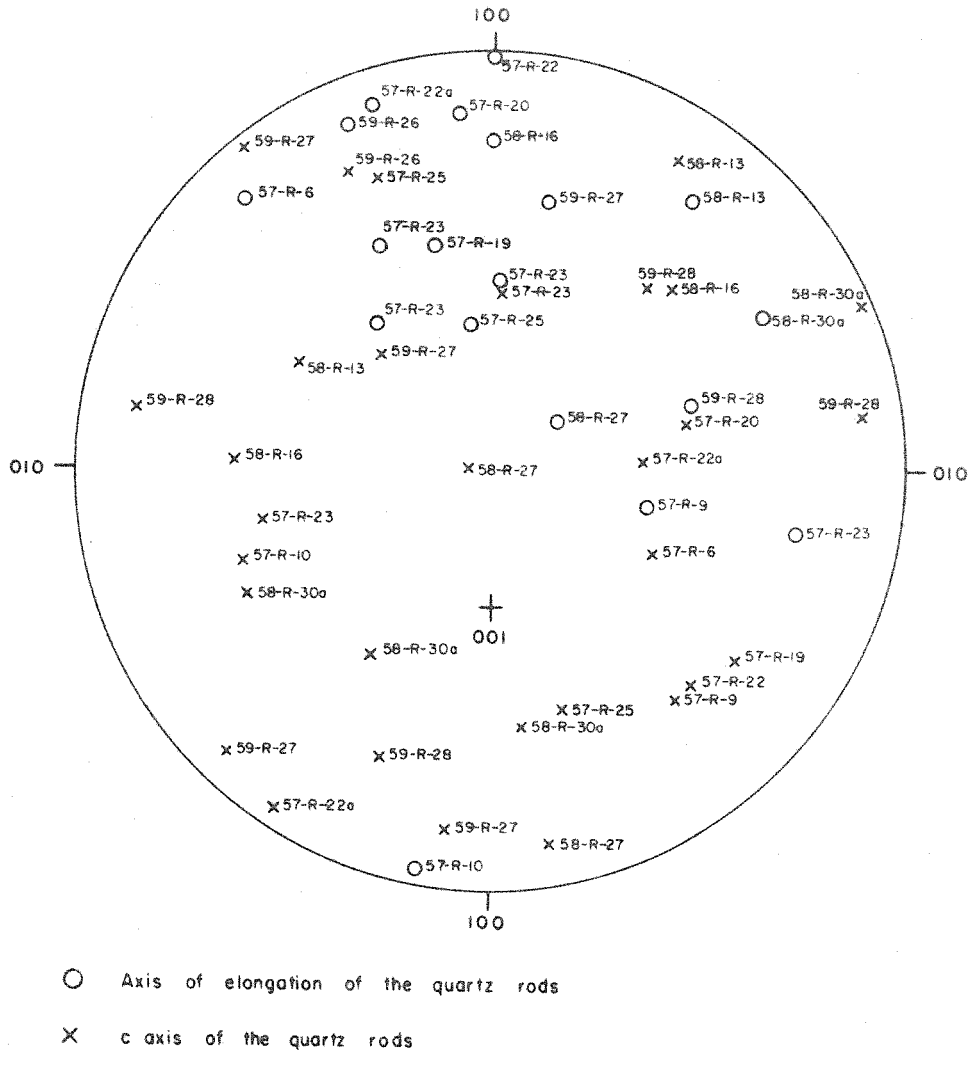

Figure 15. Orientation relationship of the c axis and axis of elongation of the quartz rods in the graphic granites from the Ramona district. The data is plotted on an equal area projection of a monoclinic potash feldspar.

TABLE 10

ROCK DESCRIPTION AND DISTRIBUTION OF c AXIS POSITIONS OF QUARTZ IN GRAPHIC GRANITE WITH TWO HOST PERTHITE CRYSTALS

Specimen Number	Distribution of c Axis Positions of Quartz in an Equal Area Projection	Number of Quartz Rods Measured	Rock Description
58-R-11 Perthite Host I	Unidirectional	8	Quartz rods about 2 mm. by 6 mm. in a host perthite crystal with a poorly developed graphic character.
Perthite Host II	Quatre-directional	29	The rock has a poorly developed graphic character with the quartz rods smaller in perthite host II than in perthite host I.
58-R-20 Perthite Host I	Bidirectional	16	Perthite host crystal with quartz rods about 2 mm. by 10 mm. and minor concentrations of tourmaline. The rock has a poorly developed graphic character.
Perthite Host II	Unidirectional	8	Perthite host crystal with quartz rods larger than in host I. This part of the rock has a poorly developed graphic character.

or perthite, or they may have no relation to the crystal structures of the minerals, or they may be related to the crystal structure but not to a possible crystal face. Specimen (57-R-23) was used for this study because there is a central area with well developed graphic characters adjacent to an outer edge where the graphic character is not well developed (see figure 10). In thin section (57-R-23-2a), with good graphic characters, most of the planes of quartz-feldspar contact are oriented so that they may be prism planes of the quartz. Also, one of these planes, probably a prism plane of the quartz, seems to nearly coincide with (010) plane of the perthite. The (001) plane of the perthite also coincides with a number of the quartz-perthite contact planes. Thin section (57-R-23-1a) from an area of the rock where the graphic characters are poorly developed has the same optical orientation of both the quartz and the perthite as thin section (57-R-23-2a), a section with well developed graphic characters. The contact planes of the quartz and perthite, in the area of the specimen with poorly developed graphic characters, do not form distinct clusters when plotted on an equal area projection. These two thin sections, one with well developed graphic characters where the contact planes are probably prism planes of the quartz and the other with poorly developed graphic characters and a scatter in the orientation of the mineral contact planes, are separated in the c axis direction of quartz by about 8 cm. One possible explanation for the features in these two sections is that the thin section with the well developed graphic character is a section

cut through the termination of the skeletal crystal of quartz. Thus the scatter of the orientations of the mineral contact plane in the thin section with poorly developed graphic characters may be because the contact planes are quartz crystal faces $\{10\bar{1}1\}$, $\{11\bar{2}1\}$, $\{51\bar{6}1\}$, and possibly $\{10\bar{1}0\}$ or perthite crystal faces (010) or (001). The explanation advanced to account for the data from this study may be applicable to other graphic granite with poorly developed graphic characters. The data from this study are shown in figure 16.

Data obtained from the study of contact planes in other specimens are summarized in table 11. In most specimens studied the contact planes of quartz cannot be given definite indices because quartz cannot be uniquely oriented by optical methods. However where many of contact planes have the same angular relation to the c axis as a crystallographic plane, the indices of the crystallographic plane are listed with a query in table 11. Common contact planes for quartz and perthite are $\{10\bar{1}1\}$?, and (001), (010) respectively.

In utilizing the data from the orientation study of the quartz-feldspar contact planes, it seems that commonly the quartz is oriented so that a plane 40 to 45 degrees from the c axis of quartz coincides with the (001) or (010) plane of the perthite. To further investigate this possibility, the angle between the c axis of quartz and the (001) axis and the (010) axis of the feldspar is plotted against frequency for all the data on the composite plot of the Ramona graphic granite. As shown in figure 17 there is a concentration of c axis positions in several

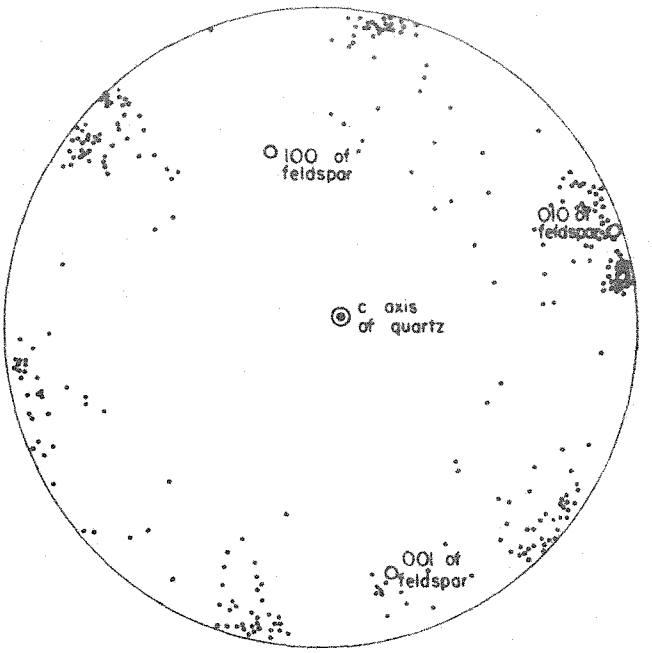

Data from thin section 57-R-23-2a

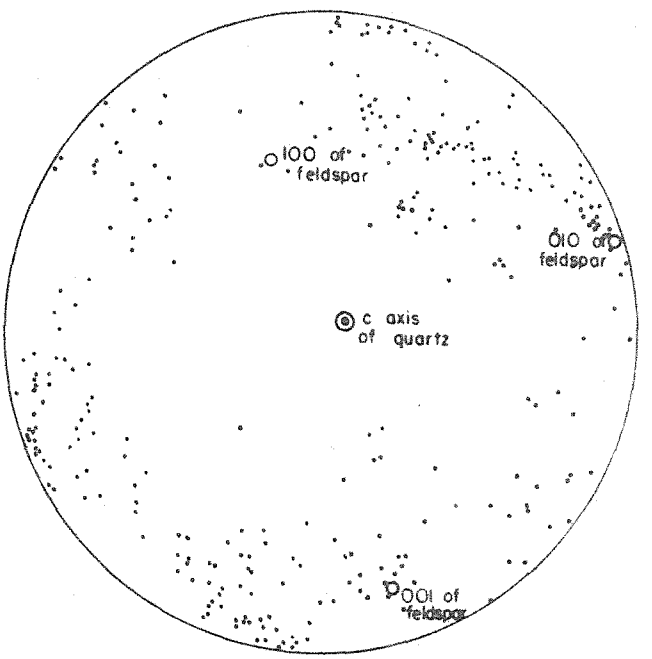

Data from thin section 57-R-23-1a

Figure 16. Equal area projection of poles to contact planes of quartz and feldspar in graphic granite specimen 57-R-23. This specimen with outlines of areas represented by thin sections is shown in figure 10.

TABLE 11

RELATIONSHIP BETWEEN THE QUARTZ-PERTHITE CONTACT PLANE AND CRYSTALLOGRAPHIC PLANES OF THE TWO MINERALS

Specimen Number	Relationship Between Quartz and Perthite
57-R-19	Perthite (001) and quartz $\{10\bar{1}1\}$? coincide forming about one half of the mineral contact planes. About one quarter of the mineral contact planes nearly coincide with (010) of the perthite and the rest are about evenly distributed in the equal area projection.
57-R-20	Mineral contact planes coincide with (001) and (010) of the perthite and $\{10\bar{1}1\}$? of the quartz.
57-R-23-1c	About 80 percent of the mineral contact planes coincide with (001) and (010) of the perthite and $\{10\bar{1}1\}$? of the quartz. The other 20 percent of the contact planes are randomly distributed in equal area projection.
58-R-18	Most of the mineral contact planes coincide with (001) and (010) of the perthite and $\{10\bar{1}1\}$ of the quartz.
59-R-26	Projection of mineral contact planes has hexagonal symmetry. One plane of this hexagonal pattern, probably quartz $\{10\bar{1}1\}$?, coincides with (001) of the perthite. Mineral contact planes near other crystallographic planes of the perthite are rare.

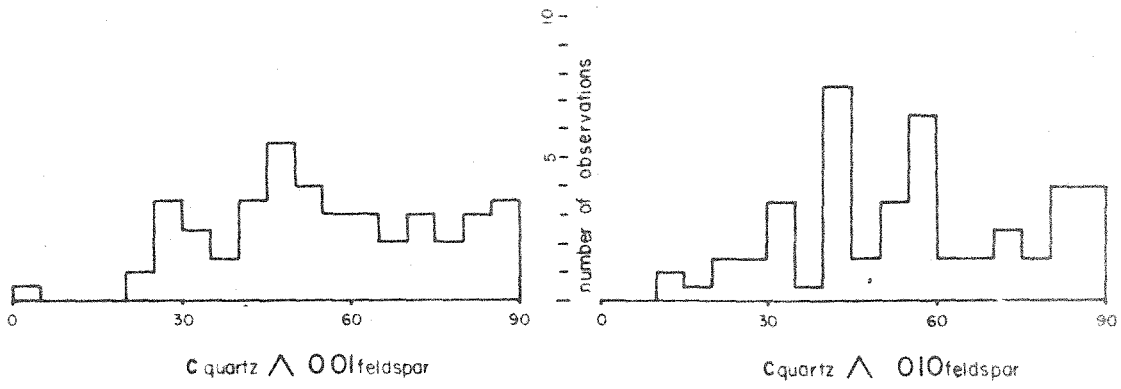

Graphic Granite from Ramona

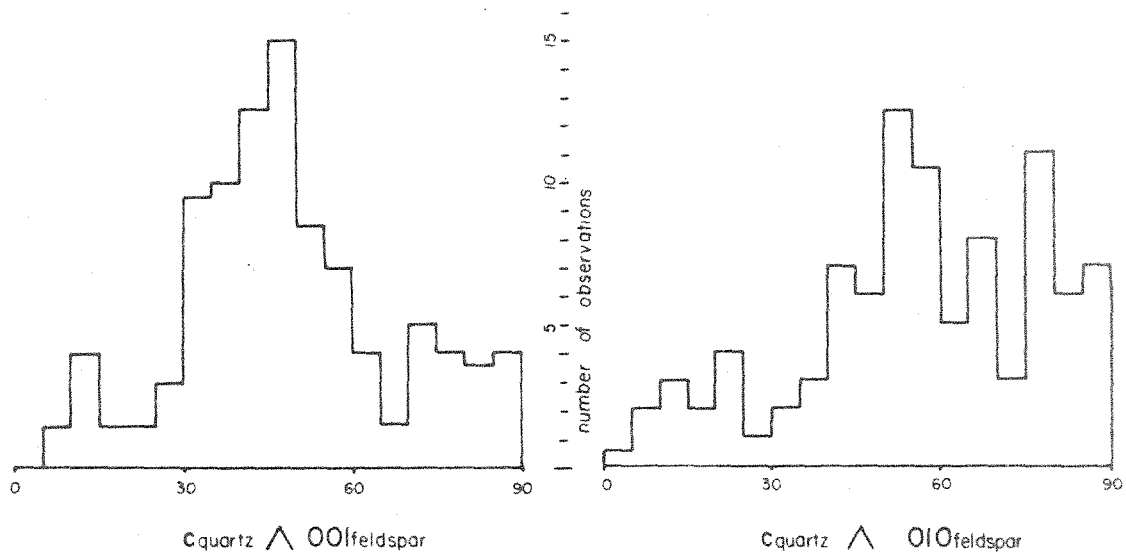

Graphic Granite Orientations shown by Wahlstrom (1939)

Figure 17. Angular relation for the c axis of quartz and crystallographic directions of the feldspar in graphic granites

areas. One concentration is found at 45 to 50 degrees from the (001) axis of the feldspar.

Wahlstrom's investigation (1939) did not show a concentration of c axis positions for quartz 42° 16' from the c axis of the feldspar, but no mention was made of attempts to find other concentrations of c axis positions for quartz. In order to investigate the possibility of other relationships, the angle between the c axis of quartz and (001) axis and (010) axis of the feldspar was measured from an equal-area projection shown by Wahlstrom. The (001) pole of the feldspar as shown in stereographic projection by Wahlstrom on an equal area projection has been relocated so that all data are consistent for an equal-area projection. Figure 17 shows the angular relationships between the c axis of quartz and (001) axis and (010) axis of the feldspar. The only significant concentration of the c axis positions for quartz is that shown at 45 to 50 degrees from (001) axis of the feldspar.

In quartz the pole to a $\{10\bar{1}1\}$ crystallographic plane make an angle of 51° 47' with the c axis. Therefore, if quartz $\{10\bar{1}1\}$ plane is coincident with the (001) plane of feldspar, the c axis of quartz would be inclined 51° 47' from (001) of feldspar. A concentration of quartz c axis positions was found at 45 to 50 degrees from (001) of the feldspar. The difference may be due entirely to observational error.

Quartz twins by reflection across the $\{11\bar{2}2\}$ plane. As Bragg (1937) points out, a number of silicon and oxygen atoms lie in this plane or close to this plane. Making an angle of

47^{o} 27' between the pole of the $\{11\bar{2}2\}$ plane and the c axis, this plane appears as a likely possibility for the quartz-feldspar contact plane, and it may well account for the c axis concentrations about 45 to 50 degrees from the (001) pole of the feldspar.

From the universal stage work it is not possible to determine whether the quartz twin planes or the quartz pyramidal faces form many of the mineral contact planes. It may be that either crystallographic plane may form the contact plane or it may be entirely circumstantial that these crystallographic planes have a similar angular relation with the c axis of quartz as the observed mineral contact plane.

The angular relationship between the c axis of quartz and a normal to the surface of the pegmatite dike was determined with four specimens of graphic granite. These specimens were first oriented in the field and then the c axis position was determined from oriented thin sections of the rocks. In these specimens the c axis direction of the quartz is not systematically related to a normal to the surface of the pegmatite dikes. A plot of the data from this study is shown in figure 18.

It is evident that the quartz rods in the graphic granites studied are not oriented by some crystallographic law, nor is their position defined by the properties of the host feldspar. One plot of the data, figure 17, suggests that quartz may statistically favor a position such that there is 45 to 50 degrees between the c axis of quartz and the (001) axis of the host feldspar. However this relationship cannot be considered a crystallographic law, because if a crystallographic law it would require specific angular relationships rather than a crude grouping of orientation directions.

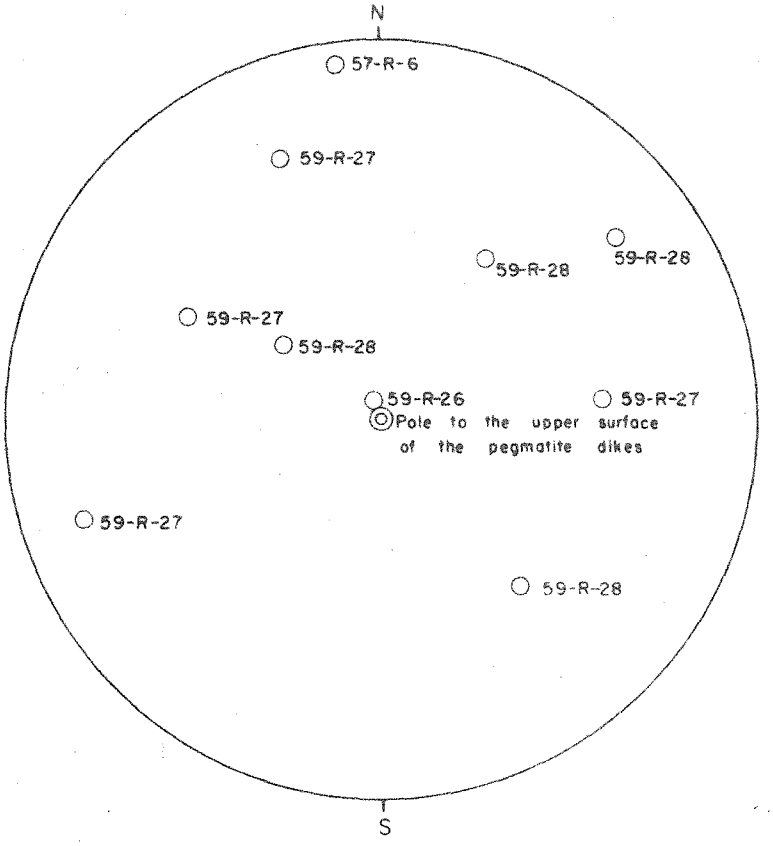

Figure 18. Equal area projection of the points of emergence of the c axis of quartz in relation to a pole to the upper surface of the pegmatite dikes.

Summary of Orientation Study

From the study of orientation relationships in graphic granite the following was found:

1. The c axis orientation of the quartz rods in a single specimen of graphic granite is most commonly unidirectional, although bi-, tri-, and quatre-directional orientations are also present in some specimens.

2. With the feldspar host crystals sharing a common orientation with each other, a plot on an equal area projection of the c axis direction of the quartz rods of all specimens does not show a fabric.

3. The graphic granites were divided into a group with well developed graphic characters and a group with poorly developed graphic characters. The data from each group were plotted in the manner described in point 2, but neither plot shows a fabric.

4. The c axis of the quartz is generally not the axis of elongation of the quartz rods.

5. Quartz rods cross perthite crystal boundaries without a change in the direction of the axis of elongation or of the c axis of the quartz rods.

6. Specimens of graphic granite with well developed graphic characters have contact planes between the quartz and perthite that are probably also prism faces for the quartz.

7. Contact planes between quartz and perthite in graphic granites with poorly developed graphic characters may also be r, z, x, or s faces for the quartz.

8. Data of all graphic granites studied from Ramona and those listed by Wahlstrom plotted with frequency against angle between the c axis of quartz and 001 of feldspar show a slight maximum for the interval 45 to 50 degrees.

9. In four specimens studied, the direction of the c axis of quartz does not have a systematic angular relationship to the surface of the pegmatite.

Connection of the Quartz Rods

Failing to find a suitable mechanism to explain the orientation of quartz rods in graphic granite, the writer investigated the possibility that the quartz rods are connected within a given host crystal of perthite. To do this a block of graphic granite was cut and a face showing good graphic character was ground flat and photographed. After this the face was reground and rephotographed. In this manner a series of photographs of the surface of a block of graphic granite were obtained, with an interval 50/1000 of an inch between surfaces of the block, mapping a 0.85 by 0.90 inch block of graphic granite to a depth of 0.8 inch.

It was found that the quartz rods branch and unite to form, within 0.8 of an inch, a pattern that is completely different from the original pattern. There is a major change in the form of the quartz rods in the 50/1000 of an inch interval, and for this reason the actual connection between the quartz rods is not always found. However, the numerous interconnections that were found clearly indicate that all the quartz rods probably represent the same quartz crystal. Figure 19 shows the first and last photographs of the sequence. Figure 20 shows a quartz rod with rather simple form developing to a complicated form and finally dividing into two simple forms, and the same figure

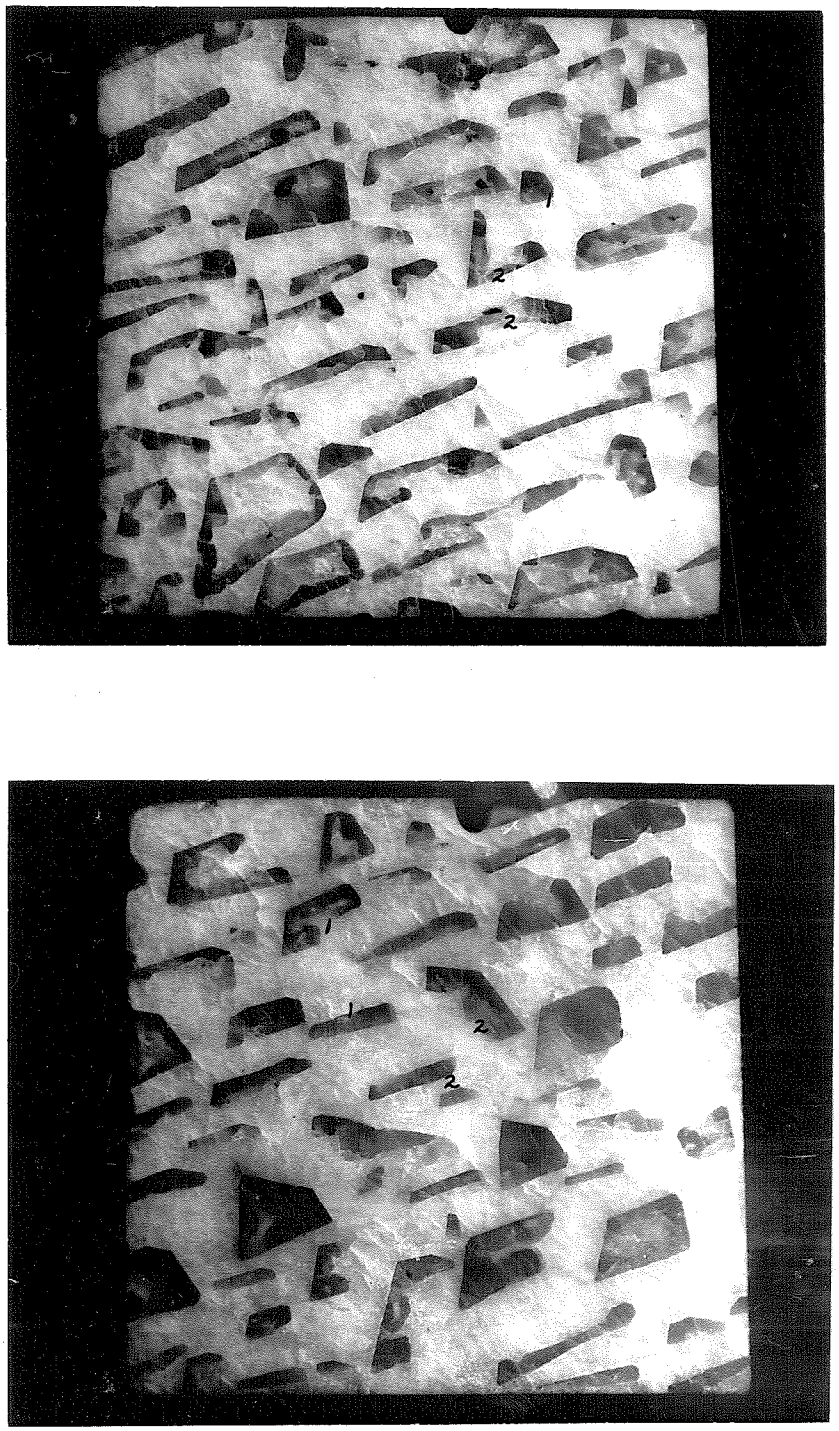

Figure 19. Surfaces of a block of graphic granite. The surfaces are separated by 0.8 inches along the axis of elongation of the quartz rod. Note rods 1 and 2 corresponding to drawing figure 20. (X4)

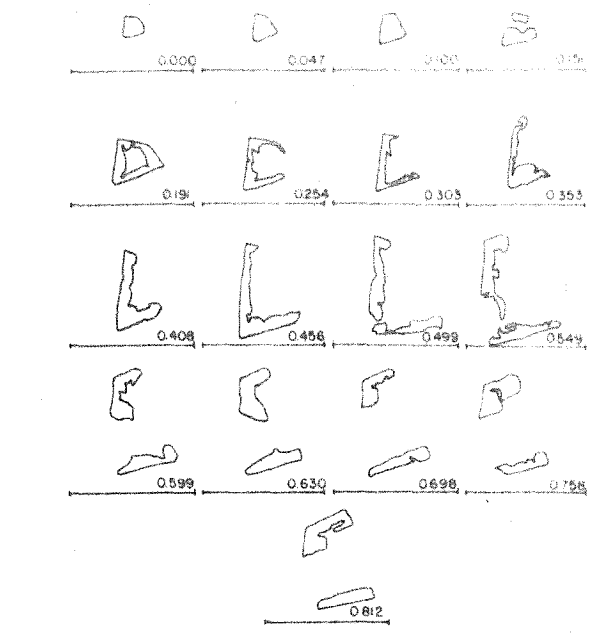

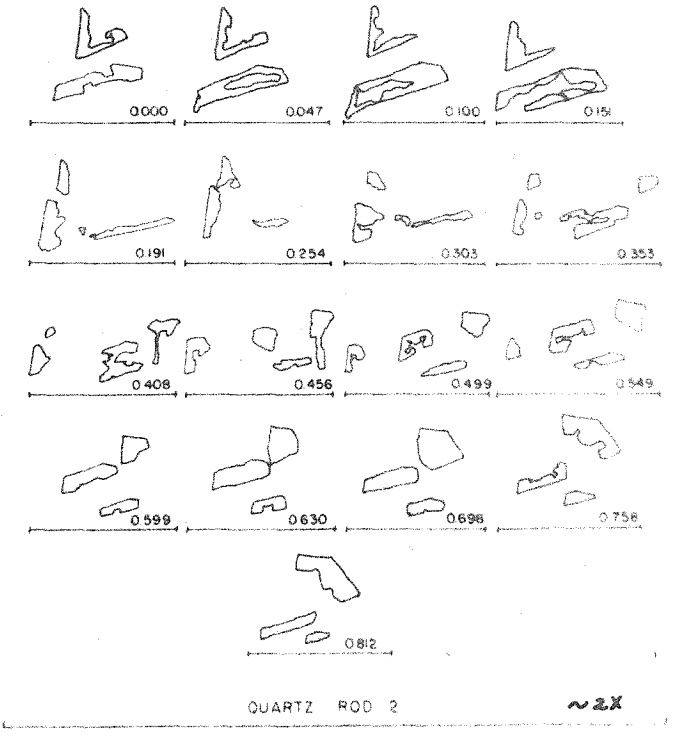

Figure 20. Sections of two quartz rods in graphic granite. Interval, in inches, between successive sections indicated by difference of numbers below sections.

also illustrates the more general case where the connection of the quartz rods is by a rather narrow passageway.

Coarse-Grained Pegmatite

A medium-to-coarse-grained variety of pegmatite rock occurs in many of the dikes. This variety of pegmatite consists mainly of quartz and perthite and has, on a large scale, a hypidiomorphic-granular texture. These rocks will be called quartz-perthite rocks instead of pegmatite so that there will be no confusion resulting from having the same name for the rock type and the rock body.

The quartz-perthite rocks are one of the major rock types in the pegmatites dikes. They occur as an inner unit in the thicker dikes and also as the only rock unit comprising the thinner dikes. Outcrops of this rock type are characterized by euhedral crystals of perthite standing out in high relief on a weathered rock surface.

A common type of this rock is mineralogically a quartz-perthite rock with minor concentration of albite, tourmaline, garnet, and muscovite. The perthite crystals mainly are in a size range of 0.1 to 6 cm. and average about 2 cm. These crystals are typically euhedral in form. Quartz, mostly interstitial to the perthite crystals, is anhedral in form and averages about 1 cm. in diameter. The quartz is commonly fractured, and consequently it is easily removed by weathering processes. Albite is sporadically distributed as subhedral to anhedral crystals about 1 to 2 cm. in diameter. On a weathered surface of

the rock, this mineral appears white to light gray with no distinctive texture in contrast to the perthite being tan and showing a perthitic texture.

Tourmaline, present in minor amounts, is conspicuous as black crystals in a white gray rock. This mineral generally is in the size range of 0.4 to 0.8 cm. in diameter by 4 to 6 cm. in length. Garnet, tan to red-brown in color, is sporadically distributed in the quartz-perthite rocks. Rarely are these garnets larger than 1 cm. in diameter. Muscovite, in books about 1 to 2 cm. in diameter by about 0.2 to 0.4 cm. thick, is present in these rocks. Although muscovite is only a minor constituent in these rocks, its presence is emphasized by its common occurrence as aggregates of books. Typically this rock has a hypidiomorphic-granular texture.

A second common type of quartz-perthite rocks is one with a porphyritic texture. The mineralogy of this rock is very similar to the rock previously described. The major difference in the rock, and the feature that results in it having a porphyritic texture, is that some perthite crystals are much larger than the other minerals. These perthite crystals that occur as phenocrysts are generally about 6 to 8 cm. in diameter with an euhedral crystal form. These phenocrysts of perthite commonly contain other minerals as quartz, tourmaline, or garnet. Quartz in the perthite phenocrysts is generally equant, but in some hosts it is rod shaped and on a fractured surface may appear with a graphic texture. Perthite is also in the groundmass of these rocks and commonly has a subhedral to anhedral crystal form.

Another common type of quartz-perthite rock contains blocks of graphic granite. The mineralogy and texture of the groundmass of this rock type may be similar to either of the prior described rocks so that the only major difference in the rock types is the presence of the blocks of graphic granite. These included blocks of graphic granite give the rock unit a gross porphyritic texture. Where best shown the blocks average about 25 cm. in length and 15 cm. in width with edges that commonly appear corroded and embayed. Mineralogically and texturally these blocks of graphic granite are similar to the typical graphic granite that occurs on the hanging wall of the dikes.

Albite-Quartz Pegmatite

Coarse crystalline albite-quartz rocks are present as fracture filling and irregular masses in the pegmatites.

The fracture fillings transect coarsely crystalline graphic granite. The mineralogical and textural contact between the two rocks is sharp and well defined by the color contrast of the perthite of the graphic granite and the light blue-green albite of the fracture fillings. Megascopically the fracture fillings consist of cleavelandite and quartz and therefore the rocks will be called cleavelandite-quartz rocks. Similar rocks, in which the albite does not have the typical cleavelandite habit, will be referred to as albite-quartz rocks.

Within the cleavelandite-quartz rocks, the quartz is anhedral in form and extremely inconstant in size, but it averages about 5 mm. in length. Roughly parallel to the graphic granite

contact, the cleavelandite-quartz rock contains a layer of euhedral to subhedral quartz crystals about 1.8 mm. in diameter by about 3.5 mm. in length. Because of large concentrations of bubbles in subparallel layers, the quartz appears fractured, but with few exceptions it shows little undulatory extinction under the microscope.

Cleavelandite, also a major mineral in the fracture-filling rocks, forms curved aggregates commonly 4 to 6 mm. in section. The smallest units in these curved aggregates are the individual cleavelandite crystals. These crystals have an average size of about 0.2 mm. in width by 0.4 mm. in length. The cleavelandite crystals have fine albite twinning and in thin section some of these twins appear distorted or bent. The individual crystals occur in platy aggregates of cleavelandite about 2 to 3 mm. in diameter. As well shown by the twin planes of the cleavelandite, there is a curvature of the individual crystals resulting in the aggregate appearing curved (see figure 21). The apparent radius of curvature may be as much as 20 degrees for the aggregates. Microlites of tourmaline and rare small crystals of garnet are present in the cleavelandite aggregates. The long axis of the microlites is not systematically related to any particular direction in the curved aggregates of cleavelandite.

Other minerals in the cleavelandite-quartz rock are microcline, muscovite, tourmaline, and garnet. The muscovite is present in minor amounts as subhedral books as much as 8 mm. in diameter. The larger books of muscovite are in areas of high concentrations of quartz. Tourmaline present in accessory

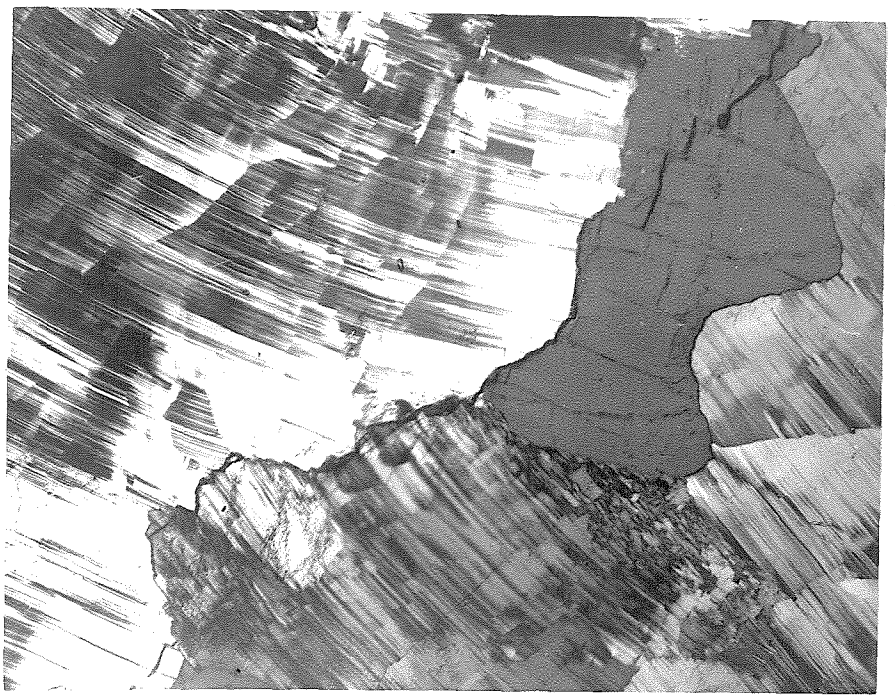

Figure 21. Cleavelandite-quartz rock. Crossed nicols, X 43. Specimen 57-R-8.

TABLE 12

MODAL ANALYSES OF ALBITE-QUARTZ ROCKS

(area of about 7 cm^2 sampled with 1000 or more points)

Specimen Number	Quartz	Potassium Feldspar	Albite	Muscovite	Tourmaline	Garnet	Total
Cleavelandite-quartz rocks occurring as fracture filling							
57-R-8-1	25.3	0.1	66.9	7.3	0.4	0.0	100.0
57-R-8-2	33.2	0.1	58.2	8.4	0.0	0.1	100.0
57-R-8-3	23.8	0.3	72.1	3.9	0.1	0.0	100.2
Albite-quartz rocks occurring as irregular masses							
57-R-15-1	35.2	1.0	62.6	0.0	0.9	0.3	100.0
57-R-15-2	22.8	0.9	69.2	0.2	3.7	3.5	100.3
57-R-16	36.5	2.5	50.7	0.1	10.3	0.0	100.1
57-R-17	35.2	1.5	50.9	0.0	12.5	0.0	99.8
57-R-26	33.6	0.9	65.2	0.0	0.2	0.0	99.9
58-R-18	28.6	3.5	64.1	0.5	2.8	0.5	100.0

concentrations is of two types. One is pleochroic from blue to a light blue-pink, whereas the other is nearly clear and shows no pleochroism. The garnet is orange-red in color and forms crystals about 8 mm. in diameter.

Albite-quartz rocks occur as irregular masses in other pegmatite zones. Microscopically some of these rocks are similar to the cleavelandite-quartz rocks, but others have a subgraphic texture and the albite does not have a cleavelandite form. Minor mineralogical differences are the following: muscovite is generally absent in the albite-quartz rocks, tourmaline (schorlite) commonly has a lighter colored internal zone or cores of quartz and feldspar, and some orange-red garnet is present.

The modes of the cleavelandite-quartz rocks and the albite-quartz rocks are listed in table 12; and figure 22 is a plot of compositions of these rocks. These rocks are about 30 percent quartz and 60 percent plagioclase.

Euhedral-Crystal Pegmatite and Pegmatite Pockets

Characteristics and Occurrence

Pockets of euhedral crystals have been found in all zones of the pegmatite. These pockets range from several mm. to about 30 cm. in diameter and are generally subspherical in shape. Quartz and cleavelandite are the most abundant minerals in these pockets although other minerals as tourmaline, topaz, and muscovite, are also present. It is primarily from the pockets that the prized pegmatite mineral specimens are collected. These

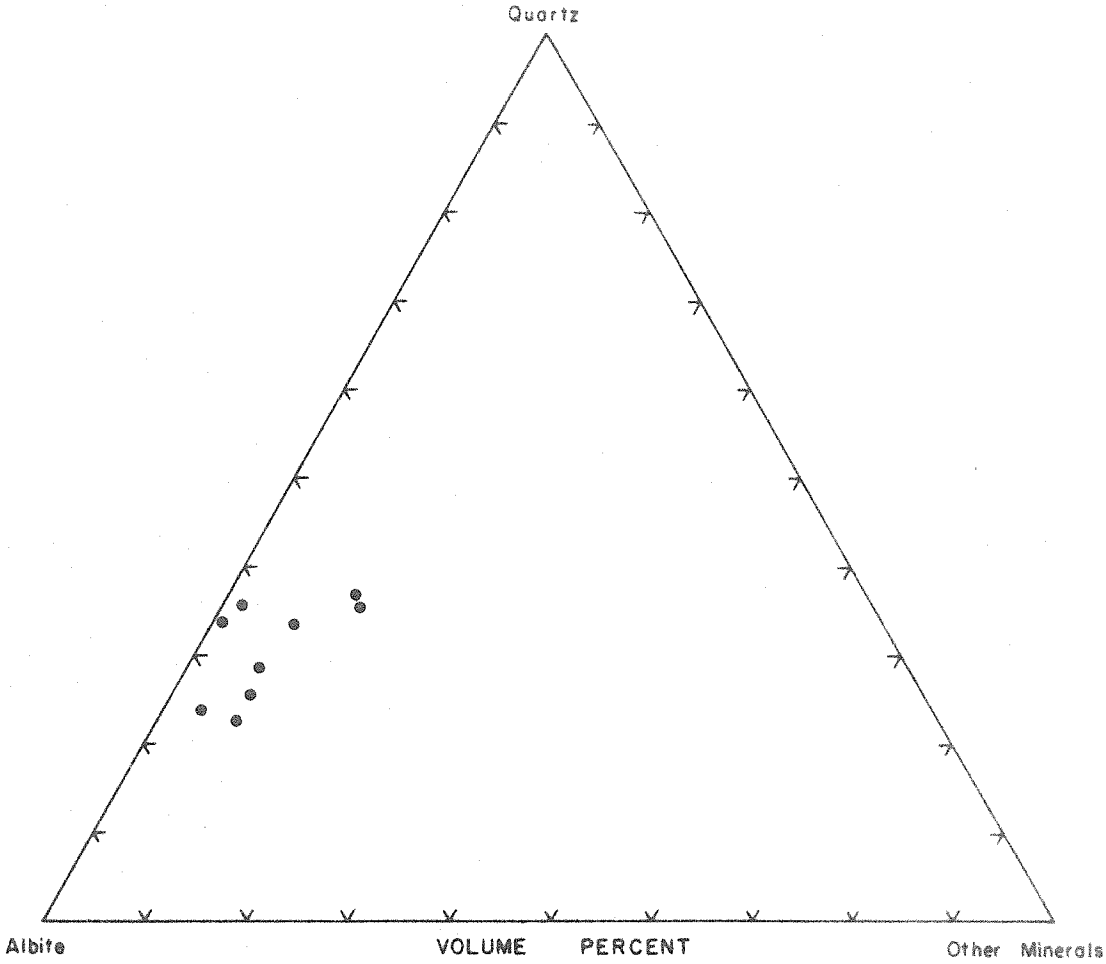

Figure 22. Volume percent relationship of quartz, albite, and other minerals in the quartz–albite rocks from the Ramona district

pockets are the largest and contain the better mineral specimens when they occur in the inner units of the pegmatite body or on the contact between the inner units and the graphic granite or the layered aplite.

Euhedral-crystal pegmatite occurs as a layer generally in or on the boundaries of the inner units of the pegmatite dikes. This layer, commonly about 8 cm. thick, is concordant with the attitude of the dike but very irregular in outline. The Little Three pegmatite contains an euhedral-crystal pegmatite layer that is several feet wide and about 6 feet long. This layer, labeled "Pocket Zone", is shown on the map of the Little Three pegmatite, plate 4 of this report. The mineralogy of this euhedral-crystal pegmatite is similar to that described for the pockets of euhedral crystals.

Because the euhedral-crystal pegmatite and the pockets of euhedral crystals differ only in form of the unit, in subsequent discussions no distinction will be made between the units and they will be termed pocket pegmatite. The term "pocket pegmatite" is particularly applicable to the cavities lined with euhedral crystals as found at the Little Three mine. However many of the so-called pockets contain little open space, being commonly filled with crystals in contact with one another, loose crystals, or clay.

It is difficult to define the limit of the pocket pegmatite because there is no distinct contact with other pegmatite rocks. For example, euhedral crystals projecting into pocket cavities commonly have an anhedral base that can not be distinguished

from anhedral crystals in an adjoining pegmatite unit. In this study the limit of the pocket pegmatite is defined as the base of those minerals with well formed crystal faces that form the walls of the pocket pegmatite.

Mineralogy and Bulk Composition

Because of the value of even an estimate of the bulk composition, three areas of the pocket pegmatite were sampled. From these samples the mineralogy is described and an estimate is made of the bulk composition of sample. In addition, a fourth sample found as float is described because it is the only sample containing light blue topaz. A more complete sampling program was not feasible because of uncertainties in determining whether material has been removed from the pockets and in defining the limits of the pocket minerals.

Sample (57-R-2) is a collection of three specimens of quartz and cleavelandite. The largest specimen is 15 cm. long by 8 to 10 cm. in diameter. Megascopically these specimens, from the euhedral-crystal pegmatite of the Little Three dike, are representative of other quartz-cleavelandite specimens from pocket pegmatites. The cleavelandite occurs as aggregates of radiating blades as much as 2 cm. in length and width by 2 mm. in thickness. Euhedral crystals of quartz about 6 cm. in diameter, commonly terminated, project from the cleavelandite aggregate. The base of the projecting quartz crystals is intergrown with the cleavelandite. Trapezohedral faces are poorly formed on the quartz, which shows a light smoky color. Many of the

crystal faces have a tan coating or are lightly frosted. A single crystal of schorlite, about 1 cm. in diameter is present on a fractured surface of one of the specimens.

A surface coating, generally about 0.5 mm. in thickness, is present on the quartz and cleavelandite. This coating appears sandy textured with a clayey cement. Under the microscope it consists of clear euhedral crystals of tourmaline, probably elbaite, cemented by minute plates of lepidolite. Commonly the tourmaline crystals are doubly terminated, reaching a maximum size of about 0.2 mm. in length by about 0.07 mm. in width. Optical and physical properties of this mineral are listed in the section on mineralogy.

The composition of sample (57-R-2) was estimated by laying a one-quarter-inch grid over the top and bottom of each of the three fragments and then point counting the minerals that fall under the cross lines. A total of more than 600 points were counted, giving a bulk composition (table 13) of about equal amounts of quartz and cleavelandite.

Sample (57-R-3) was collected from the euhedral-crystal pegmatite or pocket pegmatite of the Little Three dike about 2 feet from specimen (57-R-2). This is a collection of all of the minerals with well formed crystal faces from an area 15 to 20 cm. in diameter. It consists of two compact aggregates, one about 15 cm. and the other about 8 cm. in diameter, of quartz, cleavelandite, and tourmaline along with crystal fragments of quartz and topaz. The quartz has a very light milky to smoky color. Individual crystals of quartz range from 4 to

5 cm. in maximum dimension. The cleavelandite, present only in the aggregates, has a platy form with the plates generally about 1 mm. thick by about 1 cm. in length and width. Crystal fragments of topaz about 1 to 2 cm. in diameter are present. The good development of the {120} forms and the (001) cleavage gives the fragments a cubic appearing form. Topaz is also present in the quartz-cleavelandite aggregates as subhedral crystals. Green euhedral to subhedral crystals of tourmaline in the aggregates reach a maximum diameter of about 2 cm.

The aggregate specimens are fractured and sheared so that the quartz and tourmaline tend to break into plates. Commonly the fractures are coated with plates of pink tourmaline. In one area, a zone of deep pink tourmaline about 0.5 mm. thick is in crystallographic continuity with a green tourmaline. In contact with the pink tourmaline is an altered topaz crystal with the pink color of the tourmaline being best developed where in immediate contact with the topaz.

Because most of the specimens of sample (57-R-3) are crystal fragments, the bulk composition of the specimen was determined by weighing the fragments of each mineral. In the case of the mineral aggregates, the weight of the aggregate was obtained and this weight was divided among the volume percent of each mineral present, as determined by counting the minerals under the intersecting grid lines. The results of the composition measurements, listed in table 13, show the pocket minerals to be mostly quartz with a minor amount of cleavelandite.

Specimen (57-R-9) is a collection of most of the euhedral crystals projecting into a cavity about 15 cm. in diameter. This pocket occurs just below the graphic granite on the northwest cut of the Little Three mine. The pocket, when uncovered by the mining operation, did not contain a clay filling; however it is possible that a clay filling had been present but washed away by ground water prior to the pocket being uncovered. Mineralogically the pocket is mostly smoky quartz in crystals 4 to 6 cm. in diameter and length, respectively. The smoky color of the quartz increases in depth, with a few exceptions, from the core of the crystal to the crystal faces and especially toward the upper termination of the crystal. Cleavelandite is present in crystals reaching a maximum length and width of about 2 cm. and a thickness of 2 or 3 mm. Some cleavelandite plates show a marked curvature.

Several crystals of colorless topaz averaging about 1 cm. in diameter by 2 cm. in length are present. With the exception of the clear topaz all crystal fragments are partly coated with a brown-tan porcelaneous layer. Microscopically this coating was found to be two different micas and a clay. The micas have respectively the optical properties of lepidolite and of muscovite, but the clay mineral could not be identified microscopically. Pink and green tourmaline also is embedded in the coating, and the largest crystals are about 2 mm. in length by 6 mm. in diameter.

The bulk composition of the pocket material (57-R-9) was obtained by weighing the crystal fragments of each mineral. Where two minerals occurred together, their respective volumes were estimated and the weights adjusted accordingly. The modal

composition is listed in table 13.

Table 13

Approximate Bulk Composition of Samples of Pocket Pegmatite

Specimen Number	Quartz	Cleavelandite	Tourmaline	Topaz
57-R-2	43	57	1	
57-R-3	80	13	2	5
57-R-4	66	24	9	1
57-R-9	94	4	tr.	2

Specimen (57-R-7a), containing blue topaz, is predominantly a cleavelandite-tourmaline rock. One part of the specimen shows good euhedral faces of cleavelandite with no other minerals interstitial to the plates of feldspar. The largest blue topaz crystal, about 2 cm. in diameter, is near this area of cleavelandite, and smaller blue topaz crystals are scattered through the specimen. The tourmaline is mostly black or dark green, grading in part to a pink. In one crystal fragment, lepidolite appears to have replaced dark green tourmaline. The mineralogical composition of specimen (57-R-7a) was not determined because the specimen was collected from a mine dump as a matrix specimen for blue topaz and not as a representative sample of pocket pegmatite.

In considering the mineralogy and composition of the pocket pegmatite several features are immediately evident. First, quartz is present in unusually high concentrations. Second, potassium bearing minerals such as muscovite and potassium feldspar are rare or absent. And third, some unusual

minerals such as topaz are present.

Corrosion and Secondary Mineralization

Nature and Sequence of Corrosion

A suite of cavernous feldspar rocks containing little or no quartz was collected from Spessartite Ledge. Because some of the rocks are white crenulated masses of cleavelandite, the rocks are locally called "cottonball spar" and are accepted by the miners as a field indication of spessartite mineralization. Good examples of the cavernous or corroded rocks are found in all zones of the pegmatite except the layered aplite. The attitude of the area of corrosion is not concordant with the attitude of zones in the pegmatite as is clearly shown at Spessartite Ledge. Because of this discordant attitude and veining relationships, the period of corrosion is regarded as being later than the period of formation of the pegmatite zones.

Megascopically these corroded rocks can be divided into three general categories. The first corroded rocks to be considered are ones similar to graphic granite but with voids instead of quartz rods. In these rocks the feldspar appears fresh with good reflecting cleavage surfaces that commonly show a perthitic structure. Tourmaline is commonly present in the feldspar of these rocks. This mineral occurs as well formed crystals with a black vitreous luster that reaches a maximum size of about 2 cm. On a cut surface some of the larger tourmaline crystals show a yellow border zone. In the graphic or rod shaped holes there is generally a red-brown clay-like coating. Small terminated quartz crystals are also rarely found in the holes. The

rock is best characterized as a relic graphic granite.

The second corroded rocks to be considered are blue-white cleavelandite rocks with a cockscomb structure. Tourmaline, rarely present in these rocks, is black with a vitreous luster. There is a light tan iron stain on the rocks; however, the red-brown clay-like coating so common in the holes of the relic graphic granite is generally absent in these corroded cleavelandite rocks.

The third corroded rocks to be considered are relic euhedral perthite crystals. Crystal faces and fracture surfaces have a fin-like appearance caused by thin blades of feldspar projecting beyond less corroded parts of the crystals. Some faces of these crystals are sufficiently preserved so that light reflections can be obtained from the surface. Holes in the perthite crystals that were probably former sites for quartz rods are armored with white albite. These relic perthite crystals have a tan-brown iron stain color. Typical examples of the three general types of corroded rocks are shown in figure 23.

An examination of these rocks under the microscope shows that there is a suite of minerals that crystallized in the corrosion cavities of the rock. These minerals are termed "secondary minerals" in this report to distinguish them from minerals originally present in the rock, or "primary minerals". It is difficult to determine the sequence of removal of minerals and of secondary mineralization because the same mineral species occur as primary and secondary crystals. Furthermore, there may have

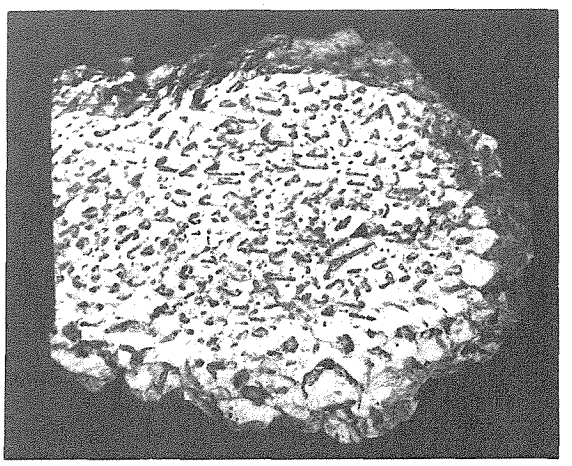

Corroded Graphic Granite

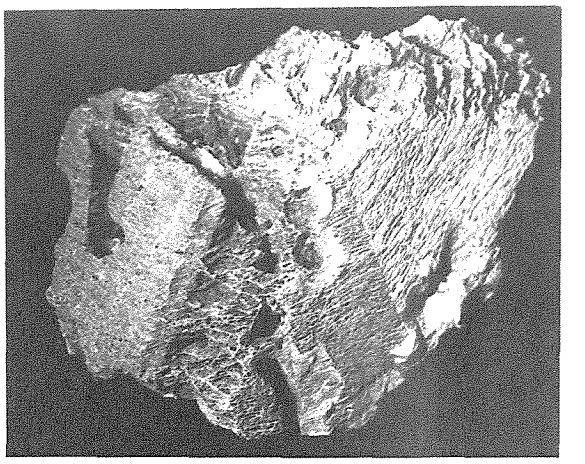

Corroded — Twinned Perthite

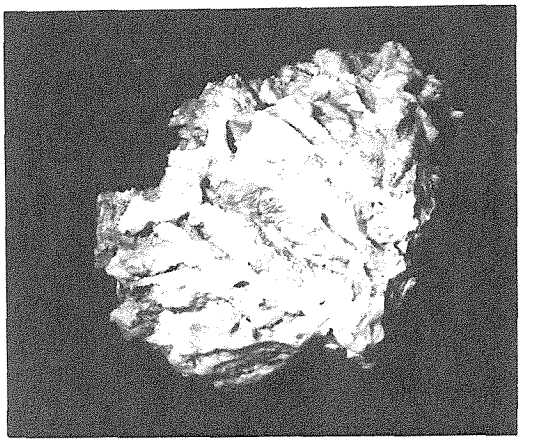

Corroded Cleavelandite Rock

1 inch

Figure 23. Corroded rocks from Spessartite Ledge

been considerable overlap in the periods of corrosion and deposition of the different minerals. Because of these complications the microscopic descriptions will be directed toward an understanding of the points on which the sequence of events was determined rather than a detailed description of the many rocks studied.

Attention will be first focused on establishing the sequence of events during corrosion of the rocks. The mineral most conspicuous by its absence is quartz. However, quartz was found in several specimens of relic graphic granite. This quartz generally does not fill the cavity in which it occurs, and it has commonly been found as terminated or doubly terminated crystals in the cavity. In thin section the quartz occurs as subhedral to euhedral crystals without undulatory extinction. On the basis of the well developed crystal form, the incomplete filling of the cavity, and the absence of undulatory extinction, this type of quartz in the corroded rocks is considered to be secondary.

Several specimens of perthite with good microcline twinning are found partially corroded. In all occurrences it is found that the microcline was corroded in preference to or at a greater rate than the albite. The absence of signs of corrosion of the albite in the cleavelandite rocks indicates that albite was probably stable during the corrosion period.

In the perthite rocks the quartz was completely removed before there was corrosion of the feldspar. During corrosion of the feldspar the microcline is removed in preference or at

a greater rate than the albite. This suggests that the sequence of removal of material from the rock is quartz, microcline, and albite. Figure 24 illustrates the corrosion features mentioned.

Nature and Sequence of Secondary Mineralization

In the most distinctive occurrences, the secondary albite is coarsely twinned or untwinned and occurs roughly perpendicular to the exsolution lamella of the host perthite. Some of this secondary albite is in optical continuity with one of the albite twin sets in the perthite host. A good example of this veining relationship is shown in figure 25. Secondary albite also occurs as euhedral crystals projecting into sites of former quartz rods as shown in figure 26.

Secondary potassium feldspar has a habit that is the result of the dominance of the (110) faces with the resulting crystal appearing diamond shaped in section. When intergrown, the crystals generally appear bladed. The secondary potassium feldspar commonly occurs as an untwinned overgrowth having a bladed habit on primary potassium feldspar with grid-iron twinning. The overgrowth characteristics of this secondary feldspar is also shown in figure 26, and the bladed habit of the mineral is shown in figure 27.

Secondary quartz, present as euhedral crystals, some being doubly terminated, occurs in cavities of the corroded rocks. These crystals of quartz have a maximum length of about 4 mm. and an average length of about 2 mm. Under the

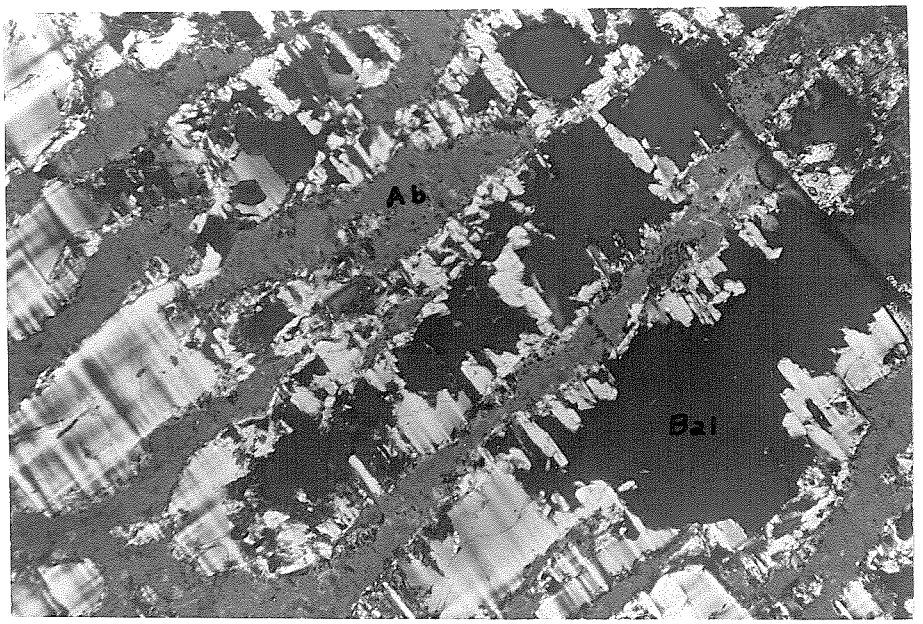

Figure 24. Corroded perthite crystal. Cross nicols, X 43. Note that microcline was corroded in preference to or at a greater rate than albite. Specimen 59-R-34.

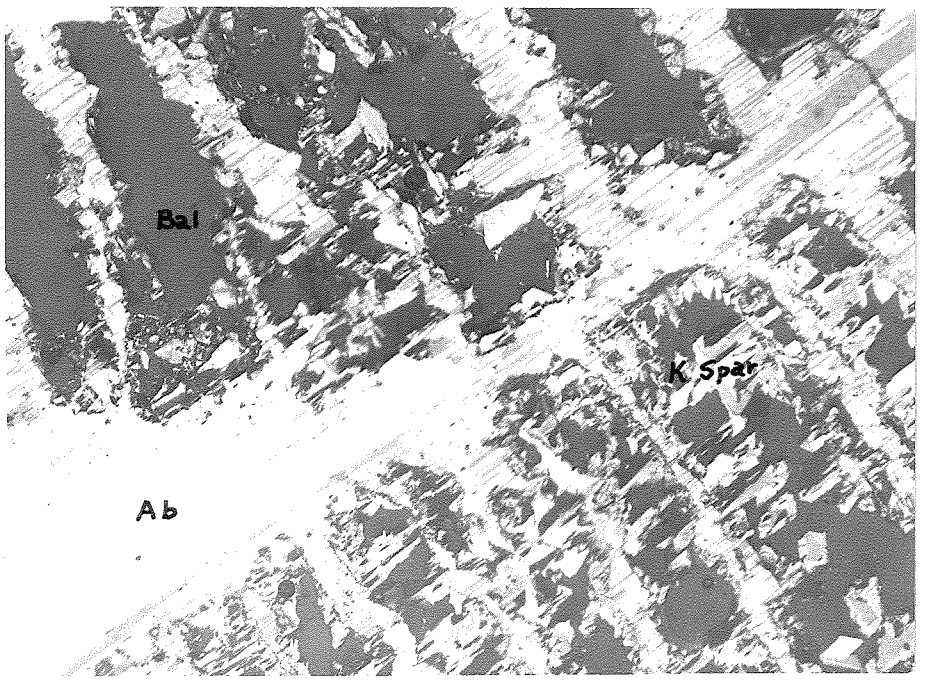

Figure 25. Secondary albite veining corroded perthite. Cross nicols, X 43. Specimen 59-R-34.

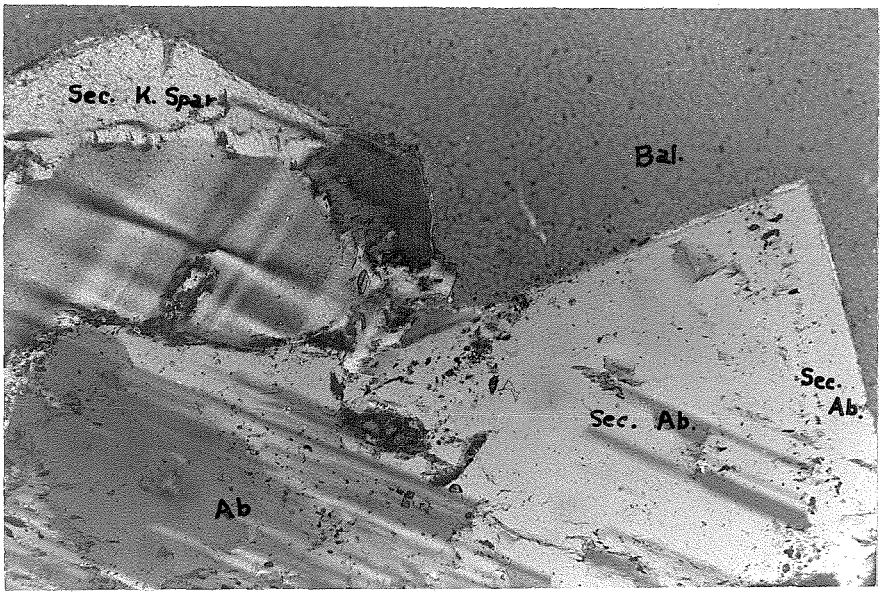

Figure 26. Secondary albite and potassium feldspar overgrows. Cross nicols, X 100. Specimen 59-R-37.

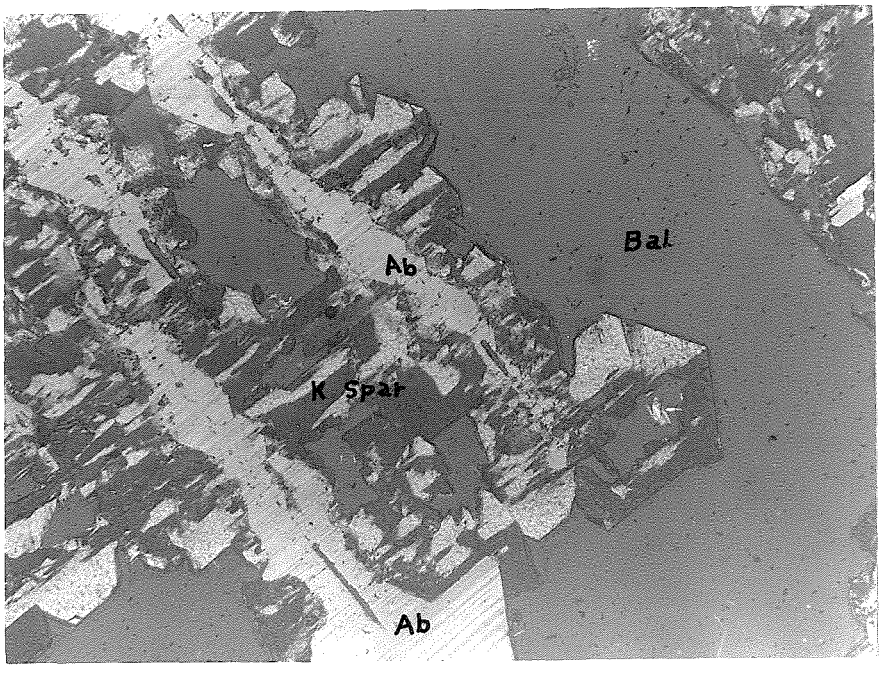

Figure 27. Secondary potassium feldspar with adularia habit. Crossed nicols, X 100. Specimen 59-R-34.

microscope these crystals of quartz do not show undulatory extinction.

The secondary tourmaline occurs as elongate euhedral needles that are pleochroic in thin section from a green-blue to nearly colorless. These needles occur in a large range of sizes; their average diameter is somewhat less than 0.5 mm. and average length about 1 cm. The needles are generally unfractured.

The primary tourmaline in the corroded rocks is equant to elongate and commonly has a color zonation. Where the color zonation is best developed, the core of the tourmaline is pleochroic from dark blue to pale violet, the intermediate zone is pleochroic from various shades of a greenish-yellow-brown to nearly colorless, and the outer zone is pleochroic from a dark blue with a green tinge to nearly colorless. The primary tourmaline is generally fractured, and the intermediate and outer zones commonly enclose or are intergrown with secondary feldspar.

It is in the corroded rocks that spessartite garnet is found. Megascopically this garnet can be recognized by its light orange-red color, as contrasted with the red-brown almanditic garnet commonly present in the pegmatite. Unfortunately the distinction between these species cannot be made under the microscope.

Before a sequence of deposition of these secondary minerals could be determined it was necessary to establish criteria that could be used for distinguishing between primary and secondary minerals. The occurrence of minerals as overgrowths

or veining other minerals was the best criterion that there are two generations of minerals, and that the secondary minerals have habits, forms, and for some colors that are different from the primary minerals. Therefore, when applicable, the habit, form, and color of the minerals was also used as criteria for distinguishing between primary and secondary minerals.

Secondary albite veins and truncates elongate cavities in the corroded perthite host, as shown in figure 25. Secondary potassium feldspar crystals have been deposited at the base of the cavities against the secondary albite veins. Rarely cavities are found containing crystals of secondary albite with an overgrowth of secondary potassium feldspar. These relationships indicate that the secondary albite mineralization was prior to the secondary potassium feldspar mineralization.

The relationship between secondary quartz and secondary feldspars is not well defined. Figure 28 shows secondary potassium feldspar on the edges of a cavity partially filled with quartz. This indicates that potassium feldspar crystallized prior to the quartz. Rarely euhedral quartz crystals are found perched on euhedral feldspar crystals. This overgrowth confirms the suggestion that the potassium feldspar crystallized prior to the quartz.

The primary tourmaline probably crystallized during the period of crystallization of the primary quartz and feldspar. However, the intermediate and outer zones of these tourmaline crystals appear to have undergone a later alteration. The period

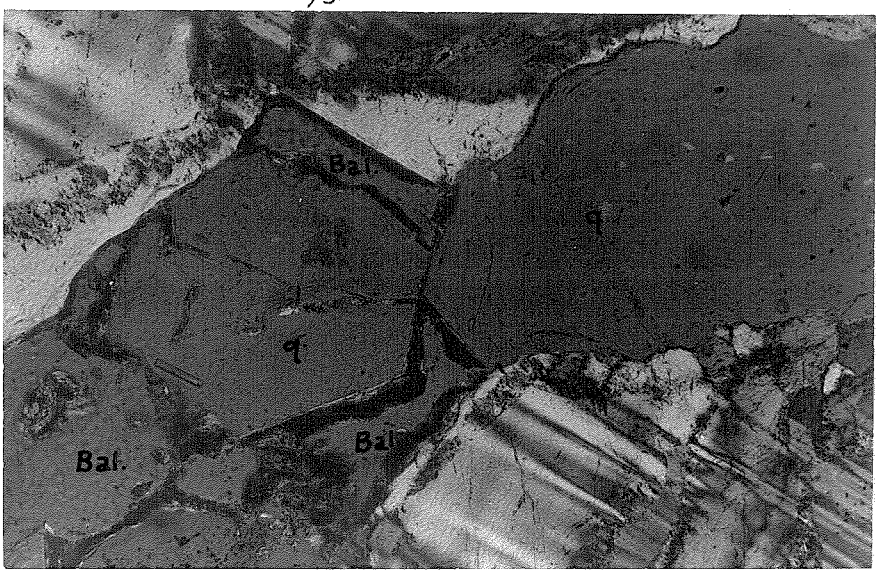

Figure 28. Euhedral quartz in cavity of corroded graphic granite. Cross nicols, X 100. Note that the cavity is partially rimmed with secondary potassium feldspar. Specimen 59-R-7d.

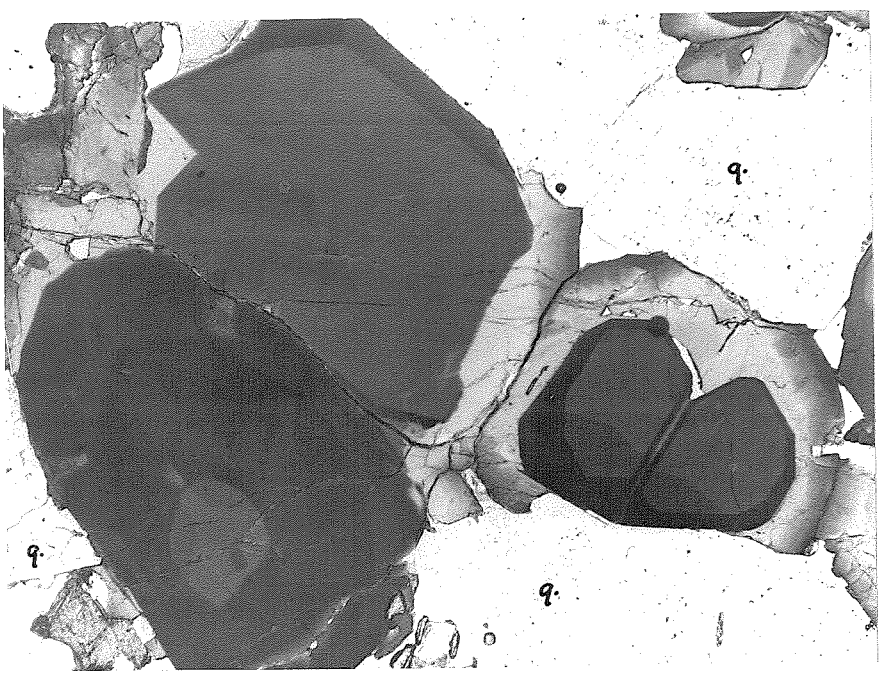

Figure 29. Tourmaline showing dark core and lighter rim. X 43. Note that rim does not completely enclose the core. Specimen 59-R-31.

of the alteration can not be precisely determined; however fractures and inclusions in the tourmaline indicate that at least some of the color zonation was developed earlier than the secondary albite mineralization. The reason being that the color zonation of the tourmaline occurs on the periphery of the crystals, but the color zone does not occur on fractured surfaces. This indicates that the fractured surface did not exist during the period that the color zonation developed. Secondary albite is present in some of the fractures and outer zones of the tourmaline crystals substantiating the sequence indicated. The properties of the individual zones of the tourmaline crystals are listed in the section on mineralogy, and a typical example of the zonation is shown in figure 29.

The secondary tourmaline generally occurs in a brecciated fine-grained vein or cavity filling material that characteristically consists of fragments of feldspar, mostly albite, and tourmaline. The angular fragments of feldspar and tourmaline, averaging about 0.03 mm. in maximum dimension, along with euhedral needles of tourmaline, about 0.1 mm. in length by 0.003 mm. in width, indicate that the rock has been granulated and later mineralized.

A distinction between spessartite and almandite garnet cannot be made by a microscopic examination of thin sections. For this reason textural relationships found in thin sections containing garnets cannot be used in determining the position of the spessartite garnet in the paragenetic sequence. Specimen (59-R-37) has both secondary albite and potassium feldspar. Spessartite garnet is also present in this specimen; however, in no place is

the garnet perched on what appears to be euhedral secondary feldspars. Rather, the euhedral feldspar appears to be enclosing the spessartite garnet. On this basis and because the spessartite occurs in corrosion cavities, it is thought to have crystallized after corrosion and before remineralization of the feldspars. Spessartite also is embedded in fractures in the large zoned crystals of tourmaline, indicating that this garnet crystallized after the zonation and fracturing of the tourmaline.

The entire sequence of corrosion and secondary mineralization is shown diagramatically in figure 30. The length of the horizontal lines is not correlative with the duration of the events. A solid horizontal line indicates the most probable sequence, whereas a dashed line with queries indicates a possible but less likely sequence.

Altered Rocks and Minerals Not Related To Pegmatite Zones

Distribution, Occurrence, and General Features

From the Little Three mine two samples were collected that show extensive alteration of tourmaline and of another mineral, probably garnet. Some of the specimens show alteration to a manganese oxide while in the other specimens the alteration is to a mica. Both samples were collected from the hanging wall of the pegmatite; however, the distribution of samples was so restricted that it was impossible to delimit a zone of alteration.

Figure 30

SEQUENCE OF CORROSION AND SECONDARY MINERALIZATION

Corrosion and Alteration	Secondary Mineralization
(-)Quartz ?	Quartz
(-)Microcline	? Potassium Feldspar var. Adularia
(-)Albite ? ?	Albite
	Spessartite garnet
Zonation of the Tourmaline ? ? ?	Secondary ? Tourmaline

Mineral Alteration To Manganese Oxides

In two specimens a massive submetallic to earthy lustered mineral was found. The mineral has a hardness greater than fluorite, a black streak, and gives a strong positive test for manganese. On this basis, the mineral has been identified as pyrolusite or one of the hydrated manganese oxides. This mineral is in masses 2 to 3 cm. in diameter and appears to be pseudomorphous after garnet. As shown in figure 31, a black to brown halo surrounds the pseudomorphic mineral. In thin section this halo is found to be cleavages and fractures in quartz and feldspar impregnated with a brown to black mineral that is translucent in very thin plates. This impregnating mineral has also been identified as pyrolusite or a hydrated manganese oxide.

Also in the rock specimens are small crystals of tan garnet, dark green and black tourmaline, and muscovite. Several small crystals of lepidolite and pink tourmaline are adjacent to the pseudomorphic mineral. Even though the quartz and feldspar matrix is pervasively fractured and sheared, there is little undulatory extinction in the quartz. In some specimens there is some weathering of the feldspars, but the tourmaline and garnet appear unaltered.

In specimen (57-R-26) tan-brown garnet is rimmed with black manganese oxide and minute crystals of lepidolite. Also in this specimen are euhedral plates of cleavelandite, green tourmaline, and quartz. Late alteration of the garnet is indicated by manganese staining of the cleavelandite and tourmaline.

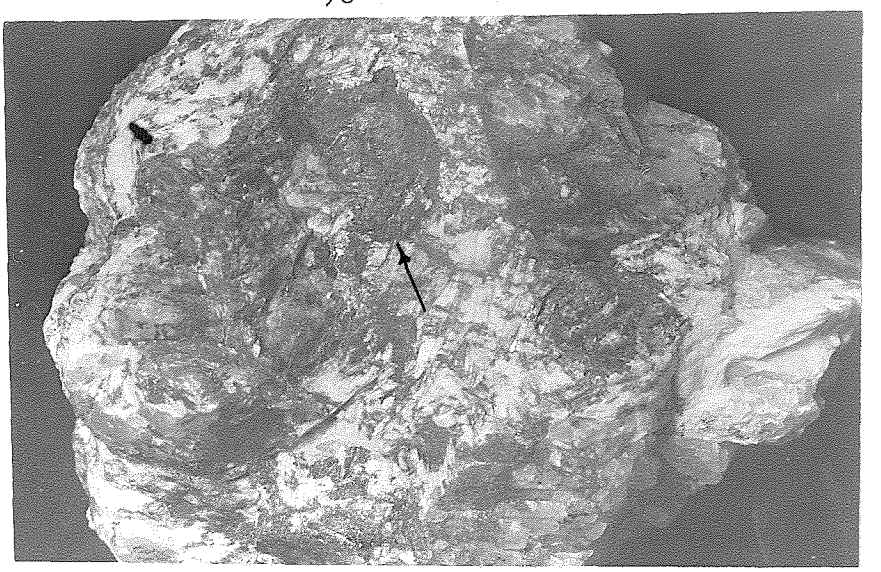

Figure 31. Manganese oxide pseudomorph after garnet (?) in a cleavelandite matrix. Natural size.

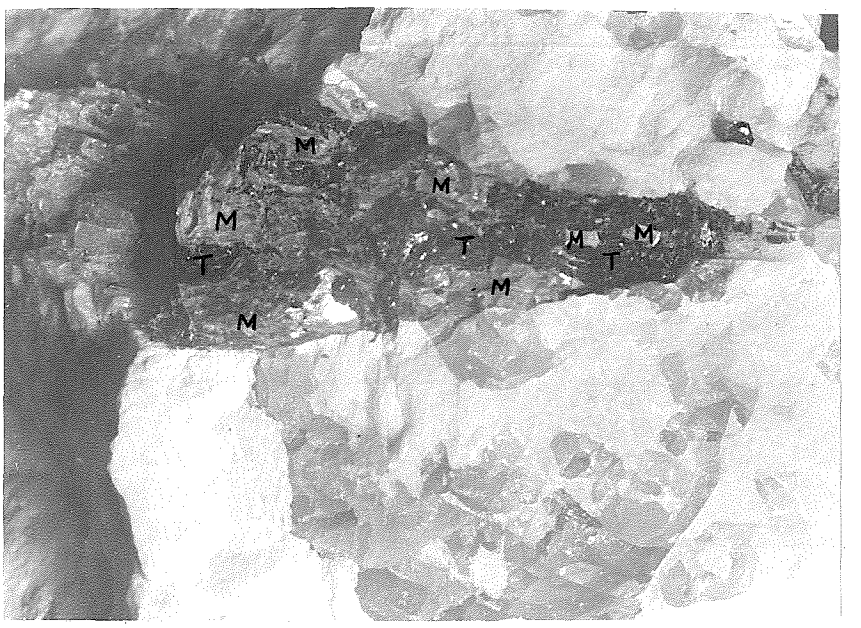

Figure 32. Tourmaline partially altered to muscovite. X 2.

Because of the limited occurrence of this garnet alteration, it is not possible to relate it to the corroded and mineralized rocks at Spessartite Ledge.

Alteration of Tourmaline To Muscovite

Two specimens were found in which tourmaline is partly altered to green muscovite. One was collected from the lower Little Three prospect, and the other from a dump adjacent to this prospect. Both specimens are coarsely crystalline, in part graphic textured, rocks in which quartz, perthite, and albite are the major minerals. Other minerals present are tan to red-brown garnet, tourmaline, and muscovite. The garnet is in the matrix of the specimens and commonly in the proximity of the tourmaline. In one area garnet is embedded in unaltered tourmaline, thus indicating that this garnet is probably not an alteration product of the tourmaline. Typical relationships are shown in figure 32.

Light blue albite and quartz occur as irregular masses and as veins in the perthite. The altered tourmaline is at least partly enclosed but not veined with these masses of albite and quartz. Consequently the black tourmaline is considered to have crystallized earlier or contemporaneous with the albite and quartz.

Microscopically no evidence was found to indicate an intermediate alteration product or other minerals being formed as a result of the alteration of tourmaline to muscovite. Generally the muscovite occurs as books approximately 4 mm. in

diameter, and it partially fills the cavity left by the removal of tourmaline. The crystal structure of the tourmaline had no apparent control on the orientation of the muscovite. Because of the presence of open cavities and the lack of other alteration minerals, it is concluded that material has been removed from the system, but there is no indication of where this material has been deposited. The properties and compositions of some of the minerals in the altered rocks are listed in the section on mineralogy.

These altered rocks clearly indicate that there has been a period of alteration different in nature from the period of corrosion and secondary mineralization at Spessartite Ledge; however, it is not possible to determine the time relation between the two periods of alteration.

IV. MINERALOGY AND BULK MINERALOGICAL COMPOSITION OF THE PEGMATITES

Mineralogy

General Features

It is not the purpose of this study to discuss in detail all of the minerals of the Ramona pegmatites. Instead, attention is directed toward those minerals from which information can be obtained concerning the genesis of the pegmatite.

In comparison to the Pala and Mesa Grande pegmatites, the mineralogy of the Ramona pegmatites is exceedingly simple. The minerals noted and recorded from the Ramona pegmatites are listed in table 14. The most abundant and widespread minerals in these pegmatites are quartz, microcline, and albite.

Principal Minerals

QUARTZ. Quartz is present in all the pegmatite units. It ranges in size from microscopic crystals to rods and plates about 20 cm. long. The quartz is present as spindles, rods, plates, masses with irregular forms, and also euhedral crystals. The euhedral crystals of quartz in the pocket pegmatite are generally 3 to 5 cm. in diameter. In hand specimen, the quartz in a matrix of other minerals is clear to milky-white translucent, whereas the euhedral crystals of quartz from the pockets are generally smoky.

Fluid inclusions present in the quartz are extremely minute. Inclusion thermometry was attempted by measuring the diameters of the fluid cavity and of its contained bubble, but

TABLE 14

LIST OF MINERALS IN PEGMATITES OF THE RAMONA DISTRICT

Mineral	Abundant and Widespread	Common	Rare	Rare and Found Only in Dumps
Albite (including cleavelandite)	X			
Beryl*			X	
Biotite			X	
Columbite-tantalite				X
Garnet		X		
Hambergite				X
Lepidolite			X	
Manganese oxide (Psilomelane)			X	
Microcline	X			
Muscovite		X		
Orthoclase (Andularia habit			X	
Quartz	X			
Topaz			X	
Tourmaline		X		

*Reported by Kunz (1903) and by Spaulding (personal communication)

it was found that the bubbles are too small to permit reproducible measurements.

ALBITE. Albite is abundant in the pegmatite rocks as small equant crystals, exsolution lamella in the perthite, and tabular crystals.

The equant crystals of albite occur in the layered aplite. By measurement of the indices of refraction and the angles between the extinction position and the (001) and (010) cleavage direction, it is found that an average composition of this albite is Ab_{93} An_7 with a composition range of Ab_{97} An_3 to Ab_{91} An_9. Typically this feldspar shows albite twinning and some pericline twinning.

Albite that occurs as exsolution lamellae in the perthite crystals commonly shows albite twinning, but pericline twinning is absent. Alteration of the perthite is found mostly along contacts between the albite phase and the microcline phase.

White euhedral albite, variety cleavelandite, is present in the late forming zones and other units of the pegmatite. Indices of refraction and angles between the optical extinction and the cleavage directions indicate that these crystals are almost pure albite. An x-ray determination of one sample (57-R-8) shows the separation of (131)-$(1\bar{3}1)$ reflection to be 1.06° 2θ; thus indicating that the cleavelandite is low-temperature albite. This mineral either crystallized as the low temperature form or has inverted to the low temperature polymorph subsequent to its formation.

The cleavelandite forms platy crystals as much as 3 mm. thick by about 2 cm. in length and 1 cm. in width, but the average sized cleavelandite plate is about one half as large. Many individual plates of the cleavelandite are warped or bent. The reason for this curvature of the cleavelandite crystals is not known. The mineral typically has albite twinning, and it may have other forms of twinning. In comparison to the other albite in the pegmatites, the cleavelandite is exceptionally fresh.

Table 15 lists the optical properties and mode of occurrence for representative samples of the albite. All samples studied are within the albite composition range except one sample of pegmatite feldspar collected about 1 cm. from the Lakeview Mountain tonalite.

MICROCLINE AND ORTHOCLASE. Microcline is one of the most abundant minerals in the pegmatites. In crystal size it ranges from less than 1 mm. to more than 30 cm. with the large crystals characteristically perthitic. A weathered surface of the microcline has a dark tan color, in contrast to the nearly white to light tan fresh surfaces.

Microcline is abundant in the graphic granite and the layered aplite zones, however the character of the microcline is different in the two zones. In the layered aplite it occurs as anhedral grains commonly less than 1 mm. in diameter. This microcline has well developed grid-iron twinning but does not show perthitic texture. The microcline in the graphic-granite zones occurs as large crystals with good grid-iron twinning and

TABLE 15

OPTICAL DATA FOR ALBITE

Specimen Number	Extinction from cleavage when on cleavage: 010	001	Indices of Refraction ± 0.002 α	β	γ	Specimen Description
57-R-7a	22	4	1.528	1.532	1.540	White cleavelandite with tourmaline
57-R-8	19	3	1.530	1.535β	1.540	Curved white cleavelandite with muscovite
57-R-9	21	4	1.529	1.535	1.540	White cleavelandite with topaz and smoky quartz
57-R-10	21	4	1.529	1.535	1.541	Light blue cleavelandite in graphic granite
57-R-14	14	3	1.532	1.537	1.543	Albite from layered aplite
57-R-16	17	3	1.530	1.535	1.542	White albite with quartz and black tourmaline
57-R-26	21	3	1.528	1.533	1.540	White cleavelandite with green tourmaline and garnet
57-R-28	18	4	1.533	1.537	1.543	Albite from layered aplite
58-R-28	15	3	1.532	1.536	1.542	White albite with quartz and tourmaline
59-R-1	10	2	1.540	1.546	1.549	White albite in pegmatite 1 cm. from Lakeview Mountain tonalite
59-R-34	21	3	1.529	1.534	1.540	Translucent secondary albite veining corroded perthite crystal
59-R-35	18	4	1.529	1.534	1.541	Cleavelandite with cockscomb structure from corroded rock zone, Spessartite Ledge

perthitic textures. As shown in table 16, there is no significant difference in the optical properties between the microcline of the graphic granites and of the layered aplite. An x-ray diffraction pattern of specimen (57-R-30) showed by the separation of (130)-($1\bar{3}0$) reflections that the potassium feldspar is maximum microcline.

Potassium feldspar with an adularia habit occurs in the corroded rock of Spessartite Ledge. This feldspar is generally clear and has well formed {110} crystal faces. It has extinction parallel to the (010) cleavage while resting on the (001) cleavage and an x-ray diffraction pattern shows no separation of the (130) reflection. These features along with the optical properties indicate that the mineral is orthoclase. Its optical properties are listed in table 16.

This orthoclase with the adularia habit occurs most commonly as overgrowths on the corroded feldspars of the host rock; however it has also been found as euhedral crystals, 1 to 2 cm. in diameter, in secondary mineralized pockets.

TOURMALINE. Tourmaline is commonly found in all zones of the pegmatite. Although several species of tourmaline are present, the black schorlite is the most widely distributed and abundant.

Schorlite occurs as small prismatic crystals in the layered aplite. Megascopically it is black with a vitreous luster. These crystals in thin section are pleochroic from light blue to violet or pink. Commonly they are zoned with the internal zone

TABLE 16

OPTICAL DATA FOR POTASSIUM FELDSPAR

Specimen Number	Extinction from cleavage when on cleavage: 010	001	Indices of Refraction ± 0.002 α	β	γ	Specimen Description
57-R-14	5	15	1.518	1.523	1.527	Microcline from layered aplite
57-R-20	4	15	1.518	1.523	1.527	Microcline from graphic granite
57-R-23	3	15	1.518	1.523	1.526	Microcline from graphic granite
57-R-28	5	16	1.517	1.523	1.527	Microcline from layered aplite
57-R-30	5	17	1.518	1.523	1.528	Microcline from euhedral perthite crystal
58-R-24	5	16	1.517	1.522	1.526	Microcline from euhedral perthite crystal
58-R-29	6	16	1.517	1.524	1.528	Microcline from euhedral perthite crystal
58-R-30	5	15	1.517	1.523	1.527	Microcline from quartz-perthite-troumaline pegmatite
Adularia	5	0	1.518	1.523	1.527	Euhedral crystal of orthoclase with adularia habit from Spessartite Ledge
59-R-34	5	0	1.518	1.523	1.526	Orthoclase from corroded perthite crystal from Spessartite Ledge

being rotated, relative to the outer zone, approximately 60 degrees about the c axis. Both the outer and the internal zones show the typical rounded triangular habit of tourmaline. The schorlite crystals range in length from less than 1 mm. to more than 1 cm. with an average size of approximately 5 mm. Rarely are these crystals found altered.

Large crystals of schorlite are present in the graphic granite and quartz-perthite pegmatite. These crystals, as much as 20 cm. in length, have optical properties similar to the small crystals described above. Commonly the mineral exhibits well formed trigonal prisms with distinct vertical striations. Rarely the crystals have well formed terminations. They have an earthy luster on weathered surfaces of the pegmatites, but on a fractured surface they have the typical vitreous luster. Some large schorlite crystals are fractured and mineralized with other minerals such as albite and quartz.

In some schorlite crystals a core of some combination of quartz, microcline, and albite is found. These cores are commonly about one half the diameter of the host crystal and extend nearly the entire length of the tourmaline crystal. In cross section the cores have an irregular shape with no relation to the external form of the tourmaline. This textural feature of the tourmaline is interpreted as resulting from simultaneous crystallization of the salic core minerals and the tourmaline.

The indices of refraction and pleochroism of schorlite from the layered aplite, graphic granite, and the quartz-perthite

zones were determined to ascertain whether there is a variation in optical properties of the tourmaline between zones of the pegmatite. From the results of this study, shown in table 17, it can be seen that there is no consistent variation of indices or of pleochroism between the different zones of the pegmatite. A chemical analysis of schorlite, from work by Schaller (unpublished) is shown in table 20. This analyzed crystal of tourmaline is from the Little Three mine.

Other varieties of tourmaline are present in several zones of the pegmatite. An olive-green tourmaline, pleochroic in thin section from a very faint yellow to clear, is present in the albite-quartz zone and the pocket pegmatite. Rarely this olive-green tourmaline occurs as large well formed crystals, but more commonly it is pervasively fractured. The optical properties of this tourmaline are listed in table 18. By comparison with Winchell's diagram (1951, p. 466), the composition of this tourmaline would be about elbaite$_{70}$ schorlite $_{30}$.

Tourmaline crystals, less than 1 mm. in length, are present with mica as a coating on quartz crystals. Although these crystals are small, they have exceptionally well developed forms that commonly are doubly terminated. Microscopically this tourmaline is clear with no detectable pleochroism. The optical properties of this mineral, listed in table 18, indicate, by comparison with Winchell's tables, that the mineral is about elbaite$_{80}$ schorlite$_{20}$.

Small needles of tourmaline are abundant as one of the

TABLE 17

OPTICAL DATA FOR BLACK TOURMALINE

(Megascopically all specimens are black, and under the microscope the tourmaline in pleochroic from dark blue to light purple.)

Specimen Number	Indices of Refraction ± 0.002 ω	ε	Host Rock	Specimen Location*
58-R-1	1.664	1.636	Layered aplite	A-A'
58-R-2	1.664	1.636	Layered aplite with perthite	A-A'
58-R-3	1.662	1.632	Quartz-perthite pegmatite	A-A'
58-R-4	1.662	1.636	Quartz-perthite pegmatite	A-A'
58-R-5	1.662	1.633	Layered aplite	B-B'
58-R-6	1.658	1.632	Quartz-perthite pegmatite	B-B'
58-R-7	1.660	1.636	Quartz-perthite pegmatite	B-B'
58-R-8	1.661	1.636	Graphic granite	B-B'
58-R-9	1.662	1.636	Layered aplite	C-C'
58-R-10	1.666	1.636	Quartz-perthite pegmatite	C-C'
58-R-12	1.662	1.636	Layered aplite	D-D'
58-R-13	1.662	1.634	Graphic granite	D-D'
58-R-14	1.662	1.636	Layered aplite	E-E'
58-R-15	1.665	1.638	Layered aplite	F-F'
58-R-17	1.664	1.637	Layered aplite	G-G'
58-R-18	1.665	1.637	Quartz-perthite pegmatite	G-G'
58-R-20	1.662	1.636	Graphic granite	G-G'
58-R-21	1.662	1.635	Quartz-perthite pegmatite	G-G'
58-R-22	1.670	1.640	Quartz-perthite pegmatite	H-H'
58-R-23	1.666	1.635	Quartz-perthite pegmatite	H-H'
58-R-28	1.662	1.634	Quartz-perthite pegmatite	I-I'
58-R-30	1.660	1.632	Graphic granite	I-I'
58-R-31	1.666	1.636	Quartz-perthite pegmatite with graphic granite	J-J'
58-R-25	1.666	1.636	Quartz-perthite pegmatite	Not shown
58-R-27	1.666	1.636	Graphic granit	in sections

*Referenced to Plate 2, Cross Sections of the Ramona Pegmatites

TABLE 18

OPTICAL DATA FOR COLORED TOURMALINE

Specimen Number	Indices of Refraction ± 0.002 ω	ε	Color	Pleochroism for 0.03 mm. Thick Sections	Mode of Occurrence
57-R-26	1.645	1.620	Olive green	Light yellow to clear	Small crystals in cleavelandite-quartz rock
57-R-8	1.663	1.636	Black	Blue-black to yellow-pink	Large crystal in cleavelandite-quartz rock
	1.665	1.628	Green black	Light green-blue to clear	Core of large crystal from pocket zone
57-R-7a$_1$	1.646	1.622	White	Clear to clear	Intermediate zone of large crystal
	1.646	1.622	Olive green	Light yellow to clear	Outer zone of large crystal
	1.656	1.628	Green black	Light green-blue to clear	Inner zone of large crystal
57-R-7a$_2$	1.646	1.621	White	Clear to clear	Intermediate zone near top of crystal
	1.648	1.623	Pink	Clear to clear	Intermediate zone near top of crystal
	1.644	1.621	Olive green	Light yellow to clear	Outer rim of large crystal
57-R-7a$_3$	1.648	1.624	Rose pink	Clear to clear	Bicolored tourmaline fragment
	1.656	1.628	Olive green	Light blue-green to clear	Bicolored tourmaline fragment
57-R-2	1.642	1.620	Clear	Clear to clear	Euhedral, 1 mm. long crystals as coating on pocket quartz
	1.658	1.632	Yellow	Yellow to yellow	Outer zone of black tourmaline from corroded rocks
59-R-7d-1	1.658	1.634	Black	Dark blue to yellow-pink	Core of black tourmaline from corroded rocks
59-R-29	1.654	1.626	Black	Blue to pink	Large crystal from brecciated rock, Spessartite Ledge
59-R-35	1.650	1.624	Black	Blue-green to yellow-pink	Small euhedral needle-like crystal from brecciated rock, Spessartite Ledge

late-forming secondary minerals in the corroded rocks of Spessartite Ledge. This tourmaline is commonly about 0.2 mm. in diameter and 1 cm. in length. The crystals have well developed forms generally with one termination. Megascopically these crystals are black with a vitreous luster. Their optical properties and pleochroism, as listed in table 18, indicate that they are about $elbaite_{60-50}$ $schorlite_{40-50}$.

Color zonation in tourmaline was studied by determining the variation in optical properties between zones. Pleochroism and indices of refraction are listed in table 18 for three of the zoned tourmalines. In general, the crystals studied were found to have green-black or dark olive-green cores with intermediate and outer zones that range from olive-green to white to rose in color. The contacts between zones are gradational over several millimeters. The indices of refraction of the intermediate and outer zones are within about 0.004 of each other, but the indices of the cores are about 0.010 greater than the indices of the other zones. In view of the small differences in the indices of refraction, little can be concluded concerning compositional variations in the outer zones, but the color, pleochroism, and indices of refraction suggest that the green-black core of the zoned tourmaline contains more iron or manganese than the other zones.

Tourmaline in the corroded rocks of Spessartite Ledge is distinctly different from needle-like crystals of tourmaline in the same rocks. The larger crystals of tourmaline were present

in the host rock prior to the period of corrosion, and it appears very similar in habit and occurrence to the common schorlite except that it has a yellow outer zone. As shown in table 18, the indices of the yellow border and the dark blue core are nearly identical; yet there is a pronounced color difference. The color change may be due entirely to compositional changes, or it may be the result of an oxidation reaction similar to that found in hornblende. Two suggested oxidation reactions are:

$$Fe^{+2} + (OH)^{-} \rightarrow Fe^{+3} + 0^{=} + \frac{1}{2}H \uparrow$$

and

$$Mn^{+2} + (OH)^{-} \rightarrow Mn^{+3} + 0^{=} + \frac{1}{2}H\uparrow$$

With optical data it is impossible to determine whether the change in color of the tourmaline is a result of the substitution of one ion species for another, or whether it involves the oxidation of certain ions initially present in the mineral.

MICAS. Muscovite is widely distributed in the pegmatites. In the layered aplite, the muscovite constitutes less than 1 percent of the total rock. It occurs as colorless subhedral plates that rarely exceed 1 to 2 mm. in diameter. In the graphic granite, quartz-perthite pegmatite, and albite-quartz rocks, muscovite is a prominent mineral because it occurs as large books. These books, colorless to pale green, are subhedral crystals reaching a maximum diameter of about 5 cm. and thickness of 1 cm. In some pegmatites a brown, earthy textured alteration occurs around the edges of the books. Rarely books of muscovite, subhedral to euhedral in form, occur in small pegmatite pockets.

These books are colorless to pale green and about 0.5 to 1 cm. in diameter and 2 mm. thick.

A pale green muscovite is found as a replacement or pseudomorph of tourmaline. This muscovite occurs as euhedral books 1 to 2 mm. in diameter, which in general do not fill the cavity left by the tourmaline. A typical example of this replacement is shown in figure 32.

Optical properties and mode of occurrence for some typical muscovite specimens are listed in table 19. The optic angles (2V), as listed, were measured by the interference figure method with a universal stage. By comparison with Winchell's diagram for muscovite (1951, p. 368), it is found that the mica from the graphic granite, quartz-perthite pegmatite, and albite-quartz rocks has optical properties very similar to the end-member muscovite, whereas the mica from the layered aplite and alteration of tourmaline has optical properties that are at variance with those of the end-member muscovite and also with muscovite in which there is magnesium and iron substitution for aluminum.

Pink-colored micas occur as scaly aggregates near altered garnet and as a coating on some pocket minerals. The optical properties of this mica, as listed in table 19, show that it is in the lepidolite group.

An analysis of a terminated crystal of lepidolite, as listed by Stevens (1938, p. 615) is shown in table 20. This crystal is reported to be from the Little Three mine and has the United States National Museum number 93924. Over 2 percent manganese oxide is listed in the analysis.

TABLE 19

OPTICAL DATA FOR MICAS

Specimen Number	Refractive Index, β ±0.002	Optic Angle (2V)	Color	Remarks
				MUSCOVITE
57-R-2	1.588	46°	Colorless	Small crystals in pocket pegmatite
57-R-6	1.588	46°	Colorless	Scaly aggregate with green tourmaline in graphic granite
57-R-8	1.588	46°	Colorless	Books 1 to 2 cm. in diameter
57-R-8	1.588	45°	Colorless	Small crystals in scaly masses
57-R-9	1.588	45°	Colorless	Scaly aggregate with green tourmaline in graphic granite
57-R-10	1.588	44°	Light green	Books 1 cm. in diameter in cleavelandite-quartz rock
57-R-10	1.593	39°	Light green	Books 2 to 4 mm. in diameter in tourmaline
57-R-15	1.588	46°	Colorless	Books 1 to 2 cm. in diameter in cleavelandite-quartz rock
57-R-28	1.592	38°	Light green	Small crystals from layered aplite
58-R-9	1.592	40°	Colorless	Small crystals in layered aplite
58-R-15	1.594	41°	Colorless	Small crystals in layered aplite
				LEPIDOLITE
57-R-9	1.550-1.555	30°-47°	Pink	Scaly aggregate near altered tourmaline
57-R-42	1.553	42°	Pink	Coating on quartz crystals

TABLE 20

COMPOSITION OF MINERALS FROM THE RAMONA DISTRICT

	Lepidolite[a]	Tourmaline[b]	Spessartite[c]
SiO_2	54.40	35.21	
Al_2O_3	17.95	36.07	
Cb_2O_5	--		
TiO_2	0.02	0.23	
FeO	0.21	11.11	
MgO	0.30	0.19	
MnO	2.06	0.98	41.7
Li_2O	6.18	tr	
CaO	tr	0.25	
Na_2O	0.72	1.92	
K_2O	10.28	--	
Rb_2O	1.22		
Cs_2O	0.24		
H_2O^-	0.81	3.51	
H_2O^+	0.58		
F	9.19	0.00	
B_2O_3		10.43	

a. Analysis reported by Stevens (1938) as Sample 15, Terminated crystal, pink, Little Three mine, Ramona, U. S. N. Mus. 93924.

b. Analysis from unpublished paper by Schaller, reported as black crystal from Ramona.

c. Partial analysis of garnet from Ramona. Information from Jahns (personal communication).

If, like the lepidolite, some muscovite contains an appreciable quantity of manganese, it may be that the anomalous optical properties of the muscovite from the layered aplite and altered tourmaline are the result of manganese substitution for aluminum in the mica structure.

GARNET. Garnet is widely distributed in all zones of the pegmatites. Because of the difficulty of determining the composition and the sub-species of garnet, the following discussion will be limited primarily to the physical appearance of the mineral. In all rocks the garnet is isotropic, a feature characteristic of the garnet species pyralspite. One analysis, (table 20), of an orange garnet shows that the mineral is nearly pure spessartite. The garnet ranges in color from orange-tan-red brown. On the basis of the isotropism, color, and one chemical analysis, the garnet is probably of the almandite-spessartite series.

In the aplite, layers of garnet are present. This garnet commonly forms dodecahedral crystals that are generally about 0.1 mm. in diameter, orange-red in color, and unaltered.

Garnet in the graphic granite and pegmatite zone is commonly tan to red-brown in color. These crystals range in size from less than 1 mm. to more than 2 cm., but they are rarely free of fractures and other imperfections. Rarely is this garnet altered.

Spessartite occurs in the corroded rocks of Spessartite Ledge. Some of these crystals are free of cracks and other

imperfections and are suitable for gem cutting; however, most of the larger crystals are marred by fractures. This garnet, ranging from anhedral to euhedral in development of crystal form, is characterized by a deep orange color.

BERYLLIUM MINERALS. Pink beryl has been reported from most of the older mines (Kunz, 1903); however none was found during this investigation.

Small vertically striated crystals of hambergite, $Be_2(OH)BO_3$, have been recovered from some of the mine dumps. Most of the crystals appear corroded and stained, but broken surfaces show that the mineral is clear. The mineral association of hambergite could not be determined because only loose fragments of the mineral have been recovered.

TOPAZ. Euhedral crystals of topaz occur with cleavelandite and quartz. These topaz crystals, averaging about 1 cm. in diameter, are clear and colorless to somewhat yellow. The crystal form of the mineral is well developed; commonly the crystals are internally fractured. Indices of refraction of the topaz are 1.614 ± 0.002 for α and 1.618 ± 0.002 for β for sodium light at 25°C. The optical properties indicate that the mineral is about $[Al(F)_2SiO_4]_{85}[Al(OH)_2SiO_4]_{15}$.

Topaz is also present in a cleavelandite matrix as anhedral crystals with a light blue to aquamarine color. Megascopically these crystals can be distinguished from beryl only by the perfection of cleavage. Under the microscope the light blue topaz cannot be distinguished from the clear to yellow topaz.

COLUMBIUM-TANTALUM MINERALS. Iron black columbite-tantalite has been recovered from the older mine dumps. Because only loose specimens have been recovered, the mineral association of the columbite-tantalite is not known.

ALTERATION MINERALS. Psilomelane occurs as rounded masses that probably are pseudomorphous after garnet. This mineral is steel-gray to black in color with an earthy luster. Other alteration minerals, such as clays, are also present.

Bulk Mineralogical Composition of the Pegmatites

General Method

If experimentally determined phase relations are to be applied to a natural system, or if a material balance is considered for a metamorphic or metasomatic process, it is necessary to establish the bulk composition of the system. For this reason, the mineralogic and chemical composition of the Ramona pegmatites was determined quantitatively by an indirect method. Because of poor exposures, large variations in mineralogy and grain size, and the zonal nature of the pegmatites, a detailed sampling program was beyond the scope of this study. However, a good approximation to the bulk composition of the pegmatites could be obtained by making dimensional measurements of the pegmatite units or zones, determining the proportions of the minerals in these units, and determining or assuming the composition of the mineral species.

To determine the dimensions of the pegmatite units, 10 cross sections of well exposed dikes were prepared in the field

at a scale of 2 feet to the inch. These cross sections are shown in plate 2. The well exposed dikes appear to be lithologically similar to dikes that are less well exposed. In general, the extent of exposure of the pegmatite dikes seems to be related more to the local topography than to the lithology of the rocks, and therefore the prepared cross sections of well exposed dikes are considered to be representative of the pegmatites. From these cross sections the thickness or the relative areas of the units or zones were measured.

The method of determining the proportions of minerals in the units or zones depended on the grain size of the rocks. Where the rock is fine to medium grained, a megascopically representative sample was taken, thin sectioned, and a modal analysis of 1000 to 1500 points made from the thin section. With coarse grained rocks, or rocks containing large phenocrysts, a modal analysis was made in the field by counting the minerals that fall on the intersection lines of a 1/4 inch grid. In the case of very coarsely crystalline rocks, points were counted along a linear traverse with a spacing of an inch or more between points. Generally modes of 300 to 500 points were obtained in this manner. If the rock samples contained a perthitic feldspar, a thin section was made of the perthite crystals, and the ratio of microcline to albite was obtained from a modal analysis of this thin section.

Each modal analysis was weighted by the relative thickness of the zone or unit that it represented in relation to the total thickness of the dike as shown in the corresponding cross

section. The summation of all the weighted modal analyses of rocks representing the zones or units gives the mineralogical composition of the dike represented by the cross section. Then the average of the mineralogical composition of the dikes shown in the cross sections is taken to be the average composition of the pegmatites.

Mineralogical and Chemical Composition of the Dikes

The data from the quantitative analysis of the pegmatites are listed in table 21. As shown, the average of the mineralogical composition of the 10 areas of the pegmatite dike studied is about the same as that of an average granite except for the presence of about 3.5 percent tourmaline in the pegmatites.

The quantitative mineralogical composition of the pegmatites can be compared to modal analyses of samples used in the course of the hydrothermal studies. Two of these samples are typical rocks from specific units or zones of the pegmatite. The third sample is a mixture of several rocks so that the modal analysis of the mixture is nearly the same as the mineralogical composition of the pegmatites. The three samples are the following:

1. Layered aplite (57-R-28). Megascopically, microscopically, and modally the rock is representative of the average layered aplite described in a previous section. The quartz has numerous inclusions that are probably tourmaline, muscovite, and fluid. The tourmaline is commonly euhedral, zoned, pleochroic from light to dark blue, and ϵ of the tourmaline is 1.642 ± 0.002 indicating that it is almost pure schorlite. Muscovite in the aplite is light green with

TABLE 21

MODES OF UNITS AND ZONES IN THE RAMONA PEGMATITE DIKES

Location[a]	Weighting factor	K-feldspar Quartz		Albite	Tourmaline	Muscovite	Garnet	Unit or Rock Description	Type of Mode[c]
A-A'	0.0464	32.68	23.86	40.08	3.18	0.13	0.00	Layered aplite	ts.[d] of aplite
A-A'	0.0019	6.21	74.93	17.53	1.05	0.07	0.21	Perthite crystals in layered aplite zone	ts. of perthite crystals
A-A'	0.0052	26.94	48.15	22.85	1.71	0.00	0.34	Layered aplite with perthite crystals	ts. of groundmass
A-A'	0.0036	100.00	0.00	0.00	0.00	0.00	0.00	Massive quartz	
A-A'	0.0172	6.21	74.93	17.53	1.05	0.00	0.34	Perthite phenocryst in quartz-albite-perthite-pegmatite	ts. of perthite crystals
A-A'	0.0257	32.34	5.49	54.36	7.80	0.00	0.00	Quartz-albite-perthite-rock with phenocrysts of perthite	ts. of groundmass
B-B'	0.0643	33.27	31.78	31.53	3.10	0.31	0.00	Layered aplite	ts. of aplite
B-B'	0.0064	10.75	70.19	17.81	1.25	0.00	0.00	Perthite rock with minor quartz	ts. of rock
B-B'	0.0046	0.00	79.90	20.10	0.00	0.00	0.00	Perthite phenocrysts in quartz-albite-perthite-pegmatite	ts. of perthite crystals
B-B'	0.0082	43.58	14.23	34.11	6.40	1.57	0.13	Quartz-albite-perthite-rock with phenocrysts of perthite	ts. of rock
B-B'	0.0092	28.00	30.90	34.40	6.00	0.00	0.70	Graphic granite with tourmaline	Field mode
B-B'	0.0073	31.54	31.34	34.86	1.86	0.13	0.20	Layered aplite	ts. of aplite
C-C'	0.0409	34.63	20.09	37.34	1.76	6.11	0.06	Layered aplite	ts. of aplite
C-C'	0.0055	0.00	23.80	76.20	0.00	0.00	0.00	Perthite phenocrysts in quartz-albite-perthite-pegmatite	ts. of perthite crystals
C-C'	0.0170	47.87	12.19	38.97	0.97	0.00	0.00	Quartz-albite-perthite-rock with phenocrysts of perthite	ts. of groundmass
C-C'	0.0366	29.00	54.51	15.90	0.21	0.36	0.00	Graphic granite in quartz-perthite pegmatite	ts. and field mode
D-D'	0.0693	33.79	14.72	45.06	5.25	0.14	1.04	Layered aplite	ts. of aplite
D-D'	0.0307	28.30	55.00	14.42	2.10	0.18	0.00	Graphic granite	ts. and field mode
E-E'	0.0662	30.24	29.87	34.97	4.91	0.00	0.00	Aplite	ts. of aplite
E-E'	0.0338	32.20	50.71	11.89	5.20	0.00	0.00	Graphic granite with tourmaline	ts. and field mode
F-F'	0.0572	35.97	4.72	47.29	6.29	0.88	4.84	Layered aplite	ts. of aplite
F-F'	0.0428	21.10	58.40	15.40	5.10	0.00	0.00	Graphic granite in quartz-perthite pegmatite	ts. and field mode
G-G'	0.0347	32.11	20.22	43.49	4.12	0.00	0.00	Layered aplite	ts. of aplite
G-G'	0.0125	22.30	3.70	67.50	4.20	0.00	2.30	Quartz-albite-perthite pegmatite	ts. and field mode
G-G'	0.0083	80.20	14.10	5.70	0.00	0.00	0.00	Quartz with minor perthite	ts. and field mode
G-G'	0.0236	28.80	58.20	12.60	0.40	0.00	0.00	Graphic granite	ts. and field mode
G-G'	0.0209	31.50	8.40	50.30	6.20	0.00	0.00	Quartz-albite-perthite pegmatite	ts. and field mode
H-H'	0.0464	33.11	32.52	32.78	0.26	0.33	0.00	Quartz-perthite-pegmatite	ts. of rock
H-H'	0.0389	41.40	36.05	15.45	7.10	0.00	0.00	Quartz-perthite-tourmaline pegmatite	ts. and field mode
H-H'	0.0147	36.44	21.13	41.50	0.00	0.31	0.00	Quartz-perthite-albite pegmatite	ts. of rock
I-I'	0.0298	0.38	76.84	22.59	0.06	0.06	0.00	Long tapering perthite crystals	ts. of perthite crystals
I-I'	0.0437	41.09	12.15	40.33	6.17	0.13	0.13	Quartz-albite-perthite pegmatite	ts. of rock
I-I'	0.0063	33.18	49.90	14.70	2.64	0.04	0.00	Quartz-perthite pegmatite	ts. and field mode
I-I'	0.0202	26.57	50.75	21.03	1.39	0.25	0.00	Graphic granite	ts. of rock
J-J'	0.0122	25.66	64.53	8.77	0.77	0.32	0.00	Graphic granite	ts. of rock
J-J'	0.0189	30.47	4.67	61.49	3.09	0.07	0.07	Quartz-albite-perthite pegmatite	ts. of rock
J-J'	0.0311	27.50	56.65	7.65	4.70	2.70	0.80	Graphic granite with tourmaline	ts. and field mode
J-J'	0.0292	31.60	59.68	8.07	0.65	0.00	0.00	Graphic granite	ts. and field mode
J-J'	0.0069	37.15	9.48	50.39	0.91	0.32	0.00	Quartz-albite-perthite pegmatite	ts. of rock
J-J'	0.0017	21.13	57.68	20.38	0.00	0.31	0.00	Quartz-perthite pegmatite	ts. of rock
Weighted average	31.13	33.08		31.19	3.49	0.48	0.43		

a. Location referenced to Cross Section of the Ramona pegmatite dikes, Plate 2.

b. Weighting factor = $\frac{\text{(thickness of unit or rock type represented by the mode)}}{\text{(thickness of dike at the listed location)(Number of dikes in this study)}}$.

c and d. ts.= mode of thin section of the rock; ts. and field mode = major minerals determined by field mode and feldspar from thin section.

a 2V of about 38 degrees. Microcline shows grid-iron twinning but has no perthitic exsolution. Plagioclase by max λ+ is Ab_{95} An_5. The feldspar shows traces of alteration. The modal analysis of this sample is listed in table 22 and a chemical analysis is listed in table 23.

2. Tourmaline-muscovite-garnet pegmatite (57-R-46). Megascopically and microscopically the rock is representative of the coarse-grained pegmatite rocks described in a prior section. Mineralogically the rock contains quartz with many bubble trains, perthite, and plagioclase besides that present in the perthite. The maximum λ+ of this plagioclase indicates a composition at least as sodic as Ab_{95}. The tourmaline and muscovite are optically similar to those described for specimen (57-R-28). A modal analysis is listed in table 22 and a partial chemical analysis is listed in table 23.

3. The "Ramona Composite" sample, listed as R.C., is a crushed fraction of (57-R-46) to which was added specific minerals so that the mixed rock has the same mineralogical composition as was calculated for the Ramona pegmatites. Because this rock is basically (57-R-46), the description of the minerals is the same as listed for that rock. Table 22 lists the modal analysis of this sample and table 23 lists a chemical analysis of a fraction of the sample that was fused to a glass.

Table 22

Modal Analyses of Ramona Rocks and Pegmatites

Specimen Number	Quartz	K-Feldspar	Albite	Tourmaline	Garnet	Muscovite	Total
Ramona Pegmatites[a]	31.13	33.08	31.19	3.49	0.43	0.48	99.80
57-R-28[b]	32.3	18.6	42.0	4.9	1.4	0.8	100.0
57-R-46[c]	34.1	22.1	32.4	6.0	0.9	4.3	99.8
Ramona Composite[d]	29.6	31.1	33.6	4.4	0.6	0.8	100.1

a. Modal analysis as listed in table 21.
b. Average of modes from 9 thin sections.
c. Average of modes from 2 thin sections.
d. Average of modes from 2 thin sections.

TABLE 23

BULK COMPOSITION OF THE RAMONA PEGMATITES COMPARED WITH ANALYZED SAMPLES OF THE PEGMATITE AND GRANITES

	Ramona Pegmatites[a]	Ramona Composite Sample[b]	Ramona Sample 57-R-28[c]	Ramona Sample 57-R-46[d]	Avg. Alkali Granite[e]	Avg. Peralkaline Granite[e]
SiO_2	74.9	75.19	73.53	73.86	73.86	71.08
Al_2O_3	14.2	14.73	15.03		13.75	11.26
TiO_2	tr	0.10	0.06		0.20	0.40
P_2O_5		n.d.	n.d.		0.14	0.07
Fe_2O_3		0.35	0.41		0.78	4.28
FeO	0.5	0.46	0.75		1.13	2.19
MnO	0.3	0.28	0.32		0.05	0.11
MgO	tr	0.02	0.10		0.26	0.25
Li_2O		0.01	0.01	0.20		
CaO	0.5	0.03	0.56		0.72	0.84
Na_2O	3.5	3.51	5.01	4.69	3.51	4.92
K_2O	5.5	4.48	2.96	2.67	5.13	4.21
Rb_2O		0.09	0.00			
Cs_2O		0.01	0.00			
H_2O^+	0.2	0.11	0.44		0.47	0.39
H_2O^-		0.01	0.24			
CO_2		n.d.	n.d.			
F		0.03	0.01			
B_2O_3	0.4					
		99.39	99.43			
$<O \equiv F$		0.01				
		99.38	99.43			

a. Analysis calculated from modal data.
b. Sample fused to a glass. C. O. Ingamells, analyst.
c. Layered alpite. C. O. Ingamells, analyst.
d. Partial analysis by flame photometry. Art Chodos, analyst.
e. Quoted from Nockolds, S. R., 1954, Chemical Composition of Igneous Rocks, Geol. Soc. Amer., Bull. 65, pp. 1012-1013.

The chemical composition of the pegmatites was determined by using end-member compositions for quartz, potassium feldspar, muscovite, biotite, and spessartite. The average composition of the albite, as previously discussed, is about Ab_{93} An_7, and the composition of the tourmaline is taken as the analysis of tourmaline that is listed in the section on mineralogy. Thus, the figures should be regarded as approximate because deviation from end-member compositions have, in general, not been considered. A refinement of data on mineral compositions is probably not warranted in view of other uncertainties; for example, whether the available exposures reflect the true composition of the pegmatite units.

The chemical composition of the Ramona pegmatite, as calculated from the data in table 21 and assumed chemical composition for the minerals is listed in table 23, which also shows analyses of chemically analyzed samples from the Ramona pegmatites and of average granites as listed by Nockolds (1954). It is readily apparent that the composition of the pegmatite does not differ greatly from that of average granites, and that the "Ramona Composite" sample is very nearly the same chemically as the Ramona pegmatites.

The chemical analyses by Ingamells, as listed in table 23, do not include B_2O_3. The amount of B_2O_3 indicated by the modal tourmaline in (57-R-28) and the "Ramona Composite" is respectively 0.48 and 0.44 percent. These amounts of B_2O_3 added to the chemical analyses bring the total to about 100 percent.

V. HYDROTHERMAL INVESTIGATION OF RAMONA PEGMATITE ROCKS

Scope and Purpose of the Hydrothermal Work

It has long been known that volatiles play an important role in the genesis of igneous rocks and much attention has been directed toward determining the extent of the role played by the volatile water. Some of the most significant contributions in this field have been made by Goranson (1931), by determining the quantity of water soluble in a granite magma, and by Tuttle and Bowen (1958) by determining the phase relations in the $NaAlSi_3O_8$-$KAlSi_3O_8$-SiO_2-H_2O system and the melting relations of two natural granites. However, little work has been done to evaluate the effect of volatiles other than water or to study the form and distribution of crystalline products obtained from a melt. Preliminary studies on the melting and crystallization of the Harding pegmatite by Jahns and Burnham (personal communication) indicated that besides water other constituents also have a marked effect on the melting relations of an igneous rock and that a zonal distribution of minerals can be obtained during the crystallization of a melt of a pegmatite rock.

In order to evaluate possible temperature and pressure conditions that may have existed at the time of formation of the Ramona pegmatites, hydrothermal studies were conducted on samples of pegmatite rock. In particular, the temperature at which the rock begins to melt, the temperature at which the rock is completely molten, and the quantity of water soluble in a melt of pegmatite rock were determined for different water vapor

pressures. In addition, some studies were made with volatile phases other than water. Conditions, rate of formation, and features of the crystalline product were also studied.

The Ramona pegmatites are particularly interesting for an investigation of this nature because their chemical composition is very similar to a granite, yet these pegmatites have all the textural features characteristic of a pegmatite. By using natural samples of this pegmatite rock, it is possible to consider the effect of minor constituents that are not present in such concentrations in granites or included in artificially prepared samples. The samples used in the hydrothermal studies are "Ramona Composite", (57-R-46), and (57-R-28). Modal and chemical data for these specimens are listed in tables 22 and 23.

Hydrothermal Equipment and Method

The well-proven "test-tube" bombs or reaction vessels, suspended in an electrical furnace were used for most of the hydrothermal studies. Because packaged units utilizing the test-tube reaction vessel for high pressure-high temperature studies became commercially available during the latter part of this study*, only a brief description will be given of the equipment used in these hydrothermal investigations.

The reaction vessel used is basically the "cold-seal pressure vessel" first designed by Tuttle (1949) and later modified by Roy and Osborn (1952). The only other modification in

---

*A packaged unit of four reaction vessels, furnaces, gauges, temperature controllers, pressure generators, and all pressure connections is available from Tem-Pres Inc., State College, Pennsylvania.

the vessel actually used was the introduction of the thermocouple well into the side rather than the end of the vessel.

The pressure generator found to have the greatest reliability and ease of operation was a Sprague pump model S-216C, manufactured by the Sprague Engineering Corporation. This multiplying piston type pump, operating with compressed air, generates by the differential area principle a water pressure of about 2 kilobars.

A pressure intensifier was used for runs above 2 kilobars. This intensifier was simply a commercial hydraulic jack driving a stellite alloy number 25 ram, with a neoprene Bridgman-type seal, into a stainless steel jacket.

Heating of the reaction vessels was with electrical resistance furnaces. These furnaces, wound with chromel wire, operate at temperatures as high as 900 degrees C.

Bourdon-type gauges were used to measure the system pressure. These factory-calibrated gauges were connected in series so that it was possible to check pressure reading for several gauges. Based on these checks among gauges, the pressure measurements are considered precise to within 10 percent of the stated pressure value.

Nearly constant temperature of the reaction vessel was maintained with a Brown indicating controller. Charge temperatures were obtained with a Leeds-Northrop galvanometer measurement of the thermocouple e.m.f. The thermocouple is in the well on the side of the reaction vessel about 6 mm. from the charge. Temperature records obtained from a Honeywell recorder indicate that there is about 5 degrees C. temperature

fluctuations during the course of a run.

Rock samples for the hydrothermal studies were prepared by hand grinding small separates or by ball milling large samples. The hand ground samples were ground to about -200 mesh and the ball milled samples were ground to about -300 mesh. The ground sample with water or acid was crimped or welded into a capsule made from a segment of thin-walled gold tubing. At high pressure the capsule collapses so that the system pressure becomes the pressure on the charge.

Most charges were quenched by plunging the bomb in water while maintaining a constant pressure on the system. In this manner charges could be quenched in about 30 seconds.

Beginning of Melting of Ramona Rocks

Melting of the Layered Aplite (57-R-28)

Beginning of melting of the layered aplite was studied in order to determine the minimum temperature and water vapor pressure conditions under which a liquid or melt could exist in an early crystallizing zone of the pegmatites. To determine the conditions for the beginning of melting of the rock, the rock was ground to a fine powder and sealed with water in a gold capsule. This capsule and its contents, under a constant pressure, were then heated to a specific temperature and held at this temperature for a certain duration of time, after which the run was abruptly terminated by rapidly lowering the temperature, or quenching the charge. If a silicate melt existed at the maximum temperature of the run, it will be present in the quenched charge

as a glass. Thus the presence or absence of glass in the charge indicates whether the maximum temperature and pressure of the run was above or below the conditions at which the rock begins to melt. For the beginning of melting studies all runs were made in 2.5 mm. gold tubing containing about 30 mg. of rock and 10 mg. of water. The ends of the gold tube were crimped shut.

There are two possible sources of error in these determinations: 1) the composition of the charge may change somewhat during the experiment, and 2) minute traces of glass may escape notice. It is unlikely that compositional changes will be large because of the low fluorine and carbon dioxide content of the original rock and the short duration of the runs. Failure to detect minute traces of glass would result in the experimental curve being established at a higher temperature and pressure than the true beginning of melting curve. In most runs, an oil immersion objective was used in searching for glass. It is unlikely that much glass escaped detection.

The experimental data are listed in table 24, and the beginning of melting curve is shown in figure 33. The melting point at one atmosphere pressure is taken as 960 degrees C. from the data of anhydrous synthetic granite as listed by Tuttle and Bowen (1958).

Melting of the Pegmatite Rock (57-R-46)

Melting relations were studied for a muscovite-rich rock (57-R-46) to ascertain the effect of the small concentrations of the mineralizers lithium and fluorine present in the

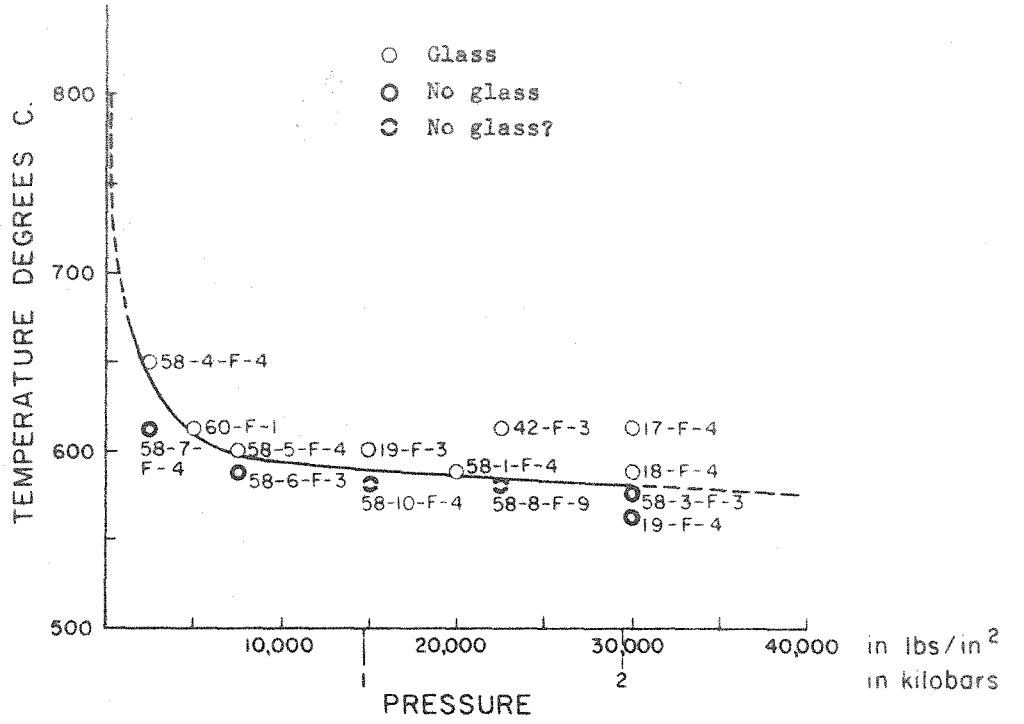

Figure 33. Pressure-temperature projection of the solidus for the layered aplite (57-R-28).

Table 24

Beginning of Melting of Layered Aplite (57-R-28).

Run Number	Temperature °C. Start of Run	Temperature °C. End of Run	Pressure lb/in^2 Start of Run	Pressure lb/in^2 End of Run	Time in hours	Results
58-4-F-4	650	650	2500	2500	6	Glass
58-7-F-4	612	610	2500	2500	6	No glass
60-F-1	609	610	5000	5000	5	Glass
58-5-F-4	600	601	7500	7500	6	Glass
58-6-F-3	587	583	7500	7500	6	No glass
19-F-3	596	597	15,000	15,000	12	Glass
58-10-F-4	580	580	15,000	15,000	6	No glass?
58-1-F-4	590	590	20,000	20,000	6	Glass
42-F-3	612	613	22,500	22,500	5	Traces of glass
58-8-F-9	580	576	22,500	22,500	6	No glass?
17-F-4	607	612	30,000	30,000	10	Glass
18-F-4	586	591	30,000	30,000	15 1/2	Glass
58-3-F-3	575	582	30,000	30,000	6	No glass
19-F-4	560	564	30,000	30,000	12	Some recrystallization, no glass

muscovite. Modally this rock is similar to the layered aplite specimen except that there is over 4 percent muscovite present. The data from these determinations are listed in table 25, and the beginning of melting curve is shown in figure 34.

Melting of Fluorine Rich Rock Sample [(57-R-46)+(Topaz)]

To investigate further the effect of fluorine on beginning of melting relations, sample (57-R-46) was mixed with topaz from sample (57-R-9). The α and β indices of the topaz are respectively 1.614 ± 0.002 and 1.618 ± 0.002. Comparison of the optical data with composition curves as published by Winchell (1951) indicate that the topaz contains about 17.3 percent fluorine. The final mixture was 90.4 percent (57-R-46) and 9.6 percent topaz (57-R-9), or there was about 1.7 percent fluorine in the mixture.

There may have been some fluorine loss during the run, but the short duration of the runs and the known retention of fluorine in glasses suggests that fluorine losses were not large. However, even in runs of short duration there was considerable recrystallization in many charges where no glass could be detected. Thus the curve established for this sample is subject to greater interpretation error because of the recrystallization problem, and also there is less compositional control on the system. The data from this study are listed in table 26 and the beginning of melting curve is shown in figure 35.

Summary and Interpretation of Beginning of Melting Studies

No attempt will be made to generalize about melting

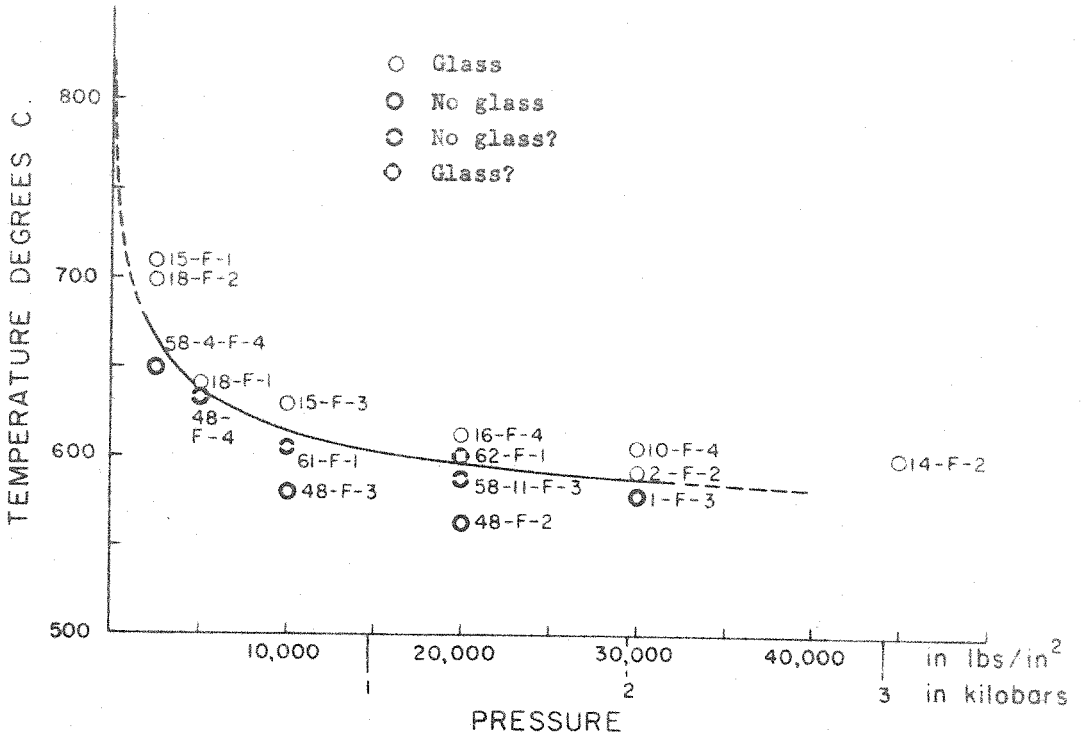

Figure 34 Pressure-temperature projection of the solidus for pegmatite rock (57-R-46).

Table 25

Beginning of Melting of Pegmatite Rock 57-R-46

Run Number	Temperature °C. Start of Run	Temperature °C. End of Run	Pressure lb/in² Start of Run	Pressure lb/in² End of Run	Time in hours	Results
15-F-1	712	708	2500	2500	13	Glass
18-F-2	699	689	2500	2500	15 1/2	Glass
58-4-F-4	650	650	2500	2500	6	No glass?
18-F-1	641	630	5000	5000	15 1/2	Trace of glass
48-F-4	620	634	5000	4500	5	No glass?
15-F-3	629	622	10,000	10,000	13	Glass
61-F-1	600	606	10,000	10,000	5	No glass?
48-F-3	570	574	10,000	10,000	5	No glass
16-F-4	607	612	20,000	20,000	10 1/2	Glass
62-F-1	603	601	20,000	20,000	5	Glass?
58-11-F-3	587	587	20,000	20,000	5	Recrystallization, no glass?
48-F-2	559	563	20,000	20,000	5	No glass
10-F-4	605	604	30,000	30,000	11	Glass
2-F-2	591	587	30,000	30,000	12	Trace of glass
1-F-3	576	578	30,050	27,000	9 1/3	No glass
14-F-2	598	600	45,000	45,000	12	Glass

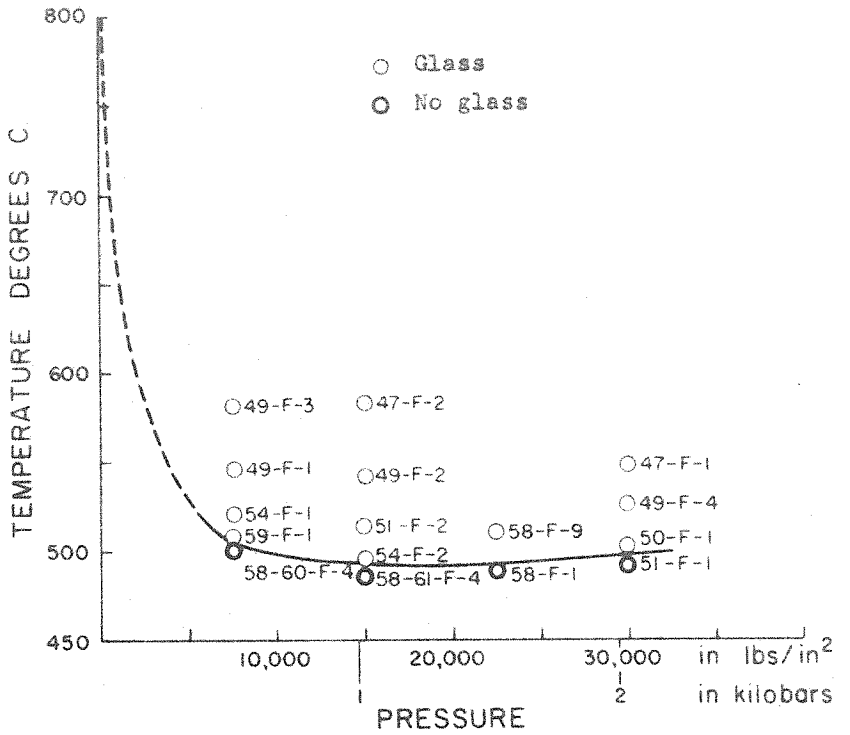

Figure 35 Pressure-temperature projection for the solidus for fluorine rich pegmatite sample [(57-R-46)+(topaz)].

Table 26

Beginning of Melting of Fluorine Rich Specimen [(57-R-46)+(Topaz)]

Run Number	Temperature °C. Start of Run	Temperature °C. End of Run	Pressure lb/in^2 Start of Run	Pressure lb/in^2 End of Run	Time in hours	Results
49-F-3	581	578	7500	7500	5	Glass
49-F-1	546	546	7500	7500	5	Glass
54-F-1	518	520	7500	7500	5	Trace of glass
59-F-1	508	503	7500	7500	5	Trace of glass
58-60-F-4	500	500	7500	7500	5	No glass, recrystallization
47-F-2	581	583	15,000	15,000	5	Much recrystallization, glass
49-F-2	540	543	15,000	15,000	5	Glass
51-F-2	510	513	15,000	15,000	5	Glass
54-F-2	485	494	15,000	15,000	5	Trace of glass
58-61-F-4	485	485	15,000	15,000	5	No glass, recrystallization
58-F-9	500	500	22,500	22,500	5	Much recrystallization, glass
58-F-1	486	486	22,500	22,500	5	No glass, recrystallization
47-F-1	547	546	30,000	30,000	5	Much recrystallization, glass
49-F-4	526	522	30,000	30,000	5	Glass
50-F-1	497	504	30,000	30,000	5	Much recrystallization, glass
51-F-1	490	492	30,000	30,000	5	No glass, recrystallization

conditions for pegmatitic rocks with only three beginning of melting curves; however some important conclusions relevant to genesis of the pegmatites can be drawn from this work. In the first place it is shown that a liquid could exist with crystals in about the same pressure temperature conditions in the foot-wall unit as in the hanging wall units of the pegmatite. Second, in the pressure temperature range investigated, it is found that the Ramona samples melt at a considerably lower temperature than do granites under the same conditions. Third, fluorine and lithia in concentrations similar to those of sample (57-R-46) do not appreciably effect the melting temperature; however an excess of fluorine, above that normally found in the Ramona samples, materially lowers the melting temperature. Consequently if the fluorine originally present in the Ramona pegmatite magma is now in chemical combination in the minerals, the temperature at which the last liquid could exist is illustrated by curves as found for samples (57-R-46) or (57-R-28). However if fluorine has escaped from the system, melting relations as found for the topaz rich sample would probably be more representative of the conditions under which the last liquid could have existed in the pegmatites.

Liquidus and Water Solubility Investigations

The study of the beginning of melting of the pegmatite rocks was followed by a study of liquidus relations in order to define the range of conditions under which liquid and crystals can coexist. Liquidus determinations could be made on any rock

unit of the pegmatites, as with the beginning of melting work; however the liquidus of greatest petrologic importance to pegmatite genesis is the one defining the conditions under which a pegmatite magma begins to crystallize. For this reason, a composite sample of pegmatite rock that is considered to approximate very nearly the composition of the original pegmatite magma was used for the liquidus determinations. This sample, the "Ramona Composite" was fused to a glass at 1500°C. and 1 atm. pressure so that the starting material for all these runs was a super-cooled liquid of the composition of the pegmatites.

Charges for the liquidus and water solubility determinations were prepared by sealing a weighed sample of glass and a weighed sample of water in a gold tube. If the quantity of water in the charge is greater than that which is soluble in the melt, it will at high temperatures exist as a separate vapor phase. This separate vapor phase in the quenched charge will appear as a bubble at the end of the capsule or as a series of bubbles in the glass. If the quantity of water initially present in the charge is less than the quantity soluble in the melt under the conditions of the run, there should be no bubbles in the quenched product of the run.

At the beginning of this investigation, it was thought that liquidus data and data on the amount of water that is soluble in a magma could be obtained from the same set of runs by considering the presence of bubbles as evidence of oversaturation with water and the presence of crystals as evidence of a temperature below the liquidus temperature of the system. Unfortunately, neither bubbles or crystals unambiguously

indicate that the system is oversaturated or that the temperature is below the liquidus temperature because they were found in all runs.

All of the charges examined contained some bubbles, but the cause of bubbles in the glass is readily explained by considering the method of preparing the charge. In particular, the charge is in a welded gold tube 4mm. in diameter and about 25 mm. long. Assuming that about one half of the capsule is air, that the perfect gas law is valid under the pressure-temperature conditions of interest, and that air is not soluble in the melt, it is found that microscopically visible bubbles could be present in all the charges. All charges were thin sectioned and the volume percent bubbles were measured. In all cases, except three where disequilibrium conditions were thought to exist, the bubbles in the undersaturated charges could be explained by the air originally present in the charges.

Having roughly calibrated the percent bubbles likely to be present, it is possible to determine saturation with water by a presence of an excess of bubbles over those present as a result of the trapped air. Furthermore, if the run is below the liquidus it is still usable for water solubility determinations because the amount of water excluded from the anhydrous phases present is negligible in comparison to the total amount of water present in the charge.

Liquidus determinations are complicated by the presence of minute hexagonal red-brown crystals that are probably hematite. At temperatures above the liquidus there should be no

crystals present in the quenched charge. However to melt the hexagonal red-brown crystals requires temperatures that are geologically unrealistic for pegmatites; therefore the liquidus in this study is considered as the temperature representing the maximum solubility of the feldspar, quartz, tourmaline, garnet, or muscovite solid phases in the liquid phase.

In several runs there are sufficient crystals to give x-ray diffraction patterns that show the primary phases to be quartz and feldspar. Other minerals may be present but in quantities below the limit of sensitivity of x-ray diffraction. In maximum dimension the crystals in these runs may reach as much as 0.01 mm.; although they are generally considerably smaller. These crystals characteristically show low first order birefringence and have a roughly equant form.

A needle-like crystal form is also present in the final products of some runs. These crystals reach 0.05 mm. in length and show birefringence, and they have parallel or nearly parallel optical extinction. Commonly a bubble is found at the center of a radiating cluster of these crystals; however single crystals and radiating groups without a bubble at the center demonstrate that the growth of these crystals did not require the presence of a central bubble. These crystals cannot be identified from either optical or x-ray data, but their colorless nature and low birefringence suggest that they may be feldspar or quartz.

The data for the critical runs in this study are listed in table 27, and figures 36 and 37 show the liquidus and water solubility curves. For comparison, the water solubility curve

TABLE 27

WATER SOLUBILITY AND LIQUIDUS DETERMINATIONS FOR THE RAMONA COMPOSITE SAMPLE

Run Number	Pressure in P.S.I.	Temp. in °C	Time	% Water in Charge	% Bubbles in Quenched Charge	Results	Conclusions
RC-6	7,500	866	3 h	2.25	0.53	Small equant and prismatic crystals	Oversaturated and below the liquidus
RC-52	7,500	887	12 h	2.01	0.08	Small equant and prismatic crystals	Undersaturated
RC-10	7,500	862	10 h	1.95	0.17	Small equant and prismatic crystals	Undersaturated
RC-53	7,500	880	12 h	1.70	0.05	Small prismatic crystals	Undersaturated
RC-28	7,500	882	4 h	Excess	--	Small needle-like crystals	Above the liquidus
RC-5	15,000	780	3 h	3.74	0.56	Cavities on surface of the charge, many equant crystals	Oversaturated and below the liquidus
RC-49	15,000	810	12 h	3.47	0.55	Many equant crystals	Oversaturated and below the liquidus
RC-9	15,000	765	3 h	3.37	0.10	Many equant crystals	Undersaturated and below the liquidus
RC-54	15,000	811	12 h	3.08	0.17	Many equant crystals	Undersaturated and below the liquidus
RC-31	15,000	804	4 h	2.59	0.10	Equant crystals and some skeletal crystals	Undersaturated and below the liquidus
RC-27	15,000	804	4 h	Excess	--	Many equant crystals	Below the liquidus
RC-1	22,500	750	4 h	4.76	0.28	Many equant crystals	Oversaturated and below the liquidus
RC-3	22,500	752	3 h	4.58	0.86	Many equant crystals	Oversaturated and below the liquidus
RC-7	22,500	746	3 h	4.41	0.20	Cavities on the surface of the charge, many equant crystals	Oversaturated and below the liquidus
RC-50	22,500	771	12 h	4.06	0.07	Few equant crystals	Undersaturated and below the liquidus
RC-55	22,500	773	12 h	3.89	0.10	Many equant crystals	Undersaturated and below the liquidus
RC-11	22,500	715	3 h	3.73	0.05	Many equant crystals	Undersaturated and below the liquidus
RC-14	22,500	715	3 h	3.46	0.12	Many equant crystals	Undersaturated and below the liquidus
RC-26	22,500	777	4 h	Excess	--	Equant crystals as in RC-1 and RC-3 are not present	Above the liquidus
RC-30	22,500	762	4 h	Excess	--	Equant crystals as in RC-1 and RC-3 are not present	Above the liquidus
RC-218*	30,500	750	5 h	6.80	2.1	Small external cavities, no crystals	Oversaturated and above the liquidus
RC-217*	30,500	750	5 h	6.60	1.6	Few small external cavities, no crystals	Oversaturated and above the liquidus
RC-216*	30,500	750	5 h	6.40	2.0	No external cavities, no crystals	Oversaturated and above the liquidus
RC-215*	30,500	750	5 h	6.20	1.0	No external cavities, no crystals	Oversaturated and above the liquidus
RC-214*	30,500	750	5 h	5.98	1.8	No external cavities, no crystals	Oversaturated and above the liquidus
RC-213*	30,500	750	5 h	5.49	1.9	No external cavities, no crystals	Oversaturated and above the liquidus
RC-4	30,000	731	3 h	5.08	0.05	Many equant crystals	Undersaturated and below the liquidus
RC-51	30,000	758	12 h	4.75	0.0	Many equant crystals	Undersaturated
RC-56	30,000	755	12 h	4.44	0.01	Many equant crystals	Undersaturated
RC-25	30,000	762	4 h	Excess	--	Needle-like crystals	Above the liquidus
RC-29	30,000	753	4 h	Excess	--	Needle-like crystals	Above the liquidus
RC-2	30,000	730	4 h	Excess	--	Small equant and prismatic crystals	Below the liquidus
RC-8	30,000	732	3 h	Excess	--	Small equant and prismatic crystals	Below the liquidus
RC-201*	43,500	725	--	7.80	1.6	No external cavities, no crystals	Oversaturated, above the liquidus
RC-202*	43,500	725	--	8.00	1.7	No external cavities, no crystals	Oversaturated, above the liquidus
RC-203*	43,500	725	--	8.20	1.6	No external cavities, no crystals	Oversaturated, above the liquidus
RC-204*	43,500	725	--	8.40	2.3	External cavities, no crystals	Oversaturated, above the liquidus
RC-66	45,000	750	12 h	5.27	0.0	Many equant crystals	Undersaturated
RC-62	45,000	747	12 h	5.16	0.0	Many equant crystals	Undersaturated
RC-44	46,000	720	3 h	Excess	--	No crystals	Above the liquidus
RC-45	46,000	740	3 h	Excess	--	No crystals	Above the liquidus

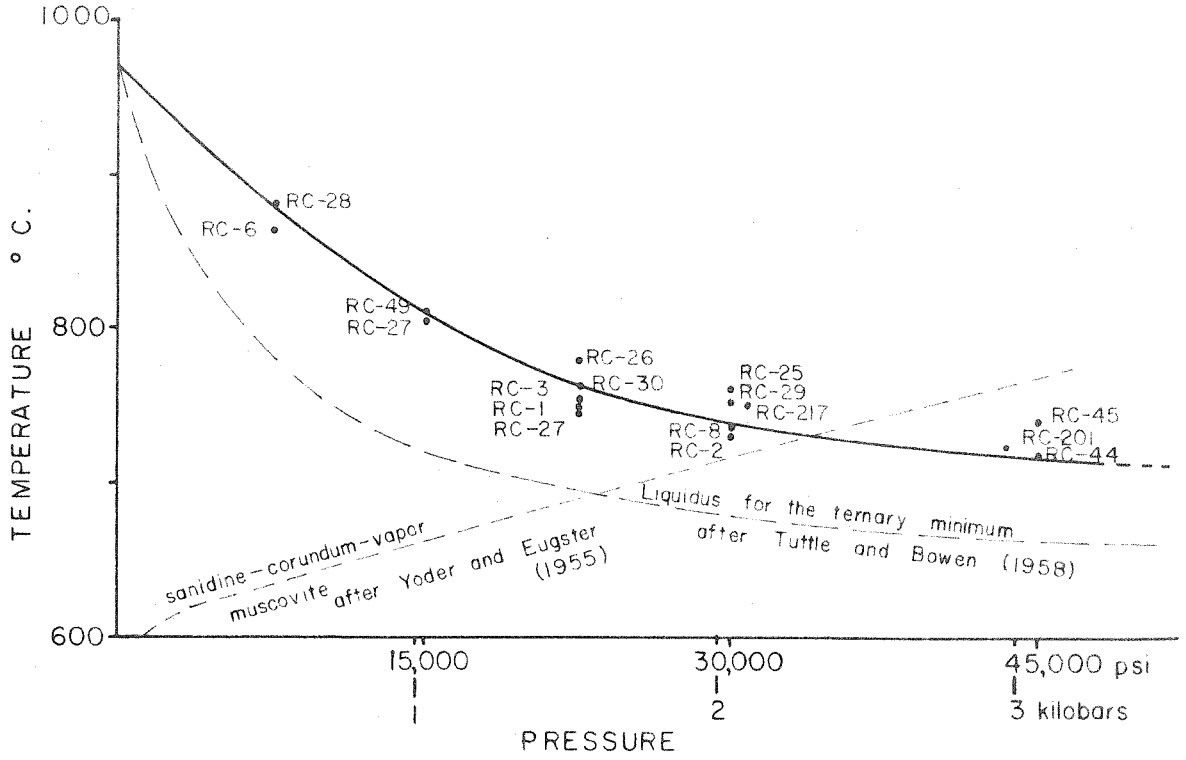

Figure 36. Liquidus of the Ramona Composite Sample

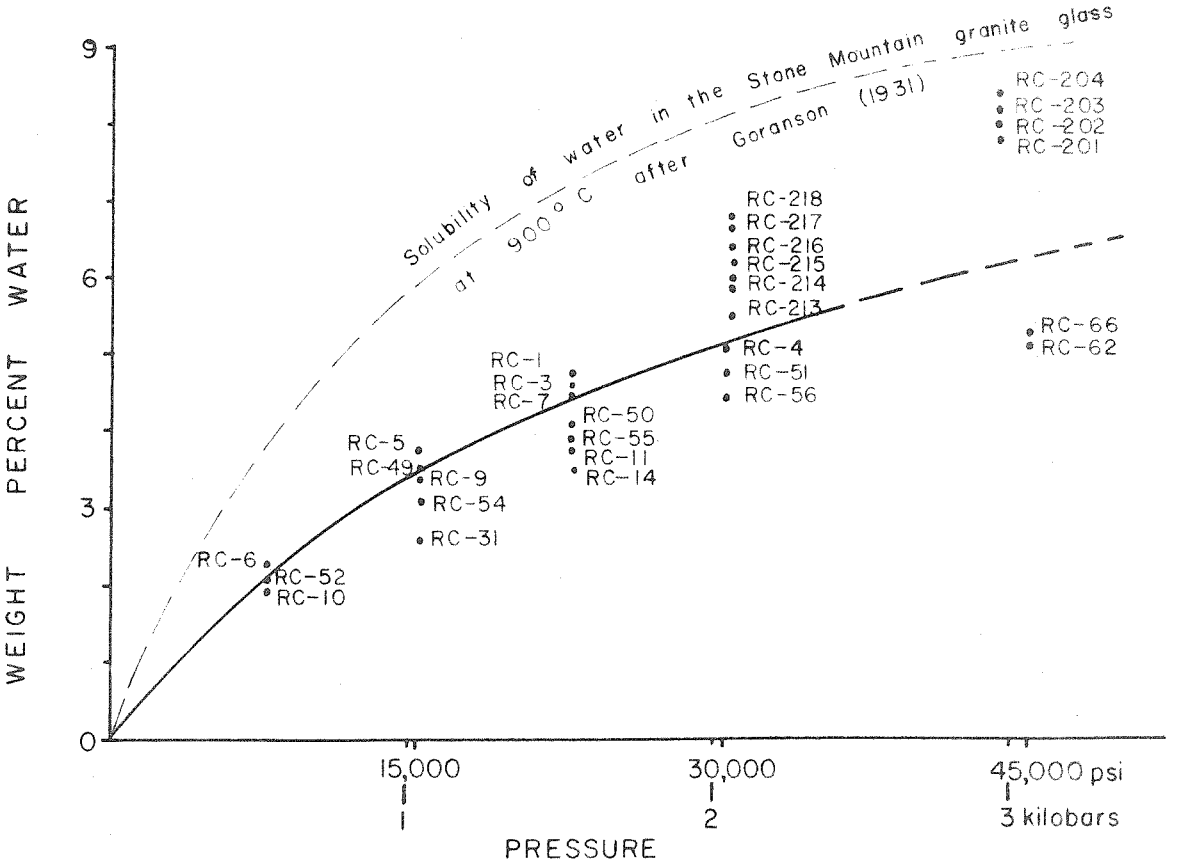

Figure 37. Solubility of Water in a Melt of Ramona Composite Sample

determined by Goranson (1931) is shown in figure 37, and the liquidus for the ternary minimum of the system $NaAlSi_3O_8$-$KAlSi_3O_8$-SiO_2-H_2O (Tuttle and Bowen, 1958) is shown in figure 36. It is evident that liquidus relations are similar for the Ramona Composite sample and the synthetic system, but less water is soluble in the Ramona Composite sample than Goranson (1931) indicated was soluble in the Stone Mountain granite.

Special Hydrothermal Studies with Ramona Samples

Effect of Pressure on the Rate of Crystallization

In the water solubility and liquidus determination runs it was observed that at the higher water vapor pressures the crystals that formed were larger and have better developed forms than those that crystallized in low pressure runs. A series of three runs was made to investigate specifically the effect of water vapor pressure on the rate of crystallization. These runs were spaced at about 1 kilobar intervals with the charges being melted at about 10 to 15 degrees above the liquidus. The temperature of the runs was lowered at about 10 degrees per day for nine days so that the final temperature was about 75 to 80 degrees below the liquidus temperature. The Ramona Composite sample, fused to a glass, was used for the starting material in the runs. The quantity of water sealed in the charge depended on the pressure of the runs, but all runs were undersaturated with water. The data concerning these runs are listed in table 28.

In all charges there were needle-like and equant crystals

TABLE 28

RATE OF CRYSTALLIZATION DATA

	Run Number		
	RC-72	RC-73	RC-74
Weight % water in the charge	4.78	4.00	2.75
Pressure constant at	45,000 p. s. i.	30,000 p. s. i.	15,000 p. s. i.
Pressure at which the charge would be saturated with water	24,700 p. s. i.	18,400 p. s. i.	11,000 p. s. i.
Temperature of the liquidus at saturation with the water present in the charge	755°C	780°C	835°C
Melting temperature	780°C	790°C	845°C
Final temperature	700°C	730°C	760°C
Cooling rate	9°C/day	6.7°C/day	9.5°C/day
Percent crystals in the charge at the completion of the run	9.6	1.2	0.4

present. The equant crystals are birefringent and appear either hexagonal or square in outline. The needle-like crystals are also birefringent and have parallel or nearly parallel extinction. In cross section the needle-like crystals appear to have a hexagonal outline. Numerous small dark crystals, possibly hematite, are present in zones in the charge. These crystals may be quench crystals; although it seems unlikely that crystals would form in a viscous silicate melt during a quench period of about one half of a minute. If these crystals formed during the main duration of the run they should be evenly distributed in the charge. The distribution of these crystals in zones and the spacing between zones suggests that the crystals were formed during the heating cycle. The spacing between the zones of these crystals is compatible with the size of the original anhydrous glass fragments used in the charge.

That water vapor pressure aids crystallization is well illustrated by this series of runs. Using modes of about 800 points and counting, in thin sections of the charges, both the needle-like and equant crystals, but not the semi-opaque crystals, it is found that there are about 10 times the volume percent crystals in RC-72 as there are in RC-74. By measuring the diameter of crystals it was found that in RC-74 the average size of the equant crystals is about 0.010 mm. whereas the average size in RC-72 is about 0.003 mm. No attempt was made to measure the needle-like crystals; however from the size distribution of the equant crystals it appears that the greater percent crystals in the high pressure run is more a function of

increased crystal size than as increased number of crystals.

Effects of Hydrofluoric Acid

One run was completed in which hydrofluroic acid (48%) was used for the vapor phase instead of water; however because of experimental difficulty, the interpretation of the results must be considered as tentative. In particular, the experimental method involved the introduction of finely ground silicate glass on hydrofluoric acid. It is unlikely that the gold capsule was welded shut before some of the evolved silicon fluoride gas was lost from the system. The weight of the capsule before and after welding checked; however this may be fortuitous.

The conditions of the run and the results are listed in table 29 in comparison to several runs with water as the vapor phase.

About the only tentative conclusion that can be drawn from this one fluorine run, is that fluorine, to a greater extent than water, aids crystallization. The few bubbles present in the charge are probably air suggesting that at least 4.25 percent fluorine is soluble in the melt at 1.5 kilobars pressure. Furthermore, for runs at about the same temperature and pressure, it appears that about 4 percent fluorine does not lower the liquidus temperature much more than about 4 percent water.

Effect of Hydrochloric Acid

Two runs were made with constant boiling, at one atmosphere pressure, hydrochloric acid to obtain information on the solubility of the acid in the melt and its effect on crystallization. The results of the two runs made for this study are

TABLE 29

EFFECT OF HYDROFLUORIC ACID

Run Number	Pressure in p. s. i.	Temp. in °C	Time in hours	Weight % Liquid Added to the Charge	Results
RC-64	22, 500	777	12	4. 25 HF	Size and distribution of crystals is uneven in the charge. Size ranges from 0. 01 mm. at one end to less than 0. 005 mm. at the other end. The crystals commonly are equant and have first order birefringence. Needle-like crystals are common as radiating aggregates in the fine-grained end of the charge. The charge contains about 10% crystals and few bubbles.
RC-50	22, 500	771	12	4. 06 H_2O	Few equant crystals present that are about 0. 003 mm. in diameter. Needle-like crystals are common and evenly distributed in the charge. Charge contains about 2% crystals.
RC-55	22, 500	773	12	3. 89 H_2O	Equant crystals about 0. 003 mm. in diameter are present in the charge. Many needle-like crystals are present, evenly distributed in the charge. About 1% crystals in the charge.

listed in table 30.

Hydrochloric acid appears to raise the liquidus temperature of the system above that to be expected if the same weight percent water had been used for the vapor phase. However this effect may be caused by the charge being undersaturated with vapor. The weight percent hydrochloric acid used in these runs is greater than the weight percent water necessary for saturation; however because of the higher molecular weight of hydrochloric acid the mole percent of acid is about that of water. X-ray diffraction patterns showed the primary phases that crystallized to be quartz and feldspar.

Effect of Boric Oxide and Water

One run was made in which about 2 percent boric oxide was added to the charge. The gold capsule of this charge, held at 800 degrees C. at 1.5 kilobars pressure for 12 hours, was found to have ruptured. As with the other runs, a test of whether the capsule has leaked or gained water is most easily checked by weighing the capsule before and after the run. In this run with boric oxide, the weights did not check. However, the run still gives some information. Namely the run may be considered oversaturated with water plus having some boric oxide present. At the pressure of the run, the temperature is about 30 degrees higher than the liquidus temperature of the Ramona Composite sample with water as the vapor phase.

The only crystals detected in the charge are extremely minute, about 0.001 mm., equant crystals that are in zones, and two groups of radiating acicular crystals as much as about

TABLE 30

EFFECT OF HYDROCHLORIC ACID

Run Number	Pressure in p. s. i.	Temp. in °C	Time in hours	Weight % Liquid Added to the Charge	Results
RC-65	22,500	777	12	4.45 HCl	Many equant crystals with irregular outlines. The larger crystals, about 0.003 mm., show low gray birefringence. A few radiating aggregates of needle-like crystals are present. Few bubbles are present in the charge; however the charge does not appear oversaturated. About 4% crystals are in the charge.
RC-70	22,500	800	12	5.20 HCl	Many equant crystals with irregular outlines. These crystals are about 0.006 mm. in diameter and show first order birefringence. Many needle-like crystals, commonly in aggregates, are present. Few bubbles are present in the charge, but it does not appear oversaturated.

0.03 mm. in length. These crystals are thought to be formed during the heating or quench cycle. Because the run is only 30°C. above the liquidus temperature at 1.5 kilobars water vapor pressure, it is concluded that boric oxide added to the melt does not appreciably raise the liquidus temperature by an early crystallization of some particular mineral, as tourmaline.

Hydrothermal Conditions and Crystal Morphologies

A series of runs was made to obtain specific information concerning conditions best for crystallization and the type of crystals formed under various hydrothermal conditions. Table 31 summarizes the conditions and results of these hydrothermal runs.

This study demonstrates that crystallization of the Ramona Composite sample is most favored at temperatures only slightly below the liquidus temperature. This is well shown by a comparison of runs RC-61 and RC-41. During the cooling of RC-61 about 100 times as many crystals formed as during the more rapid cooling of RC-41; yet the total duration of run RC-61 was less than twice that of RC-41.

Run RC-40 is the only run in which spherulites formed in abundance. This run was cooled over about two days to 150 degrees below the liquidus temperature and then held for a week at a temperature about 150 to 175 degrees below the liquidus temperature. In comparison, run RC-48 containing few spherulites was cooled to a temperature only 75 degrees below the liquidus at a much slower rate than RC-40. With a cooling rate

TABLE 31

HYDROTHERMAL CONDITIONS AND CRYSTAL MORPHOLOGIES

Run Number	Temp. in °C	Time in hours	Pressure in p. s. i.	Weight % Water in Charge	Remarks and Results
RC-40	850 829 824 799 780 761 730 698 704	0 4 13 15 25 37 49 219 229	Constant at 22, 500	1. 9	For 1. 9% water the liquidus of the melt is about at 880°C. The change is about 40% crystalline with the crystals occurring in layers and zones. The crystals commonly occur as spherulites and show first order birefringence. Many needle-like crystals are present commonly in aggregates. Rarely equant crystals are found in the charge. These crystals are about 0. 002 mm. in diameter.
RC-41	800 757 743 722 705 686 687 687	0 4 13 15 25 37 219 227	Constant at 22, 500	Excess Water	Crystals, about 0. 001 mm. in diameter are in layers and have the appearance of flow bands. These crystals are translucent to opaque. Needle-like crystals, commonly in radiating aggregates are sparsely distributed in the charge. The liquidus of the melt at the pressure of this run is about 760°C.
RC-47	888 878 868 868 857 857 848 852 836 828	0 24 48 72 77 96 108 130 156 180	10, 000 20, 000 20, 000 20, 000 22, 500 22, 500 22, 500 22, 500 22, 500 22, 500	1. 97	For 1. 97% water the liquidus of the melt is about 870°C. About 10% crystals are present evenly distributed in the charge. Equant crystals average about 0.005 mm. in diameter, but some larger ones show first order gray birefringence. Many needle-like crystals are present with the larger ones showing birefringence and having parallel extinction.
RC-48	885 870 868 868 857 855 854 851 832 802 813 799	0 24 48 72 77 96 108 130 156 180 216 240	10, 000 20, 000 20, 000 20, 000 22, 500 22, 500 22, 500 22, 500 22, 500 22, 500 22, 500 22, 500	1. 97	For 1. 97% water the liquidus of the melt is about 870°C. The charge is about 10% crystals of which about half are equant and half are needle-like. The equant crystals are about 0. 01 mm. in diameter; however some larger ones show first order gray birefringence. The larger needle-like crystals, about 0. 2 mm. long, are birefringent and have parallel extinction. Several spherulitic forms are present with the larger ones being about 0. 03 mm. in diameter.
RC-60	870 845 845 833 822 808 854	0 48 58 70 92 118 140	15, 000 22, 500 22, 500 22, 500 22, 500 22, 500 22, 500	2. 00	For 2. 00% water the liquidus of the melt is about 865°C. About 5% crystals in the charge of which half are equant and half are needle-like in form. The equant crystals average about 0. 007 mm. in diameter, and the needle-like crystals are commonly about 0. 04 mm. in length. The larger crystals show first order gray birefringence.
RC-61	775 760 746 750 734 729 717 702	0 12 34 56 82 106 142 382	Constant at 22, 500	Excess Water	The liquidus for a melt at the pressure of this run is about 760°C. About 5% needle-like crystals about 0. 05 mm. in length. About 1% equant crystals that are commonly in zones or layers. These equant crystals are rarely larger than 0. 002 mm. in diameter.

very similar to RC-48, run RC-47 showed no spherulitic crystal forms with 50 degrees undercooling. From this information, it appears that with 150 to 175 degrees C. undercooling and about 2 percent water in the melt spherulitic crystal forms are abundant, but they decrease in abundance with less undercooling until at about 50 to 75 degrees undercooling they no longer form.

It can also be noted from the data in table 31 that equant crystals formed best in those runs that are not greatly undercooled. For example the equant crystals in run RC-40 are about 0.002 mm. in diameter; yet in runs RC-47, RC-48, and RC-60 equant crystals are about 0.007 mm. in diameter.

Ramona Hydrothermal Work in Relation to Synthetic Systems

In order to determine the applicability and thus to fully utilize existing information from other experimental studies, it is necessary to appraise the effects of slight compositional differences between the natural rocks and the synthetic system. By comparison of the data for the Ramona samples with data for the $KAlSi_3O_8$-$NaAlSi_3O_8$-SiO_2-H_2O system, as shown by Tuttle and Bowen (1958), it is found that liquidus relations are very similar for the two systems; however the solidus relations are considerably different, with the Ramona samples beginning to melt at a lower temperature than the ternary minimum of the synthetic system.

Water solubility data for the Ramona samples can be compared to work by Goranson (1931) and Jahns and Burnham

(unpublished). The comparison shows that at pressures less than about 4 kilobars, less water is soluble in the Ramona sample than the quantity that Goranson indicated was soluble in the Stone Mountain granite. At pressures less than 3 kilobars the Ramona sample also contains less water than do melts of pegmatite rock studied by Jahns and Burnham. The reasons for these variations is now known.

Because of compositional similarities and similarities of liquidus relations for the natural samples studied and the synthetic system $NaAlSi_3O_8$-$KAlSi_3O_8$-SiO_2-H_2O, it is concluded that liquidus and crystallization trends of the synthetic system may, with reservation, be applied to a melt of the composition of the Ramona Composite sample.

Composition of the Vapor Phase

The composition of the vapor in equilibrium with a melt of a composition similar to the Ramona Composite sample has not been determined experimentally. Some information concerning the composition of such a vapor can be obtained from studies of a single mineral phase and water. Kennedy (1950) established some solubility curves for the system SiO_2-H_2O. Experimental work by Morey (1957) and Morey et al. (1951) gives some information about the vapor phase in the systems SiO_2-H_2O, $NaAlSi_3O_8$-H_2O, and $KAlSi_3O_8$-H_2O. All available experimental data that are applicable to the problem of the nature of the vapor phase in a system of granitic composition are shown in figure 38. An important feature shown by this experimental work is that the solubility curve for silica has a maximum.

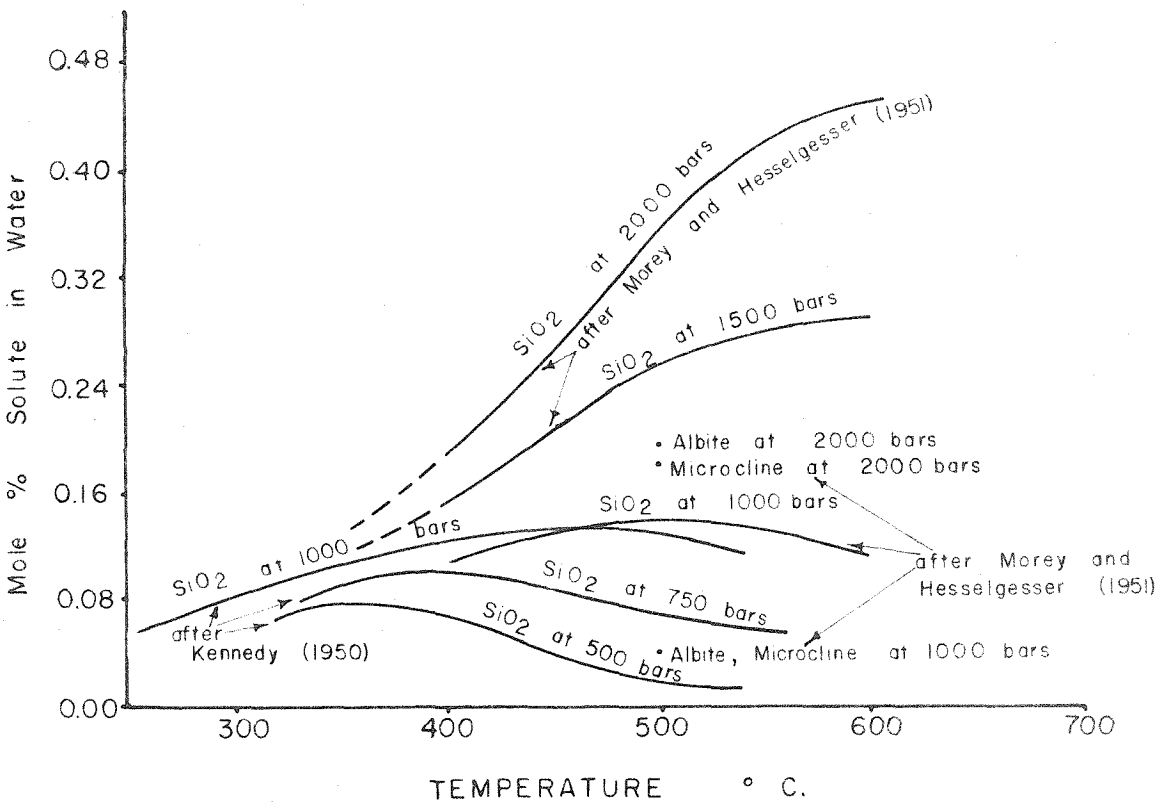

Figure 38. Solubility of Minerals in Water

VI. ORIGIN OF THE RAMONA PEGMATITES

Source and Mode of Emplacement

The pegmatite dikes at Ramona appear to have been injected as a liquid possibly with a vapor phase and crystallized in place without replacement or significant alteration of the country rock. This conclusion is based on the following criteria:

a. The Ramona pegmatites lie well within granitic rocks of the Southern California batholith with very little metamorphic terrane in the area.

b. The walls of the pegmatite dikes are roughly straight and can be traced across contacts with no change in attitude.

c. The dikes show no change in either mineralogical or bulk chemical composition, thickness, or internal structure that can be correlated with changes in wall rock lithology.

d. The country rock show no change in either mineralogical or bulk chemical composition or texture as the pegmatite contact is approached.

e. The contact of the pegmatite and the tonalites is sharp mineralogically and texturally.

The larger masses of igneous rocks in the area range from tonalite to granodiorite in composition; whereas the pegmatites are truly granitic in composition. Thus there is a break either in time or space between the pegmatites and the exposed nearby igneous rocks. The pegmatites are distinctly younger than the large masses of igneous rocks but are probably of the same general age as these rocks. For example only about 30 miles from the Ramona district, and well within the Southern California batholith, the Pala pegmatite district has been shown by absolute age determinations to be the same general age as the batholithic rocks (Jahns, 1955, p. 1054).

Thus the pegmatites at Ramona probably represent the end product of a differentiated batholithic magma; so that in waning stages of magmatic activity a pegmatitic magma could be injected into already solidified rock units. The apparent lack of a rock unit of close genetic relation to the pegmatites is no doubt a function of exposure.

A metamorphic or metasomatic origin for the pegmatite bodies is considered unlikely because the pegmatites show no relic structure of a pre-existing igneous rock and because of the criteria advanced earlier in this section. If the dikes had formed by some process as lateral secretions, it would seem likely that there would be mineralogical or textural difference in the country rock that would bear some systematic relationship to the distance of the rock from exposed pegmatites. Such a relationship was not found.

Bellemin and Merriam (1958) in discussing the origin of the rhyolite clasts in the Poway conglomerate state,

> "Toward the end of the magmatic differentiation process in the batholith magma, an acid magma (about 75 percent SiO_2) had been produced. The most salic portion was probably concentrated at the roof which, by this time was rather thin and weak. Some of this magma escaped through the roof in minor local intrusions as dikes and sills which led to the surface to form several small flows with large masses of interbedded pyroclastics.... The areas affected by these rhyolitic extrusions were small and not evenly distributed. One extrusive center was probably in the general region of Ramona."

If the ideas presented by Bellemin and Merriam are correct, the residual magma in the Ramona area would have been extruded and no longer available for pegmatite formation. Because of this it is necessary to consider the validity of Bellemin

and Merriam's proposal in regard to the origin of the clasts in the Poway conglomerate.

Bellemin and Merriam suggest a source area for the rhyolite clasts within 50 miles. In a study of high mountain streams Miller (1958) shows particle wear to be much less than the value assumed by Bellemin and Merriam (1958). On the basis of data from Miller's study the source area could be considerably more distant than 50 miles.

Because the eight analyzed Poway clasts generally fit extensions to the variation diagrams for rocks of the Southern California batholith, Bellemin and Merriam suggest a genetic relationship to the batholithic magma. However, the average of rhyolites listed by Johannsen in Volume II (1932) also fits the variation diagrams.

Furthermore, absence of feeder dikes or other evidence of extrusive activity at Ramona would require an explanation. The statement that the roof of the batholith was rather thin and weak by the time an acid magma was produced by magmatic differentiation is not justified from any evidence presented by Bellemin and Merriam.

In conclusion there does not appear to be any evidence to support a hypothesis involving extrusion of a rhyolitic magma, derived from the batholithic magma, in the Ramona area or elsewhere in the Southern California batholith. Consequently, the assumption that the pegmatite magma is a derivative magma from an unexposed granite seems reasonable.

In summary, all available evidence indicates that the

pegmatites crystallized from a liquid, possibly with a vapor phase, that was injected into the country rock.

Development after Emplacement

The post-emplacement history of the pegmatite magma is difficult to determine with certainty because the pegmatite may have crystallized in either an open system, closed system, or a restricted system. With open system conditions, the space occupied by the pegmatite represents a channel along which the pegmatite melt or vapor moved. In a closed system the pegmatitic magma is injected into the pegmatite chamber and undergoes crystallization without appreciable addition or escape of material from the system. Cameron and others (1949, p. 99) describe the restricted system as "a system closed to the extent that nothing is added to it from the source of the liquid between the time of the original injection and the end of the zone development, but open to the extent that material may escape during crystallization, and reactions of the pegmatite and its walls may take place".

If the pegmatites had crystallized in an open system it would seem likely that the crystals forming would be oriented in response to the pegmatitic liquid flowing through the system. Such flow structures have not been found, thus suggesting that the pegmatites did not crystallize in an open system. The closed system also appears unlikely for a water saturated pegmatitic magma because the crystallization of anhydrous phases would result in an increase in the water vapor pressure ultimately causing a release of this pressure either by a slow

diffusion process or by a failing or explosive process.

Crystallization of the pegmatite in a restricted system appears to best explain the observed features of the pegmatites. This in no way implies that the restricted system is the only possible system that can be used to explain pegmatite features, but rather that the features of the Ramona dikes can most readily be explained with such a system. Subsequent discussions will be limited to the restricted system hypothesis.

Sequence of Formation of the Pegmatite Zones and Units

As discussed earlier, it is most likely that the pegmatites crystallized from a liquid and probably a vapor phase. With such a situation, crystallization no doubt proceeded from the wall inward; because if crystallization was from the core outward, the early forming crystallized core would be unsupported spatially in the liquid phase. The possibility that the dikes crystallized so that a pegmatite rock unit developed shells or layers by successive peripheral replacement cannot unequivocally be denied. However detailed examinations of the peripheral or wall zones has failed to reveal any evidence of a pre-existing pegmatite rock. Other evidence against a peripheral replacement origin for the pegmatites is that material from inner zones is found to extend along fractures into outer zones, whereas the reverse is not true. Using the assumption that plagioclase having the highest anorthite content should form first from a crystallizing system, the variation of the anorthite content of the plagioclase should indicate the

sequence of formation of the zones. As shown in the section on mineralogy, the layered aplite, occurring generally as the footwall unit of the Ramona pegmatites, has plagioclase with the highest anorthite content as determined by the optical properties of the mineral.

To summarize, all available evidence indicates, although it does not unequivocally prove, that the dikes crystallized from the walls inward. In subsequent discussions the spatial position will be considered to be indicative of the relative age of the pegmatite zone or unit in those cases where other evidence is lacking.

The layered aplite generally occurs on the footwall side of the pegmatite and contains included and embayed blocks of graphic granite. Also in the layered aplites are euhedral graphic perthite crystals. In the zones of graphic granite and other coarse grained pegmatite units, there are commonly stringers or layered aplite. Definitive veining relationships between the graphic granite and the layered aplite have not been found. On the basis of the evidence cited, it seems most likely that the graphic granite and layered aplite either cocrystallized or crystallized in an alternating sequence.

In the ideal case, the graphic granite and the layered aplite form opposite wall zones of the pegmatite. Being the wall zones with no evidence of having replaced earlier units, the graphic granite and the layered aplite are considered to be the oldest zones in the pegmatites.

Because the quartz-perthite pegmatite zone lies between the border zones, it is considered on spatial relationships to be a younger zone.

Quartz cores are only rarely present in the Ramona pegmatites. Where the quartz core is found, it is between the quartz-perthite pegmatite and the layered aplite, in the quartz-perthite pegmatite and the layered aplite. Consequently, the quartz is considered younger than the quartz-perthite pegmatite. The quartz cores in these pegmatites have the appearance of local segregations and are rarely more than several inches thick.

Quartz-albite, or cleavelandite, rocks vein the graphic granite and they occur as anhedral masses and veins in the quartz-perthite pegmatite. On this basis the quartz-albite rocks are considered younger than the graphic granite and quartz-perthite pegmatite. Spatial relationships were not found between the quartz core and the quartz-albite rocks. With other units it is found the concordant units predate the discordant units. This suggests, but certainly does not prove, that the concordant quartz core predates the discordant quartz-albite rocks.

Pegmatite pockets are found on the contact or in all of the units, except the quartz-albite rocks, suggesting that the pocket pegmatite was one of the last units to crystallize.

A period of deuteric alteration and secondary mineralization followed the formation of the primary units and zones in the pegmatites. This is particularly well shown at Spessartite Ledge where the alteration zone cuts and replaces the graphic granite, quartz-perthite pegmatite, and pocket pegmatite.

Rarely tourmaline altered to muscovite and garnet altered to manganese oxide are found. The relationships of this alteration period and the period of deuteric alteration is not known.

The sequence of formation of the pegmatite zones and units is shown diagramatically in figure 39.

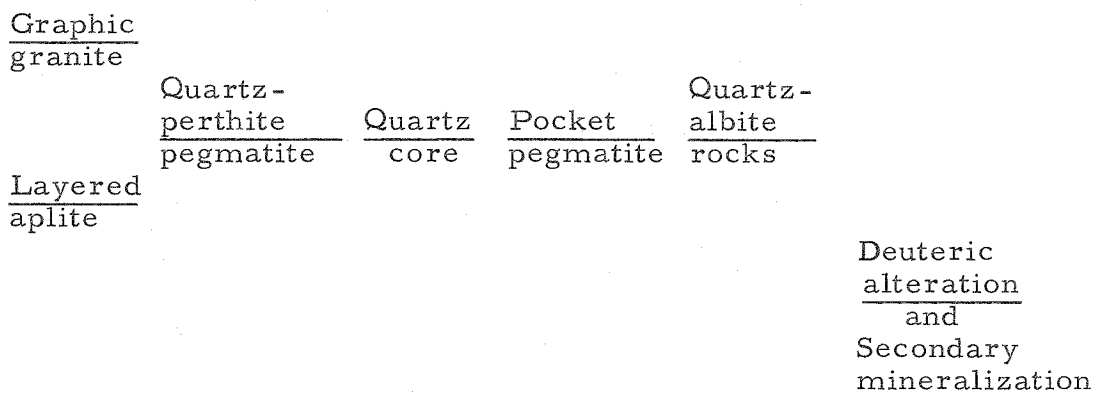

Figure 39. Sequence of formation of the zones and units of the Ramona pegmatites

Paragenesis of the Pegmatite Minerals

It is the purpose here to establish the paragenesis of the pegmatites on the basis of the paragenesis of the minerals of each unit of pegmatites as given in prior sections of this report. Several rare minerals are not listed in the paragenetic sequence because their relationships are not known. The composite paragenetic sequence for the minerals is shown in figure 40.

Formation of the Pegmatite Zones and Units

Layered Aplites

Nature of the Problem

The origin of the layered aplites that occur within borders of pegmatites is a problem common to many pegmatite districts.

FIGURE 40

DIAGRAM OF PARAGENESIS OF PEGMATITE MINERALS

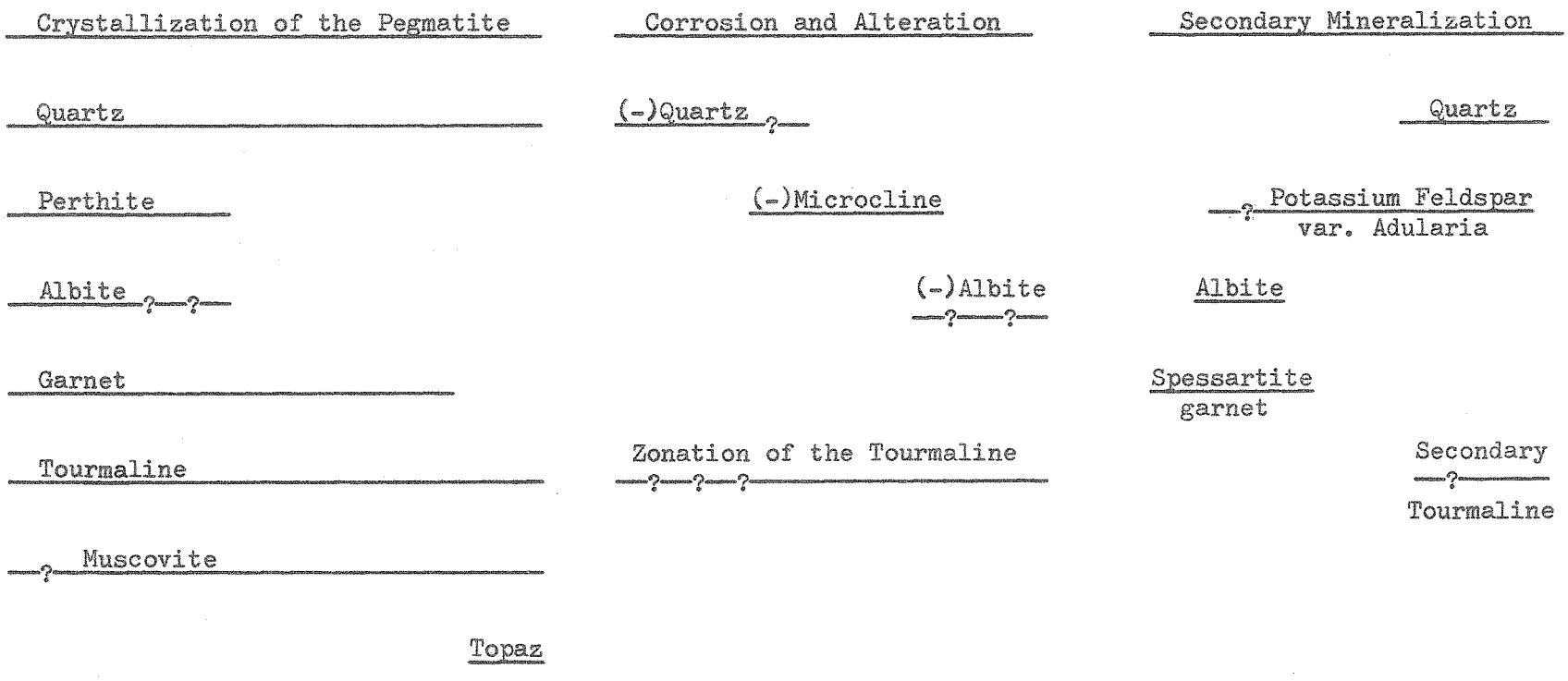

Many modes of origin have been proposed to explain the features of these rocks. Jahns (1955) summarizes the various interpretations for this rock unit as follows,

> "It (the layered aplite) was contrastingly interpreted in California occurrences by Waring (663*, p. 366) as an early product of simple crystallization from a 'hydrous magma', by Merriam (419, p. 242-243) as the result of rhythmic replacement in an early, probably primary aplite, and by Schaller (535, p. 274-277) as a late stage product of replacement of pre-existing graphic granite by soda-rich solutions. An origin by channel-controlled hydrothermal replacement of earlier pegmatite minerals was suggested for occurrences in Wyoming by McLaughlin (414, p. 62-63), whereas rhythmic primary crystallization, accompanied in some instances by streaming of liquid, was favored for occurrences in Colorado by Staatz and Trites (610, p. 23-24) and by Thurston (628, p. 30-31, 65)."

The applicability of these proposed mechanisms to explain the formation of the layered aplites at Ramona is tenuous for the following reasons:

a. There is no textural evidence indicating that some minerals have replaced other minerals to form the layers, or that there has been extensive replacement of a pre-existing rock unit.

b. The observed similarity in the quartz-microcline-albite ratios between layers of the layered aplite seems unlikely if some layers are the result of a selective replacement process.

c. If the layers were the result of a channel controlled replacement process it would seem likely that these layers would be concentrically arranged around the channel. The layers in the Ramona aplites are not concentric nor is there any evidence of a pre-existing channel way.

d. If there had been a primary crystallization accompanied by a streaming of liquid it would seem likely that elongate crystals, as tourmaline, would be

---

*Numbers refer to Selected References listed by Jahns (1955). Also listed in this report by name of investigator.

preferentially oriented in response to the streaming or flowing liquid. The tourmaline in the layered aplites at Ramona is not preferentially oriented.

Two hypotheses are presented here which might account for the features of the layered aplitic rocks. The hypotheses primarily are attempts to account for the features of the layered aplite using one intrusion of magma and processes of primary crystallization and crystal settling.

The applicability of a model using only a magma to explain the formation of the layered aplites can be initially tested by considering whether or not the accessory minerals are stable at temperatures corresponding to the liquidus temperature of the pegmatite. The accessory minerals, garnet, tourmaline, and muscovite, are useful for this consideration because, as previously considered, the accessory minerals form early in the course of crystallization of the layered aplite.

The first accessory mineral to be considered is muscovite. Because muscovite is a hydrated mineral, the range of temperature over which it is stable increases with an increase in water vapor pressure. Also the melting temperatures of a rock such as a granite or a pegmatite will decrease with increasing water vapor pressure. The point where the melting curve of the granite or pegmatite intersects the stability curve for muscovite indicates the lowest water vapor pressure at which muscovite could exist stably at liquidus temperatures of the granite or pegmatite. The probable liquidus temperatures of the pegmatites, as discussed in the section on hydrothermal investigation, and the dehydration curve for muscovite to sandine, corundum,

and water vapor, as established by Yoder and Eugster (1955), are applicable to the muscovite stability problem. From the intersection of these curves it is found that muscovite probably would not be stable at pegmatite liquidus temperatures unless the water vapor pressure of the system were greater than about 2.4 kilobars.

Tourmaline is of special interest because it was probably one of the first as well as one of the last minerals crystallizing in the layered aplite. The meager information about tourmaline stability is from work by Frondel, Hurlbut, and Collette (1947). In their study they showed black tourmaline to melt at 1550°C. They also synthesized tourmaline at 400 to 500°C in the presence of water. Unfortunately nothing is known about the tourmaline phase relations in a magmatic system of pegmatite composition. However in view of the dry melting temperature and the formation of tourmaline in the presence of water, it is tentatively concluded that tourmaline would be stable at magmatic temperatures.

The stability of almandite garnet has been investigated by Yoder (1955), and very meager information is available on the almandine-spessartite series from work by Michel-Levy (1951). Yoder shows almandite to melt incongruently to hercynite, iron cordierite, and fayalite. Temperatures for this incongruent melting at even moderate water vapor pressures are considerably higher than the liquidus temperature of the pegmatite. Assuming that the substitution of manganese for iron in almandites does not radically change the stability relation,

garnet would be stable on the liquidus of the Ramona pegmatite at about 1 kilobar water vapor pressure or greater.

In conclusion, at about 2.4 kilobars or greater of water vapor pressure, it appears likely that the accessory minerals would be stable at liquidus temperatures of the Ramona pegmatites. If these minerals could not exist stably at the magmatic temperatures, it would be necessary to consider metastable crystallization or a non-magmatic origin for the accessory minerals.

The proposed system using only relative or assumed values for the variables may be explained by considering combinations of the mineral phases grouped as "end-members" of a ternary system. In this manner one end-member comprises garnet, muscovite, and tourmaline, while the other two end-members are quartz and feldspar respectively. For obvious reasons, this proposed system is not to be confused with a three-component phase diagram. By lowering the temperature of a magma of appropriate composition, the field of garnet, tourmaline, and muscovite is entered with the separation of these crystalline phases. With the early formation of these phases the composition of the residual system moves toward the boundary curve that encloses the garnet, tourmaline, and muscovite field. At the boundary curve the accessory minerals, garnet, tourmaline, and muscovite, and quartz or feldspar will crystallize; and at a specific point on the curve all mineral phases will co-crystallize. As in the $NaAlSi_3O_8$-$KAlSi_3O_8$-SiO_2-H_2O system (Tuttle and Bowen, 1958), a water vapor pressure change is

considered to shift the position of the boundary curves. Thus the assemblage of minerals crystallizing at the minimum point could alternate with minerals crystallizing from one of the phase fields because of water vapor pressure fluctuations. If equilibrium conditions did not exist in the system, there would be some undercooling before crystallization occurred, and the observed liquidus surface would be below the equilibrium liquidus surface.

Assuming that the magma is saturated or nearly saturated with water, the liquidus temperature at moderate pressure decreases with increasing water vapor pressure. At extremely high pressures the curve may have a positive slope because of the shift of mineral phase boundaries with water vapor pressure, the effect of pressure on the solubility of water in a magma, and the pressure effects on the melting of a solid. However, investigations of the liquidus of a Ramona pegmatite sample at water vapor pressures to 3.1 kilobars did not show any indication of a reversal of the negative slope of the curve. Therefore it appears unlikely that the liquidus curve could have a positive slope at pressures that would be geologically reasonable for the formation of pegmatites. If the temperature and pressure are the two variables of interest, there are the following cases:

1. The pressure resulting from the intrusion of the magma is greater than the lithostatic pressure so that crystallization may proceed either by a loss of heat or a decrease of pressure on the magma.

2. The pressure resulting from the intrusion of the magma is about equal to the lithostatic pressure so that crystallization will proceed primarily by a loss of heat.

Hypothesis I

Where the pressure resulting from the intrusion of a water saturated magma is greater than the confining pressure, crystallization of the magma may be initiated either by a loss of heat from the system or by a decrease of water vapor pressure on the magma, assuming of course that the liquidus temperature of the magma decreases with increasing water vapor pressure. Figure 41 diagrammatically illustrates this situation.

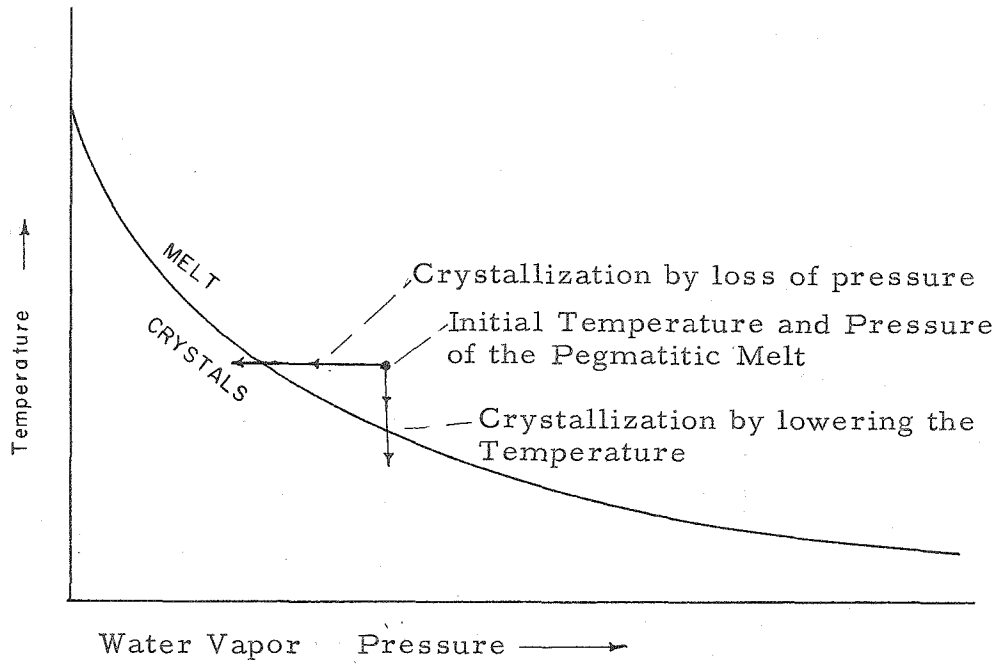

Figure 41. Sketch showing crystallization of a melt by a loss of pressure or by a lowering of temperature.

Crystallization in the system illustrated can be terminated by arresting the loss of heat from the system, exhausting the supply of magma or liquid, changing the composition of the system by the introduction of external material, or by increasing the water vapor pressure of the system. None of these mechanisms for halting crystallization adequately explain how a crystallizing magma can

be repeatedly stopped and started except for the pressure mechanism. Consider the situation where the system is isothermal, then an increasing or decreasing of the water vapor pressure can start or stop crystallization.

The absence of chilled contacts between the Ramona pegmatites and the batholithic country rock indicates that the country rock was as hot or nearly as hot as the pegmatite magma. Consequently, the heat loss from the pegmatite dikes would correspond to the slow cooling rate of the southern California batholith, and a gross error is probably not introduced by considering an isothermal model to explain the crystallization of the layered aplite. Pressure changes may be the result of forceful injections in pulses of the pegmatitic magma. Or it may be that there exists a magma chamber serving as a pressure reservoir supplying the pegmatite magma at a pressure greater than the confining pressure. Failure of the confining chamber for the pegmatitic magma may have been in discrete steps so that the cycle of pressure build up-failure-pressure release could be repeated many times.

Because of the effect of water vapor pressure on starting and stopping crystallization of a system and of shifting the boundary between cocrystallizing mineral phases, it is possible to propose a mechanism for the formation of the layered aplites as follows:

a. At the highest water vapor pressures there are no minerals crystallizing from the melt.

b. With decreasing water vapor pressure the field of garnet, tourmaline, and muscovite is entered with the formation of these minerals.

c. At still lower water vapor pressures the system crystallizes quartz and feldspar along with garnet, tourmaline, and muscovite because of a shift in the position of the boundary of the cocrystallizing mineral phases.

d. Crystallization of all mineral phases will continue until an increase of pressure effects the same sequence of steps in reverse.

Diagrammatically the sequence of steps listed for the crystallization of minerals is shown in figure 42.

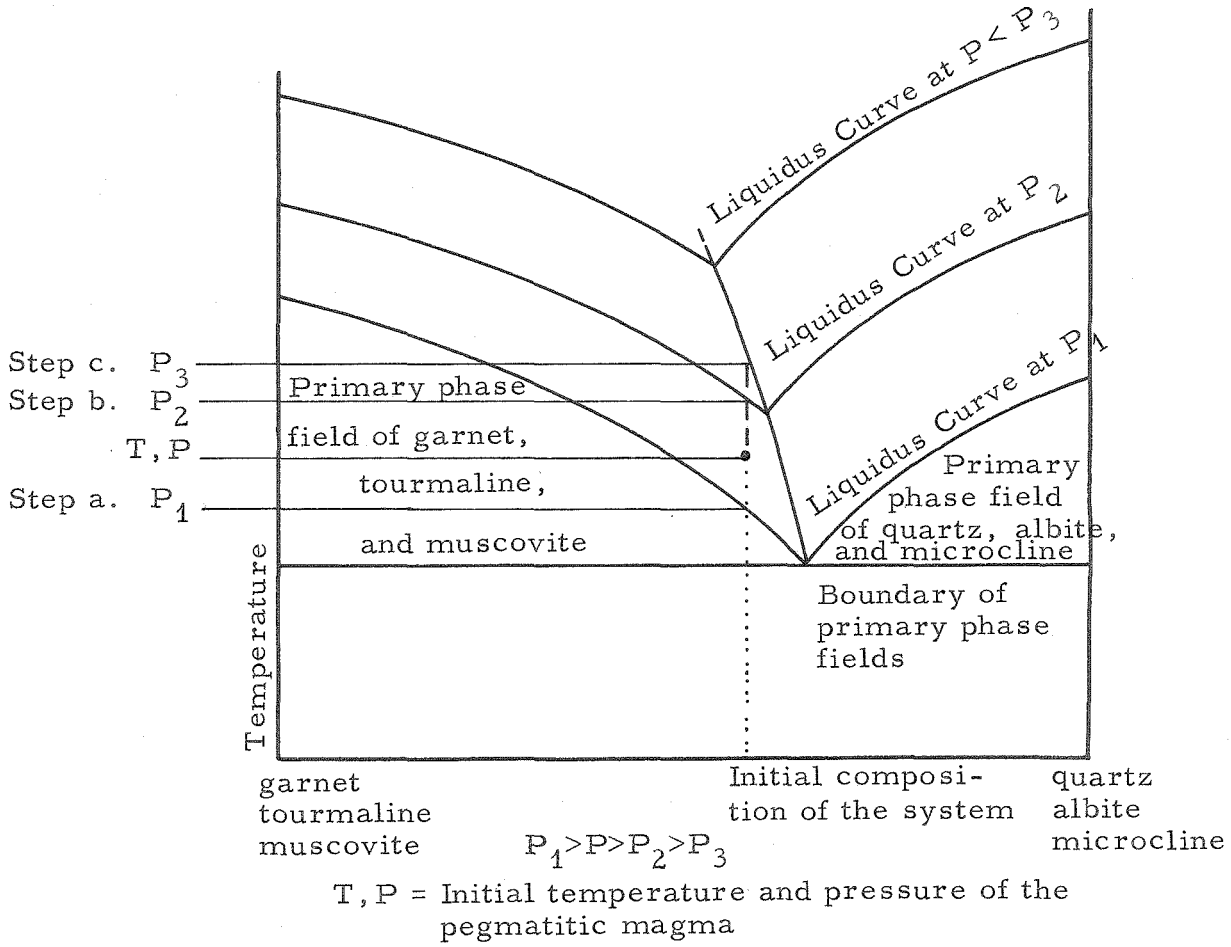

Figure 42. Suggested sequence of steps for the crystallization of the layered aplites.

If crystal settling is considered as an operative mechanism in a pegmatitic melt, it would be possible to concentrate the tourmaline and garnet in layers because these minerals would continue to crystallize and settle through the melt after the other minerals stopped crystallizing. If the overlying rock was to fail, thereby releasing the pressure, all minerals would begin to crystallize and settle through the melt. Thus the concentration of tourmaline and garnet now would be diluted by quartz and feldspar. The feasibility of a crystal settling mechanism will be discussed further when the viscosity of the magma is considered.

Hypothesis II

The major difference between this hypothesis and the one previously discussed concerns where the crystals form and how they aggregate as layers. In the first hypothesis the crystals were considered to form throughout the melt and later be concentrated in layers by gravity settling. In both hypotheses only one magma is required, the magma is considered saturated or nearly saturated with water, and the country rock is considered to be as hot or nearly as hot as the pegmatitic magma. The basic model for both hypotheses is the same in that pressure is considered to change the assemblage of minerals crystallizing by shifting the mineral phase boundaries. Thus the mineral assemblage garnet-tourmaline-muscovite because of pressure changes might alternate with quartz-albite-microcline. The model and the boundary conditions are described under hypothesis I and therefore require no further discussion in this section.

It is proposed in this hypothesis that crystallization begins where the magma is in contact with the country rock and progresses toward the center of the dike. The reason for crystallization to begin near the contact of the country rock and the pegmatite may be because the country rock is at a slightly lower temperature than the pegmatite magma. In such a situation the magma adjacent to the country rock would be the part of the magma with the lowest temperature and therefore be a likely site for formation of crystals. Subsequent crystallization, in gross relations, would be parallel to the contact between the country rock and the pegmatite and would progress as a front toward the center of the dikes.

An alternation in the assemblages of minerals crystallizing at any one time could account for the layering of the aplite with the proposed model where crystallization begins at the pegmatite-country rock contact and progresses as a front toward the center of the dike. As mentioned in a prior paragraph, the alternation in the assemblages of the minerals is probably because of water vapor pressure changes.

With the present lack of specific data on the viscosity of water saturated magmas at high pressure it is not possible to ascertain whether the explanation advanced by hypothesis I or II is the most reasonable to account for the features of the layered aplites. The layering of the aplites is not an essential part of the explanation of the origin of the pegmatite dikes. Therefore the ambiguity in the explanation of the layering of the aplite need not distract from later discussions concerning the genesis of the

pegmatites.

With either hypothesis, the large anhedral crystals of quartz, microcline, and albite could be a late stage crystalline product of liquid or melt that was interstitial to the small euhedral crystals of quartz, albite, tourmaline, and garnet.

Graphic Granite

Orientation of the Quartz Rods

It seems likely that if graphic granite were formed by replacement, the rods, tablets, and runic characters of the quartz should be preferentially oriented along cleavages or other planes related to the crystal structure of the host feldspar. In the Ramona graphic granite this relationship has not been found. Bastin and others (1931), in discussing ore textures, point out that when replacement is proceeding in two directions the replacement textures are commonly characterized by a thickening of the replacing mineral at the point of intersection of this mineral. In the Ramona graphic granite, tabular quartz crystals commonly intersect at an angle of about 60°, but commonly there is no thickening at the point of intersection. Furthermore, if the quartz replaced perthite, it seems likely that there would be areas or veins of large masses of quartz. This is not found in the Ramona graphic granite. In conclusion, there is no evidence that the graphic granite formed by replacement of a pre-existing pegmatite or that the quartz rods in the graphic granite formed by replacement of perthite.

Exsolution features, as observed in ores, metallographic specimens, and even silicate minerals, commonly appear

very similar to textural features of graphic granite. But typically exsolution occurs along some crystallographic plane, as ilmenite exsolving from a magnetite on the octahedral face. The graphic granite, in contrast, does not show a marked preferential orientation of the quartz as would be probable if exsolution took place on some crystallographic plane. More compelling evidence against an exsolution origin for the graphic granite lies in the apparent absence in nature of a homogeneous mineral that has a composition similar to the bulk composition of graphic granite. If such a homogeneous compound exists, even if metastable, it would almost certainly have been observed in the detailed investigation of the $NaAlSi_3O_8$-$KAlSi_3O_8$-SiO_2-H_2O system by Tuttle and Bowen (1958).

A remaining possibility for the formation of the texture of graphic granite is that the quartz and feldspar crystallized simultaneously. Wahlstrom (1939), in discussing the orientation of quartz in graphic granite states (p. 685) "If it is a fact that the quartz is everywhere definitely oriented, a strong point is gained in favor of a theory of simultaneous crystallization". Yet simultaneous crystallization does not require a graphic texture as is well shown by ores, metallographic specimens, and silicate minerals. Therefore the problem of why graphic granites have their unusual texture is still present.

With conditions of simultaneous crystallization in a thermal flux, there is a possible cause for orientation of the quartz rods in the graphic granite. Assuming a situation where the

country rock is cooler than the pegmatite, there would exist a heat flow roughly perpendicular to the walls of the pegmatite. In regard to this mechanism, Buckley (1951, p. 273) states, "Another means by which crystals may be oriented during growth from the molten condition is that whereby a unique crystallographic axis being also a direction of maximum heat conduction essays to align itself with the direction of flow of the heat leaving the cooling system". In view of Buckley's statement it would seem that the quartz and feldspar may be oriented so that their axes of greatest thermal conductivity are parallel to the direction of heat flow.

The thermal conductivity mechanism was considered for the Ramona graphic granites by measuring the orientation of quartz rods in relation to the surface of the pegmatite. The results of this study are shown in figure 18. It was found that for the samples measured there is no coincidence between a normal to the surface of the pegmatite and the c axis, the axis of greatest thermal conductivity, of the quartz rods. Therefore thermal conductivity is not considered as a functional mechanism for the orientation of the quartz rods in the Ramona graphic granites.

Another possible cause for the orientation of the quartz rods is that of parallel or epitaxis growth. Frondel (1936, 1940) conducted some very informative studies in this field. In particular he studied the orientation of staurolite, garnet, and zircon on muscovite from the Manhattan schist. He concluded that these crystals, after settling on the surface of muscovite, gradually rotated

to take positions of relatively low interfacial energy. Many examples of epitaxis are cited in the literature with most of them being alkali or halide salt crystallizing on other salts or on mica. One of the most important features of parallel growth is that there is a similarity in distance between like atoms or ions of the one structure and like atoms or ions of the other structure.

In view of the above discussion it would appear likely that there would be certain planes on which the quartz and feldspar of the graphic granite would have the best structural fit.

To investigate the possibility of epitaxis growth in graphic granites the unit cell dimensions were compared for the mineral contact faces listed in table 11. In general it was found that the unit cell repeats in the planes of contact are not similar for the two minerals. Translation of the trigonal quartz structure to an orthorhombic type structure failed to produce better structural fit for the quartz-feldspar contact planes. The lack of similarity of unit cell dimensions between quartz and feldspar for the contact planes suggests that epitaxis is not the mechanism for producing graphic granites.

It was found in one specimen of graphic granite that there are many connections between the quartz rods. Considering the situation where there are interconnected quartz rods, it is more easily understood how graphic textures can be developed. Crystals of quartz and feldspar form which, with growth, become in contact with each other. The contact plane need not be crystallographic planes for the minerals; however in the event that one mineral forms on the other, it is probable that the contact plane

will be a crystallographic plane. Continuing growth of the two minerals at different rates, or fluctuations in concentration of the constituents of the minerals in the liquid or the vapor, could result in rapid growth of one mineral followed by rapid growth of the other. In this manner, alternately a quartz rod and then a feldspar host could crystallize. The graphic character found in many quartz rods is no doubt the result of the development of the $\{10\bar{1}0\}$ face on the growing quartz rod.

Conditions for Crystallization of Graphic Granite

In establishing the conditions of crystallization for the graphic granite, the following features must be considered:

a. The perthite host crystals and the quartz rods are very large compared to most crystals in igneous rocks.

b. Well developed crystal faces are found as the quartz and feldspar of the graphic granite.

c. The composition of the graphic granite does not correspond to the minimum or even a cotectic in the $NaAlSi_3O_8$-SiO_2-H_2O system.

d. The graphic texture of the rocks.

e. Where the graphic granite zone is best developed it is on the hanging wall of the pegmatite dikes.

These features are most readily explained as a product of simultaneous crystallization from a vapor phase for the following reasons:

1. Well formed crystal faces are commonly found on minerals that crystallize from a vapor phase, or a watery liquid phase, for example the mineral found in vugs.

2. The occurrence of the graphic granite on the hanging wall of the dikes is consistent with where it would most likely be if it crystallized from a vapor; because the vapor would tend to be above the liquid phase.

3. The composition of the graphic granite can not be explained by crystallization from a melt without invoking some process for differentiating the liquid or changing the liquid so that the general relations in the $NaAlSi_3O_8$-$KAlSi_3O_8$-SiO_2-H_2O are not applicable.

4. Vugs and cavities are found in the graphic granite indicating that a vapor phase was present during the formation of the rock.

In the section on the orientation of the quartz rods reasons have been advanced for concluding that graphic granite formed by simultaneous crystallization.

To summarize, all evidence indicates, although it does not conclusively prove, that the Ramona graphic granite is a product of simultaneous crystallization from a vapor phase. Subsequent discussions and the model proposed for the crystallization of the pegmatites are based on this mode of formation of graphic granite.

Coarse-Grained Pegmatite

The origin of the coarse-grained pegmatite, or quartz-perthite rock, is problematic because it occurs with large variations in texture and mineralogical composition. The two most noticeable textural features of the rock are the abundant euhedral crystals or phenocrysts of perthite and the rare presence of corroded and embayed blocks of graphic granite. These corroded and embayed blocks of graphic granite might be considered to indicate that the quartz-perthite rocks formed by replacement of a pre-existing graphic granite. However, if this is the situation, it would seem likely that there would be corroded and embayed blocks of layered aplite included in the quartz-perthite rocks; because the layered aplite, like the graphic granite, is

also a zone that crystallized before the coarse-grained pegmatite. Corroded and embayed blocks of layered aplite are not found in the quartz-perthite rocks nor is there any evidence of a relic layered aplite texture. A possible explanation for the blocks of graphic granite in the quartz-perthite rock is that the blocks of graphic granite become detached from the hanging wall of the dikes and settle into the crystallizing magma. In this situation it may be that the irregular outline of the graphic granite blocks is the result of overgrowths rather than corrosion of the blocks.

Pocket Pegmatite

The pocket pegmatite contains minerals with euhedral crystal form and also rare minerals as topaz, lepidolite, and various colored tourmalines. Cleavelandite occurs in the pocket pegmatite as aggregates of platy crystals. Generally there are no other minerals interstitial to the plates of cleavelandite.

If the pocket pegmatite crystallized from a liqud or melt, it would seem likely that there would be minerals interstitial to the plates of cleavelandite that would form from trapped interstitial liquid. These interstitial minerals are not found in the cleavelandite aggregates. The euhedral form of the minerals and the rare minerals are also features of the pocket pegmatite that are not readily explained if the minerals crystallized from a liquid.

In the pocket pegmatite there is not widespread pseudomorphism of earlier minerals nor is there evidence of relic structures or textures of a pre-existing rock. Thus a replacement

origin for the pocket pegmatite seems unlikely.

To summarize, it seems most likely that the pocket pegmatite crystallized from a vapor phase rather than a liquid phase with little or no replacement of pre-existing rock.

Albite-Quartz Rocks

With the known phase relations in systems roughly comparable to the bulk composition of the Ramona pegmatites, it is difficult or impossible to crystallize albite and quartz in a ratio similar to that found in the albite-quartz rocks. There is also no evidence that these rocks formed by replacement of pre-existing rock. It is reasonable to consider these rocks as having crystallized from a vapor; and, although this is by no means proven, it will be used in subsequent discussions concerning the origin of the pegmatite dikes.

Corroded Rocks and Crystallization of Secondary Minerals

Formation of Rock Features and Major Minerals

The corroded rocks occur in a zone that transects most of the other pegmatite zones and units, thus indicating that the period of corrosion occurred after the crystallization of the pegmatites. In view of the many cavities in the corroded rocks, it seems unlikely that the corrosion was effected by a viscous silicate melt. A more likely agent for the corrosion is a hydrothermal fluid. The euhedralism of the secondary minerals and their projections into cavities also suggests that they crystallized from a hydrothermal fluid rather than a viscous melt.

There is no good indication of the duration of time between the end of crystallization of the pegmatites and the beginning of the period of corrosion.

Information concerning the temperature of the hydrothermal fluid is very meager. The secondary quartz has a typical α crystal form. The secondary potassium feldspar shows no triclinicity by either optical or x-ray methods. It is not known whether this potassium feldspar formed under metastable conditions or whether it failed to invert to the more stable triclinic form for some reason as exceptional purity of the mineral or rapid cooling. The dominant {110} crystal faces give this potassium feldspar an adularia habit. The full significance of the adularia habit is not known. Spessartite garnet formed late in the period of corrosive activity or early in the period of secondary mineralization. Michel-Levy (1951) formed spessartite garnet at 500°C. at a water vapor pressure of 1000 kg/cm^2. Thus the presence of spessartite garnet does not necessarily indicate a

high temperature.

In conclusion the best indication of temperature during the period of corrosion and secondary mineralization is the presence of secondary quartz with the low temperature or α form. For example at 2000 bars pressure this would indicate that the temperature was less than 625°C.

Because the sequence of corrosion and deposition of minerals in these rocks has been determined, it is possible to propose curves for the solubility of the mineral phases in the hydrothermal fluid. The sequence of corrosion of minerals was quartz-microcline-albite and the sequence of deposition was albite-microcline-quartz. The solubility curves for these minerals in the hydrothermal fluid based on observed features of the rocks are shown in figure 43.

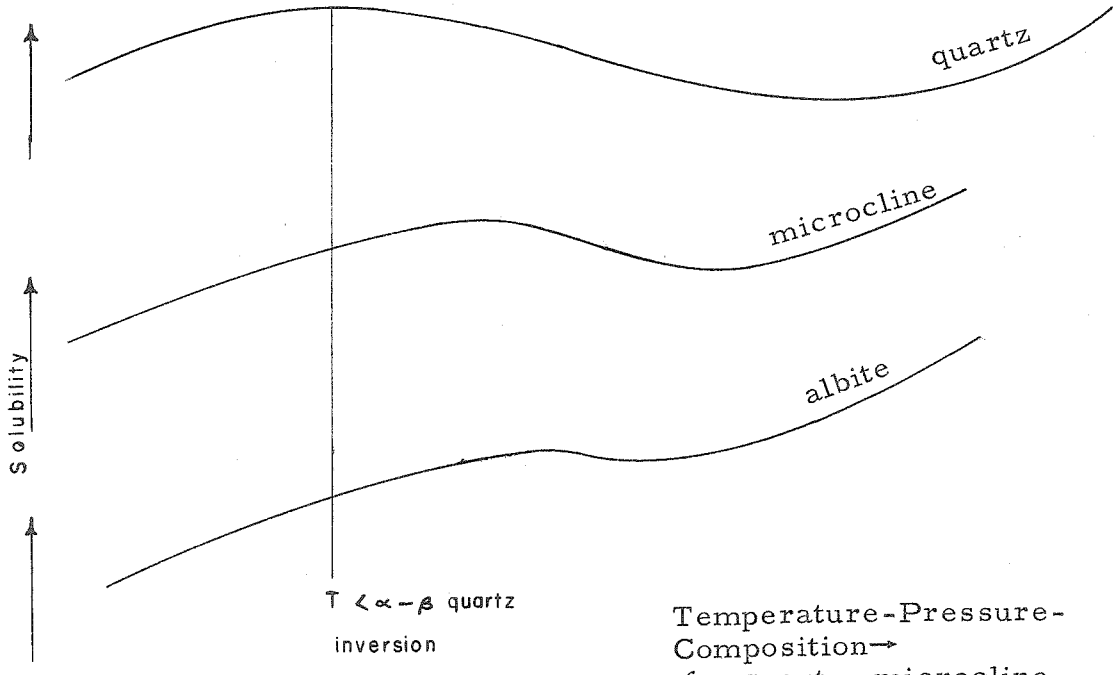

Figure 43. Proposed solubility curves for quartz, microcline, and albite.

These curves are a function of the temperature, pressure, and also composition of the system, and therefore the experimental data on the solubility of solute in water vapor shown in figure 38 may not be applicable to the curves established from the features of the corroded rocks. If the fluid pressure of the natural system equals the lithostatic load, the pressure can be considered constant. Assuming that the composition of the system does not have a great effect on the position of the maximum of the quartz solubility curve, it is then unlikely that the pressure of the hydrothermal fluid could have been much greater than 2000 bars. If the pressure had been greater than 2000 bars β quartz could form and also the corrosion would be at temperatures above the minimum melting temperature of the rock (figures 33, 34, and 35).

Crystallization of Spessartite Garnet

Spessartite garnet and its mode of occurrence have been described in previous sections. To review briefly, the spessartite garnet present in the corroded rocks is nearly pure manganese garnet. In association with this garnet is primary and secondary potassium feldspar, albite, and tourmaline and secondary quartz. Mica is not found in any of the corroded rocks.

The formation of spessartite requires a source of manganese. This source can not be determined with certainty; however there are two likely explanations. The manganese may have come from decomposition of the tourmaline or from the decomposition of mica. On the basis of an analysis of tourmaline and mica, the manganese oxide content of the minerals is about 1 and 2 percent.

Temperature and Pressure of Formation of the Ramona Pegmatites

The most plausible temperature and pressure of crystallization of the Ramona graphic granite and layered aplite is in the range of 690 to 720°C. and 3500 to 4500 bars. This temperature and pressure range is based on the point where the alkali feldspar solvus intersects the liquidus and on the composition of coexisting feldspars.

The perthite of the graphic granite and the albite of the layered aplite are coexisting feldspars because of the cocrystallization of the units. By optical methods an average composition of the plagioclase in the layered aplite and the microcline perthite in the graphic granite was found to be about $(NaAlSi_3O_8)_{90-95}$ $CaAl_2Si_2O_8)_{10-5}$ and $(KAlSi_3O_8)_{70}$ $(NaAlSi_3O_8)_{30}$.

Fortunately, Yoder et al. (1956-57) have experimentally determined tie lines connecting coexisting feldspars in equilibrium with a liquid and a gas. A plot of the experimentally determined tie lines of the coexisting plagioclase and alkali feldspar is shown in Figure 44.

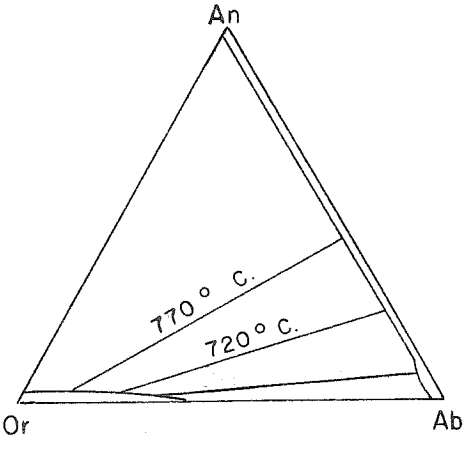

Figure 44. Plot of experimentally determined tie lines for coexisting feldspars in equilibrium with a liquid and a gas. The lowest tie line shows the composition of coexisting feldspars in the Ramona pegmatites.

In relating the natural feldspars from Ramona to an experimentally determined system the following assumptions must be made:

1. The plagioclase and microcline-perthite crystallized in equilibrium with each other.

2. Their composition has not changed subsequent to their time of crystallization as single phases.

3. The pressure of the natural system corresponds to the pressure of the experimentally determined system; or that pressure has a small effect on the orientation of the tie-line.

4. And that the compositional difference between the experimental system and the natural system does not have a significant effect on the position of the tie-line.

The first assumption is considered reasonable since field evidence indicates that the graphic granite and the layered aplite formed simultaneously. Because the feldspars do not show alteration, zoning, or exsolution other than the perthitic exsolution, it is thought that their composition has not changed subsequently to their time of crystallization. The effect of pressure on the orientation of the tie-lines has not been accurately determined. However Yoder et al. (1956-57, p. 213) states, "In general, the tie line makes a smaller angle to the Or-An side at high temperature and low pressure than at low temperature and high pressure." Therefore if the natural pegmatites crystallized at less than 5000 bars water vapor pressure, the temperature indicated by the tie-line of the coexisting feldspars would be a maximum temperature. The effect of different compositions on the ternary feldspar system is entirely unknown.

The orientation of the tie-line of the natural feldspars compared to the orientation of the experimentally determined

tie-lines suggests that the temperature of crystallization of the natural feldspars was less than 720°C.

Because the natural pegmatite is a two-feldspar rock, an indication of temperature and pressure can be obtained from the intersection of the alkali feldspar solvus and the pegmatite liquidus. Yoder et al. (1956-57) established the maximum of the solvus to be 715°±5°C. at 5000 bars total pressure, and they indicate that the maximum of the alkali feldspar solvus is raised 14°C./1000 bars pressure in the range of 1000 to 5000 bars pressure. This indicates an intersection of the alkali feldspar solvus with the Ramona pegmatite liquidus, as established hydrothermally, at about 710°C, and 4500 bars water.

There is about 0.25 percent CaO in the Ramona pegmatites, but the extent that this CaO raises the maximum of the alkali feldspar solvus cannot be quantitatively evaluated. However, it is certain that lime radically raises the maximum of the solvus, because one-feldspar rocks with more than 1.5 percent lime are an extreme rarity in nature. Therefore the 4500 bar water vapor pressure for the intersection of the solvus and the liquidus should be considered a maximum pressure for the crystallization of the layered aplite and graphic granite.

The dehydration curve for muscovite to sanidine, corundum, and vapor as established by Yoder and Eugster (1953) is plotted with the liquidus curve of the Ramona composite sample. The intersection of these curves at about 2400 bars water vapor pressure would then be a minimum water vapor pressure at which muscovite could exist on the liquidus of the Ramona pegmatite magma. This minimum value should be considered with due

reservation because of many unevaluated factors that may have an effect on the stability of muscovite.

To summarize, the most likely temperature range for the crystallization of the graphic granite and the layered aplite is about 690 to 720°C. The water vapor pressure must have been greater than about 2400 bars and less than about 4500 bars.

It should be pointed out that if the water vapor pressure equals the lithostatic pressure, 4000 bars of water vapor pressure would correspond to a depth of about 15 kilometers under sediments of average density. The Southern California batholith is considered to be early Upper Cretaceous in age and exposed batholith rocks were overlain with later Upper Cretaceous sediments. In view of the duration of the Cretaceous period, there was probably 20 million years during which the batholith was unroofed. To remove 15 kilometers of cover in 20 million years would require the very high erosion rate of 3 inches per 100 years. Erosion may have been at this high rate, or it may be that the pegmatites were intruded and crystallized at a pressure greater than the lithostatic pressure.

Viscosity of the Pegmatite Magma

There have been no experimental studies of the viscosity of a silicate melt in a temperature-water vapor pressure range comparable to the most likely conditions during the crystallization of the pegmatites. However, several studies have been made on hydrous silicate melts at relatively low pressures.

Wyart (1955) determined the viscosity of obsidian under

a water vapor pressure of 750 bars at 750°C. The viscosity of the hydrous melt was found to be 5×10^9 poises compared to 2×10^{13} poises at 750°C. and one atmosphere pressure. Saucier (1951) determined the viscosity of a retinite as about 10^7 poises at 980°C. and a water vapor pressure of 163 bars. The viscosity of the retinite at atmospheric pressure and 980°C. is about 10^{10} poises.

The composition of the obsidian, retinite (pitchstone), Ramona aplite (57-R-28), and the Ramona composite is compared in table 32. It is evident that the Ramona pegmatite magma had a composition very similar to the rocks used for the hydrous viscosity studies. However because of low water vapor pressure conditions of the experiments, the only conclusion that can be drawn is that high water vapor pressure would have a profound effect on lowering the viscosity of a pegmatite magma.

The layering in the aplite is suggestive of a rock formed by crystal settling. If gravitational settling is to be a functional process, the combination of time available for crystals to settle and the viscosity of the melt must be such that layers of crystals can accumulate.

Considering Stoke's Law to be applicable, the following assumptions were made:

1. The density of the melt is about equal to the average density of obsidian as listed by Birch (1942).
2. The viscosity of magma is about 10^5 poises.

From this it was found that the small crystals in the layered aplite could have settled from 100 to 300 cm. per year. The assumed viscosity of the magma seem reasonable in view of the

TABLE 32

COMPOSITION OF MELTS USED FOR VISCOSITY STUDIES COMPARED TO THE COMPOSITION OF RAMONA ROCKS

	Obsidian	Retinite	Ramona Aplite 57-R-28	Ramona Composite Glass
S_1O_2	74.37	72.05	73.53	75.19
Al_2O_3	12.65	11.25	15.03	14.73
Fe_3O_4	1.02	1.55	0.41	0.35
FeO	-	0.70	0.75	0.46
MnO	-	0.02	0.32	0.26
MgO	0.08	0.20	0.10	0.02
CaO	1.00	1.60	0.56	0.03
Na_2O	2.91	1.95	5.01	3.51
K_2O	6.77	3.65	2.96	4.48
T_1O_2	-	0.30	0.06	0.10
P_2O_5	-	0.02	ND	ND
H_2O^-	0.33	1.20	0.24	0.01
H_2O^+		6.40	0.44	0.11
F	-	0.05	0.01	0.03
Cl	-	0.03	-	-
SO_3	-	0.07	-	-
B_2O_3	-		0.49*	0.44*
L_1O_2			0.01	0.01
Rb_2O			0.00	0.09
Cs_2O			0.00	0.01
CO_2			ND	ND

* Calculated from tourmaline in modes

viscosity determination of hydrous melts as made by Saucier (1951) and Wyart (1955). As mentioned earlier, the temperature of the country rock at the time of intrusion of the pegmatite magma was most likely about the liquidus temperature of the pegmatites. With the cooling rate of the pegmatites controlled by the cooling rate of the country rock, there would be considerable time during which a process of crystal settling could be operative.

Formation of the Pegmatites

It has been concluded previously that the pegmatite forming material was a magma and that the magma was saturated with water early in the course of crystallization. The model proposed to explain the formation of the pegmatites will be based on these conditions for the pegmatite forming material.

If there is an increase in the specific volume of the water in the vapor relative to that in the melt, with crystallization there will be either an increase in the vapor pressure, an escape of the vapor, or expansion of the confining chamber. Unless the water vapor pressure greatly exceeded the confining pressure, it seems that vapor must have escaped from the system. Remembering the rhythmic features of the layered aplite, it is probable that the escape of the water vapor was in surges.

Equilibrium conditions do not exist continuously in a system in which water vapor pressure is being released in surges. However conditions for quasi-equilibrium could be present during much of the course of crystallization, and for the sake of simplicity such conditions will be referred to as equilibrium conditions. With these equilibrium conditions, crystallization may proceed

from the melt or from the vapor. It should be pointed out that if a vapor is in equilibrium with a magma, crystallization may proceed from the vapor or from the magma or from both the vapor and the magma. If several crystalline phases are forming, it is entirely possible that one may crystallize from the vapor and the other from the magma.

The cocrystallization of the graphic granite and the layered aplite can most readily be explained by a model in which the graphic granite crystallized from a vapor phase while the layered aplite crystallizes from the melt. This seems the feasible explanation for why neither the composition of the graphic granite or the layered aplite are in accord with the composition of the ternary minimum in the system $NaAlSi_3O_8$-$KAlSi_3O_8$-SiO_2-H_2O although the bulk composition of the pegmatite dikes is very similar to the composition of this ternary minimum. However a combination of the composition of the layered aplite and graphic granite in a ratio of about 1:1 very closely approximates the composition of the ternary minimum.

With a model where there is crystallization from a melt and vapor, it seems most likely that the coarse-grained pegmatite, or the quartz-perthite rocks, are a product of crystallization from both the liquid and the vapor. Thus the phenocrysts of the rock may have crystallized from vapor bubbles rising or streaming through the melt. It is possible that the blocks of graphic granite in these rocks are blocks detached from the hanging wall of the dike that have settled into the crystallizing melt perhaps with an overgrowth of perthite and quartz. Crystallization from

a melt could account for the allotriomorphic textured groundmass of quartz-perthite pegmatite rocks.

Evidence has previously been presented indicating that the pocket pegmatite and cleavelandite, or albite-quartz rocks crystallized from a vapor. It may be that the mineral composition of these rocks is a reflection of the change in solubility of the mineral components in the vapor with a change of the temperature or pressure of the system. For example in the cleavelandite-quartz rocks the ratio of cleavelandite to quartz is approximately 2:1. Thus over the temperature-pressure interval of formation of these rocks the change in solubility in the vapor phase is about twice as great for cleavelandite as it is for quartz. The pocket pegmatite could crystallize in the same manner but in a different temperature pressure interval.

As previously considered, the corroded rocks are a product of a hydrothermal fluid; however there is no evidence indicating a close relationship between this hydrothermal fluid and the vapor proposed to account for the crystallization of other rocks in the pegmatite.

The hypothesis proposed for the origin of the Ramona pegmatites is consistent with relations observed in the field and the laboratory during this investigation. As with any hypothesis, subsequent work may invalidate some of the conclusions in this report; however the relations observed during this study and presented in this report must be considered in any subsequent hypotheses concerning the origin of the Ramona pegmatites.

REFERENCES

Bastin, E. S., Graton, L. C., Lindgren, Waldemar, Newhouse, W. H., Schwartz, G. H., and Short, M. N., 1931, Criteria of age relations of minerals, with especial reference to polished sections of ores: Econ. Geol., vol. 26, p. 561-610.

Bellemin, G. J., and Merriam, Richard, 1958, Petrology and origin of the Poway Conglomerate, San Diego, County, California, Geol. Soc. Amer. Bull., vol. 69, p. 199-220.

Birch, F., 1942, Handbook of physical constants, Thermal Conductivity and Diffusivity, G. S. A. Special Paper 36, p. 245-266.

Bragg, W. L., 1937, Atomic structure of minerals, Cornell University Press, Ithaca, New York, 292 p.

Brögger, W. C., 1881-82, Nogle bemaerkninger om pegmatitgangene ved Moss og deres mineraler: Geol. Foren. Stockholm, Forh., vol. 5 p. 326-376.

Buckley, H. E., 1951, Crystal Growth, 571 p., John Wiley and Sons, Inc., New York.

Cameron, E. N., Jahns, R. H., McNair, A. H., and Page, L. R., 1949, Internal structure of granitic pegmatites: Econ. Geol., Mon. 2, 115 p.

Campbell, R. B., 1959, The texture, origin, and emplacement of the granitic rocks of Glenlyon Range, Yukon, Canada, unpub. Ph.D. thesis, Calif. Inst. Tech.

Chayes, F., 1956, Petrographic Modal Analysis, John Wiley and Sons, Inc., New York, New York, 113 p.

Ellis, A. J., and Lee, C. H., 1919, Geology and ground waters of the western part of San Diego County, California, U.S.G.S. Water Supply Paper 446, 321 p.

Emery, K. O., 1954, General geology of the offshore area, Southern California, California Division of Mines, Bulletin 170 p. 107-113.

Fairbanks, H. W., 1891-1892, Geology of San Diego County; also of portion of Orange and San Bernardino Counties, Eleventh Report of the State Mineralogist, California State Mining Bureau, 612 p. (esp. p. 87.)

Fersman, A. E., 1928, Die Schriftstruktur der Granitpegmatit und ihre Entstehung: Zeits. Kristall., vol. 69, p. 77-104.

REFERENCES (continued)

Fersman, A. E., 1931, Les pegmatites, leur importance scientifique et practique: Acad. Sci., U.R.S.S.; Translated from the Russian into French under the direction of R. du Trien de Terdonck and J. Thoreau, 3 vols., 675 p., Univ. of Louvain, Belgium, 1951.

Frondel, Clifford, 1936, Oriented inclusions of tourmaline in muscovite: Amer. Mineral., vol. 21, p. 777-799.

Frondel, Clifford, 1940, Oriented inclusions of staurolite, zircon, and garnet in muscovite. Skating crystals and their significance: Amer. Mineral., vol. 25, p. 69-87.

Frondel, Clifford, Hurlbut, C. S., and Collette, R. C., 1947, Synthesis of tourmaline, Amer. Mineral., vol. 32, p. 680-681.

Goranson, R. W., 1931, The solubility of water in granite magmas: Amer. Jour. Sci., 5th ser., vol. 22, p. 481-502.

Hanley, J. B., 1951, Economic geology of the Rincon pegmatites, San Diego County, California: California Div. Mines, Special Report 7-B, 24 p.

Hertlein, L. G., and Grant, U. S., 1954, Geology of the Oceanside-San Diego Area, Southern California, Geology of Southern California, California Division of Mines, Bulletin 170 p. 107-113.

Jahns, R. H., 1954, Pegmatites of southern California, in Geology of southern California: California Div. Mines, Bull. 170, Chapt. VII, p. 37-50.

Jahns, R. H., 1955, The study of pegmatites, Econ. Geol. Fiftieth Anniversary Volume, p. 1025-1130.

Jahns, R. H., and Burnham, C. W., 1958, Experimental studies of pegmatite genesis: melting and crystallization of granite and pegmatite: Geol. Soc. America Bull., vol. 69, p. 1592.

Jahns, R. H., and Wright, L. A., 1951, Gem- and lithium-bearing pegmatites of the Pala district, San Diego County, California: California Div. Mines, Special Report 7-A, 72 p.

Johannsen, Albert, 1932, A descriptive petrography of the igneous rocks. Volume II. The quartz-bearing rocks, p. 4-25, 72-97, The University of Chicago Press, Chicago, Illinois.

Kennedy, G. C., 1950, A portion of the system silica-water: Econ. Geol., vol. 45, p. 629-653.

Larsen, E. S., Batholith and associated rocks of Corona, Elsinore, and San Luis Rey quadrangles Southern California, Geol. Soc. America Memoir 29, 1948.

REFERENCES (continued)

Merriam, Richard, 1941, A Southern California ring-dike, Am. Jour. Sci., vol. 239, p. 365-371.

Merriam, Richard, 1946, Igneous and metamorphic rocks of the southwestern part of the Ramona quadrangle, San Diego County, California: Geol. Soc. Amer., Bull., vol. 57, p. 223-260.

Merriam, Richard, 1954, Geologic map of Ramona Julian area, California Div. Mines, Bull. 170, Geologic Guide No. 5, p. 43.

Merrill, F. J. H., 1914, Mines and mineral resources of San Diego County, California: California Min. Bur., Rept. XIV, pp. 691-700, 706-708, 1914.

Michel-Levy, M., 1951, Reproduction artificell des grenats ferromanganesiferes series almandin-spessartite, Compt. Rendu., Acad. Sci. Paris, 232, p. 1953-1954.

Miller, W. J., 1935, Geomorphology of the Southern Peninsular Range of California, Geol. Soc. Amer. Bull., vol. 46, p. 1535-1562.

Miller, John P., 1958, High mountain streams: effects of geology on channel characteristics and bed material, New Mexico Bur. Mines, Memoir 4.

Morey, G. W., 1957, The solubility of solids in gases, Econ. Geol. vol. 52, pp. 225-251.

Morey, G. W., and Hesselgesser, J. M., 1951, The solubility of some minerals in superheated steam at high pressure. Econ. Geol., vol. 46, pp. 821-835.

Nockolds, S. R., 1954, Chemical composition of igneous rocks, Geol. Soc. Amer., Bull., vol. 65, pp. 1007-1032.

Nolan, T. B., 1943, The basin and range province in Utah, Nevada, and California, U.S.G.S. P.P. 197-D, p. 141-196.

Roy, R., and Osborn, E. F., 1952, Some simple aids in hydrothermal investigation of mineral systems. Econ. Geol. vol. 47, p. 717-721.

Saucier, H., 1952, Quelques Experiences sur la viscosite a haute temperature de verres ayant la composition d'un granite; influence de la vapeur d'eau sous pression, Bull. Societe Francaise de Mineralogie et de Cristallographie, vol. 75, pp. 1-45.

Schaller, W. T., 1925, U. S. Geol. Survey, unpublished manuscript on Southern California pegmatites.

REFERENCES (continued)

Schaller, W. T., 1927, Mineral replacements in pegmatites: Amer. Mineral., vol. 12, p. 59-63.

Schiebold, E., 1927, Uber den Feinbau der Feldspate. Fortschr. d. Min., vol. 12, p. 78.

Sinkankas, J., 1957, Recent gem mining at Ramona, Gems and Gemology, vol. VIII, no. 12, p. 367-374.

Spagenberg, K. and Newhaus, A., 1930, Kunstlich gefarbte Kristalle als beispiele sogennanter anomaler Mischkristalle und ihre mineralchemische Bedeutung, Chemie der Erde, vol. 5, p. 438-523.

Staatz, M. H., and Trites, A. F., 1955, Geology of the Quartz Creek pegmatite district, Gunnison County, Colorado: U. S. Geol. Survey, Prof. Paper 265, 111 p.

Stevens, R. E., 1938, New analyses of lepidolites and their interpretation: Amer. Mineral., vol. 23, p. 607-628.

Taylor, W. H., 1933, The structure of sanidine and other feldspars, Zeits. Krist., vol. 85, p. 425-442.

Thurston, W. R., 1955, Pegmatites of the Crystal Mountain district, Larimer County, Colorado: U. S. Geol. Survey, Bull. 1011, 185 p.

Tuttle, O. F., 1949, The variable inversion temperature of quartz as a possible geologic thermometer: Amer. Mineral., vol. 34, p. 723-730.

Tuttle, O. F., 1949, Two pressure vessels for silicate-water studies, Geol. Soc. Amer. Bull., vol. 60, p. 1727-1729.

Tuttle, O. F., and Bowen, N. L., 1958, Origin of granite in the light of experimental studies in the system $NaAlSi_3O_8$-$KAlSi_3O_8$-SiO_2-H_2O, G.S.A. Memoir 74, 153 p.

Wahlstrom, E. E., 1939, Graphic granite: Amer. Mineral., vol. 24, p. 681-698.

Waring, G. A., 1905, The pegmatyte veins of Pala, San Diego County: Amer. Geol., vol. 35, p. 356-369.

Washington, H. S., 1917, Chemical analysis of igneous rocks, U. S. Geol. Survey Professional Paper 99, 1201 p.

Winchell, A. N., 1951, Elements of Optical Mineralogy, Part II, John Wiley and Sons, Inc., New York, 551 p.

REFERENCES (continued)

Wyart, J., 1955, Cristallisation, par voie hydrothermale, d'un verre naturel et origine du granite, Numero hors serie, Sciences de la Terre, pp. 177-187.

Yoder, H. S., 1955, Almandite garnet stability range, Amer. Mineral., vol. 40, p. 342.

Yoder, H. S., and Engster, H. P., 1955, Synthetic and natural muscovites, Geochemica et Cosmochemica Acta, vol. 8, p. 225-280.

Yoder, H. S., Stewart, D. B., and Smith, J. R., 1956-57, Feldspars, Carnegie Institution of Washington Year Book 56, pp. 206-214.